Assessing the Risks of Climate Change on Electricity Grid Infrastructure

Von der Fakultät Nachhaltigkeit

der Leuphana Universität Lüneburg zur Erlangung des Grades

Doktor der Naturwissenschaften

- Dr. rer. nat. -

genehmigte Dissertation von Marius Stankoweit

geboren am 23.07.1987 in Münster

Eingereicht am: 18.06.2019

Mündliche Verteidigung (Disputation) am: 14.02.2020

Erstbetreuerin und -gutachterin: Prof.in Dr. Daniela Jacob
Zweitgutachter/in: Prof. Dr. Markus Quante
Drittgutachter/in: Prof. Dr. Klaus Eisenack

Erschienen unter dem Titel: Assessing the Risks of Climate Change on Electricity Grid Infrastructure

Druckjahr: 2020

Abstract

In response to the challenges of the energy transition, the German electricity network is subjected to a process of substantial transformation. Considering the long latency periods and lifetimes of electricity grid infrastructure projects, it is more cost-efficient to combine this need for transformation with the need to adapt the grid to future climate conditions. This study proposes the spatially varying risk of electricity grid outages as a guiding principle to determine optimal levels of security of electricity supply. Therefore, not only projections of future changes in the likelihood of impacts on the grid infrastructure were analyzed, but also the monetary consequences of an interruption. Since the windthrow of trees was identified a major source for atmospherically induced grid outages, a windthrow index was developed, to regionally assess the climatic conditions for windthrow. Further, a concept referred to as *Value of Lost Grid* was proposed to quantify the impacts related to interruptions of the distribution grid. In combination, the two approaches enabled to identify grid entities, which are of comparably high economic value and subjected to a comparably high likelihood of windthrow under future climate conditions. These are primarily located in the mid-range mountain areas of North-Rhine Westphalia, Baden-Württemberg and Bavaria.

In comparison to other areas of less risk, the higher risk in these areas should be reflected in comparably more resilient network structures, such as buried lines instead of overheadlines, or more comprehensive efforts to prevent grid interruptions, such as structural reinforcements of pylons or improved vegetation management along the power lines. In addition, the outcomes provide the basis for a selection of regions which should be subjected to a more regionally focused analysis inquiring spatial differences (with respect to the identified coincidence of high windthrow likelihoods and high economic importance of the grid) among individual power lines or sections of a distribution network.

Contents

List of Tables

List of Figures

Acronyms

CORDEX COordinated Regional Downscaling EXperiment

ECMWF European Centre for Medium-Range Weather Forecasts

ERA-Interim ERA-interim reanalysis data

ESGF Earth System Grid Federation

EURO-CORDEX European branch of CORDEX

GERICS Climate Service Center Germany

IPCC Intergovernmental Panel on Climate Change

mHM mesoscale Hydrologic Model

REMO REgional MOdel

SAIDI System Average Interruption Duration Index

VoLG Value of Lost Grid

VoLL Value of Lost Load

WCRP World Climate Research Programme

Abbreviations

DGO distribution grid operator

FT fourier transformation

GCM general circulation model

GVA gross value added

IQR interquartile range

OHL overheadline

RCM regional climate model

RCP representative concentration pathway

RMSE root mean square error

TGO transmission grid operator

1 Introduction

In response to the challenges of the energy transition (*Energiewende*), the German electricity landscape is in the process of major transformations: In order to comply with national CO_2-mitigation targets of the electricity sector (see *Salb et al.*, 2018), large thermal power generation units are increasingly replaced by decentralized units of renewable energy capacities (*Burger*, 2019). These transformations implicate structural adaptions and expansions of the whole electricity grid infrastructure.

Electricity needs to be transported over increasing distances, since the location of installation of renewable generation capacities is predominantly guided by the availability of renewable resources (such as wind and sunlight), instead of their proximity to demand centers of electricity. In response, the German electricity transmission grid infrastructure, those parts of the grid which are responsible for the transport of electricity over large distances, are planned to be significantly expanded (*Pesch et al.*, 2014). Moreover, the grid has to be adapted to cope with variable electricity feed-ins into those parts of the grid which traditionally were mainly in charge of the distribution of electricity. This relates to the fact that a significant share of the renewable electricity generation capacities is directly connected to the distribution networks (*National Academy of Sciences and Engineering (acatech) et al.*, 2016).

While, in comparison to the transmission grid, the German medial focus on the expansion of the distribution grid is much less pronounced, the expansion requirements at these lower voltage levels of the grid are significantly higher. Depending on the underlying energy-economic scenario considered, a projected 130,000 to 280,000 km of grid extensions (8 to 16% of current total distribution grid length) are projected to be required until around 2030 (*Büchner et al.*, 2014; *Agricola et al.*, 2012).

Besides the sketched expansion requirements of the electricity distribution networks due to the energy transition, these networks need to be adapted to the climate conditions they are exposed to during their lifetime. Climatic conditions are considered in the design of electricity networks: Based on observations on wind and ice conditions, climatic conditions are for example reflected in norms that regulate the resistance of the grid with respect to the local climatic conditions (compare e.g. *Deutsches Institut für Normung*, 2005). However, potential future climate changes are not yet included in these norms. In response, a redefinition of technical standards is considered to account for climate change aspects (*Arent et al.*, 2014).

Extreme weather events may impair the secure operation of electricity distribution and transmission networks. In the course of climate change, the return periods of these events can be impacted (*Groth et al.*, 2018; *Koch et al.*, 2016). The electricity transmission and

distribution sector has been identified of being particularly vulnerable to altered storm conditions and increases in air temperature (*European Commission*, 2013; *Rademaekers et al.*, 2011).

Increased ambient temperatures lead to reduced carrying capacities of the grid (*Arent et al.*, 2014). However, their physical and monetary implications are comparably small to the damages potentially induced by events of extreme wind speeds (*Ward*, 2013a). This relates to the fact that extreme wind speeds bear potential to cause electricity outages. These may lead to the interruption of value-adding processes causing severe economic implications. Also historically, in Europe, the majority of such customer disconnections were related to storms that caused trees or other debris to damage the distribution infrastructure (*Ward*, 2013a). *Schubert et al.* (2008) and the findings in Sec. 2.4 of this thesis indicate that this general observation also applies to Germany.

Hence, besides the considerable investment requirements to adapt the electricity networks to the requirements related to the energy shift, further adaptation becomes necessary to account for climate change impacts - especially considering the long latency periods and lifetimes of electricity infrastructure projects (*Schmid et al.*, 2016).

The previous paragraphs stressed two important points: The investments into the German transmission and distribution grid infrastructure to meet the structural changes related to the energy transition are estimated to be substantial in the forthcoming years. In addition, the electricity transmission and distribution sector has been identified being vulnerable to climatic changes. Therefore, it is probably more cost-efficient to combine both aspects as part of the standard maintenance-renewal cycle: the need for extension requirements related to the energy transition as well as the need to adapt the grid to potentially altered climatic conditions.

It should be underlined that the electricity grid in its current structure was not designed according to cost-efficiency criteria. Admittedly, today's grid design to some extent unintendedly reflects economic criteria: Lower voltage levels, for example, are in general designed with a lesser degree of redundancy than higher voltage levels (*Ward*, 2013a) and, therefore, have better capacities to cope with an outage of any component within the power system. This reflects economic reasoning, since most probably more economic value generation would be affected by an interruption in the higher voltage levels of the grid than in any of the lower levels. However, in fact, the guiding regulatory frameworks in Germany base security standards primarily on engineering practices, instead of resorting to economic considerations (*Röpke*, 2013). This is common practice also in most other countries, but there are also examples of countries that include economic arguments: The Netherlands, for example, have added a rule that allows grid operators to deviate from

strict engineering practices in case the costs exceed the benefits of a certain measure (*de Nooij et al.*, 2010).

Climate change should not simply be taken into account by redefining the respective technical standards in accordance to the projections of future changes in the probability distribution of extreme weather events. Instead, also the monetary consequences of an interruption should be taken into account. As a guiding concept, this thesis suggests the risk concept as defined in the field of quantitative risk analysis. Applied to the research complex of interest in this study, risk can be represented as likelihood of the occurrence of hazardous events multiplied by the impacts if these events occur (*IPCC*, 2014). Resorting to this concept determines the structure of this thesis along the lines of the following research questions.

Which atmospheric events trigger grid interruptions?

The proposed risk concept requires the likelihood of the occurrence of hazardous events. In order to determine which events are actually hazardous in the context of electricity grid infrastructure, Ch. 2 introduces the main characteristics of the electricity networks, investigates which events led to network interruption in the past and which events are projected to constitute grid outage initiators in the future. Since the windthrow of trees is identified as a main contributor to atmospherically-related grid interruptions (compare Sec. 2.4), the conditions that influence the probability for windthrow and the relevant climatic variables determining the probabilities of windthrow are identified. In this context, also the role of overheadline as vulnerable critical infrastructure is discussed.

How does climate change impact the likelihood for grid outages?

Having identified windthrow as the most likely future source for network outages, an index to capture the conditions for windthrow is proposed (compare Ch. 3). Thereafter, regional differences in the windthrow index at the end of the 20$^{\text{th}}$ century are quantified and compared to the windthrow index as projected for a mid 21$^{\text{st}}$ century period according to an ensemble of state-of-the-art regional climate model simulations. Finally, regions of increasing and decreasing windthrow likelihood due to climate climate are identified.

What is the economic impact related to a grid interruption?

Having analyzed the likelihood of hazardous events as one component required for the quantification of risk, Ch. 4 focuses on determining the impacts related to a windthrow-induced interruption of the distribution grid. Therefore, a methodology to quantify and analyze regional differences in the economic relevance of the distribution grid infrastructure is proposed. Finally regions of comparably higher economic relevance than others are highlighted.

What is the risk associated with climate change impacts on the electricity grid infras-

tructure?

Ch. 5 combines the outcomes of the individual results of the two principal parts of this thesis (Ch. 3 and Ch. 4) and stresses relevant limitations of the suggested approach. Ch. 6 summarizes the outcomes with respect to the posed research questions and provides an outlook for a more refined analysis on a higher spatial resolution.

2 Interruptions of Electricity Networks

In Ch. 1, the research questions analyzed in this dissertation project were motivated. This chapter provides relevant background information on crucial characteristics of electricity networks with respect to its hierarchy of voltage levels and their respective duties in the context of electricity supply (compare Sec. 2.2), and on the reliability of electricity supply (compare Sec. 2.3). In addition, a dataset on electricity outage statistics is analyzed, and the windthrow of trees is identified as the dominant reason of atmospherically-induced electricity grid interruptions (compare Sec. 2.4). Subsequently, the variables determining windthrow are introduced (compare 2.5). Finally, climate change impacts on windthrow are analyzed (compare 2.6).

2.1 Introduction

The reliability of the electricity system is crucial for the availability of basic services such as health care or food- and water supply. In consequence, the electricity system is classified as critical (compare e.g. *The Council of the European Union*, 2008). The critical infrastructure of a country refers to all the assets essential for the proper functioning of a society and its economy.

Beyond its social and economic significance, investments into electricity grid infrastructure are characterized by further important aspects: Firstly, electricity grid infrastructure is very capital-intensive. Therefore, it is not economically reasonable, to have various competing grids in place (*Schwab*, 2012). In order to avoid that operators exploit this situation of a so-called *natural monopoly*, the electricity transmission and distribution business is regulated. In exchange for being granted a monopoly, an electricity transmission or distribution company has to accept that a regulatory authority (in Germany: the *Bundesnetzagentur*) determines the structural requirements of the infrastructure as well as the height of the network charges (*Schwab*, 2012), and thus, strongly influences the operators' revenues.

Secondly, large infrastructure projects are often characterized by significant latency periods during the planning process (*Schmid et al.*, 2016), and experience very long lifetime of up to 50 and more years. In Germany, for example, more than 40% of the currently installed distribution or transmission grid infrastructure has been build prior to 1969 (*Bräuninger et al.*, 2014). Therefore, the planning of required grid capacities crucially depends on robust projections of future energy transmission and distribution requirements. At the same time, it is of vital importance to account for climatic changes during the operational lifetimes of these infrastructure.

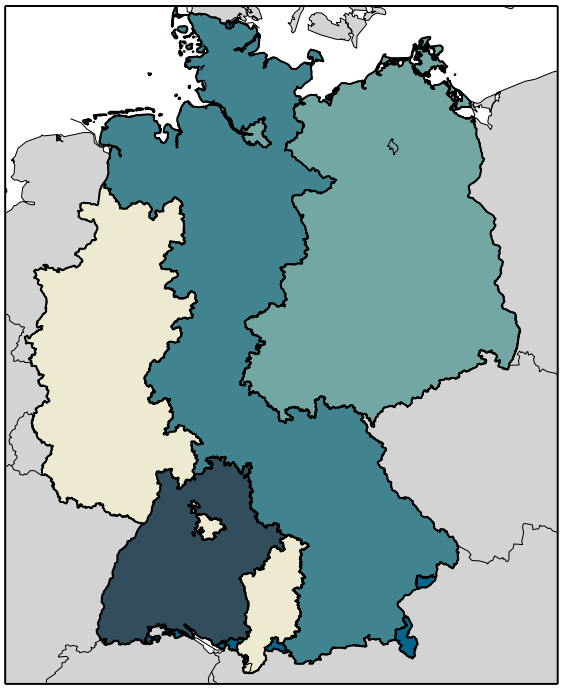

Figure 1: Domains of the four different transmission grid operators (TGOs) in Germany (Visualization based on shapefiles from *Lutum + Tappert DV-Beratung GmbH* (2016)).

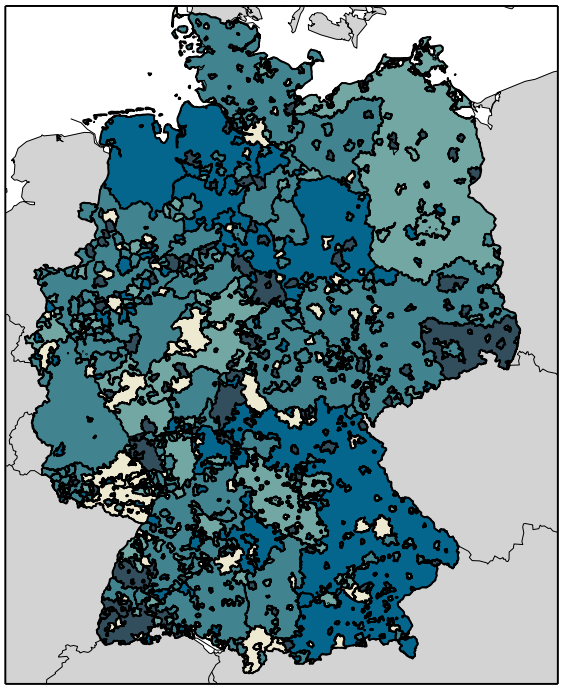

Figure 2: Domains of the almost 900 different distribution grid operators (DGOs) in Germany (Visualization based on shapefiles from *Lutum + Tappert DV-Beratung GmbH* (2016)).

2.2 The Role of Transmission and Distribution Networks of Electricity

Electricity is transported at different voltage levels. The higher the distance over which power is to be transported, the higher the voltage used. This is related to the fact that power losses decline the higher the voltage used for its transmission (*Schwab*, 2012). It is distinguished between the transmission and the distribution grid. In essence, the transmission grid's task is the supra-regional transportation of electricity, usually at peak voltage levels of 220 or 380 kV. In Germany, the transmission grid is operated by four different so-called transmission grid operators (TGOs) (compare Fig. 1). Unplanned interruptions of the transmission grid can lead to blackouts far away from the location where the interruption of transmission occurred.

Though transmission grids play an essential role for the long-distance transport of electricity, they constitute only 1.9% of totally installed grid lengths (*Lengsfeld et al.*, 2015). The remaining share of the grid is referred to as the distribution grid, usually running at between 400V to 110kV. Its primary task is to locally distribute the electricity to the electricity consumers. Currently, there are around 900 different distribution grid

operators (DGOs) in Germany of very different geographical sizes (compare Fig. 2).

The energy transition in Germany has triggered significant alterations in the structure of electricity generation. Historically, the electricity system has been designed such that large thermal power plants were located in close proximity to the demand centers of electricity. These fed into the transmission grid, from which electricity was propagated down to the lower voltage levels of the distribution grid to meet the demand of the end-customers of electricity. These conventional sources of electricity generation have the advantage that their operation can be planned and to some extent adjusted according to the projected demand for electricity. However, large thermal power plants are increasingly replaced by decentralized units of small-scale renewable generation capacities (*Burger*, 2019), which in many cases directly feed into the distribution grids (*National Academy of Sciences and Engineering (acatech) et al.*, 2016). In response to this ongoing development, a combination of measures are planned or are in the process of gradual implementation: One is, to increase electricity storage capacities in order to cope with an increased variability of renewable power generation and the limited influence on its power output (*Zander et al.*, 2017). In addition, the electricity market gets gradually adapted to these challenges by developing towards a pattern where the market incentivizes to adjust consumption to the generation of electricity (*Bayod-Rújula*, 2009), instead electricity generation responding to the timing of consumption.

These measures can to some extent compensate for investments in the grid infrastructure (*Zander et al.*, 2017). Nevertheless, sizable investments in the expansion of the German electricity transmission grid infrastructure are necessary (*Pesch et al.*, 2014). This is due to the installation of renewable electricity generation capacities being primarily determined by the availability of renewable resources, instead of a proximity to the centers of electricity demand. Wind energy is for example harvested by large (planned) offshore wind parks in the North- and Baltic Sea, while there are few (planned) renewable generation capacities close to the electricity demand centers in the South of Germany (*Knorr et al.*, 2017). Therefore, today (and even more pronounced in the future) electricity needs to be transported over larger distances than historically.

While the medial focus on the adaptation of the distribution grids to the sketched developments is much less pronounced, the absolute expansion requirements at these lower voltage levels of the grid are significantly higher. This relates to the fact that the distribution grids have originally not been designed for high shares of renewable electricity feed-ins. Due to this development, the historically mostly unidirectional power flow (from the higher to the lower voltage levels) is increasingly often replaced by a bidirectional electricity flow (*National Academy of Sciences and Engineering (acatech) et al.*, 2016). Therefore, adaptation and expansion of the distribution grid is crucial to

cope with these decentralized electricity feed-ins (*Büchner et al.*, 2014). In consequence, as already highlighted, a projected 130,000 to 280,000 km of grid extensions (~8 to 16% of current total distribution grid length) are required until 2030 or 2032 (depending on the underlying energy-economic scenario considered by *Büchner et al.* (2014) or *Agricola et al.* (2012) respectively).

2.3 Reliability of Electricity Supply

Many sectors and services significantly rely on a constant provision of electricity. Therefore, a long-lasting and large-scale electricity blackout would lead to the complete collapse of many other critical infrastructures (*Petermann et al.*, 2010). The causes of such major blackouts are manifold. They could relate to terrorist actions, system failures or natural disasters, such as extreme weather events (*Petermann et al.*, 2010). Climate change may impair the reliability of the energy system through an increased occurrence of weather extremes. In the past, the impacts of most extreme weather events were rather locally constrained and did not lead to large-scale blackouts in Germany. However, already small-scale blackouts may cause significant deadweight losses and harm the local economy (*de Nooij et al.*, 2007). An estimated 3.4 million people were for example affected by blackouts during the two winter storms *Lothar* and *Martin* (in December 1999), having caused estimated economic losses of 15 billion € (*Groenemeijer et al.*, 2015).

An individual contingency within the system does not necessarily lead to a supply interruption. In general, an electricity network is designed according to the *N-1 standard*, implying that the network has sufficient redundancy to withstand any singular fault of the system, such as the unplanned outage of a generating unit or the unplanned outage of a conductor line (*Schwab*, 2012). Consequently, a necessary condition for a supply interruption is, in most networks types, the failure of at least two system components.

However, distribution networks are generally characterized by a lesser degree of redundancy than the transmission network (*Schwab*, 2012). In certain network architectures of the lower voltage networks a single fault may already cause a number of consumers to lose supply. Radial systems are the predominant network architecture of low voltage grids, whereas on the medium voltage level, loop systems dominate (*Büchner et al.*, 2014). In a radial distribution system, a failure at one point of the grid causes a collapse for those system units located behind the point of failure. In a loop system, each system unit can be supplied from two sites, hence, a failure at one point in the loop does not necessarily imply a supply interruption for other units within the loop.

Besides the network architecture and the degree of redundancy of the grid, the share of overheadlines (OHLs) constitutes a factor of vulnerability of the system, due to their exposure to falling trees and other wind-blown debris or ice agglomeration on the lines.

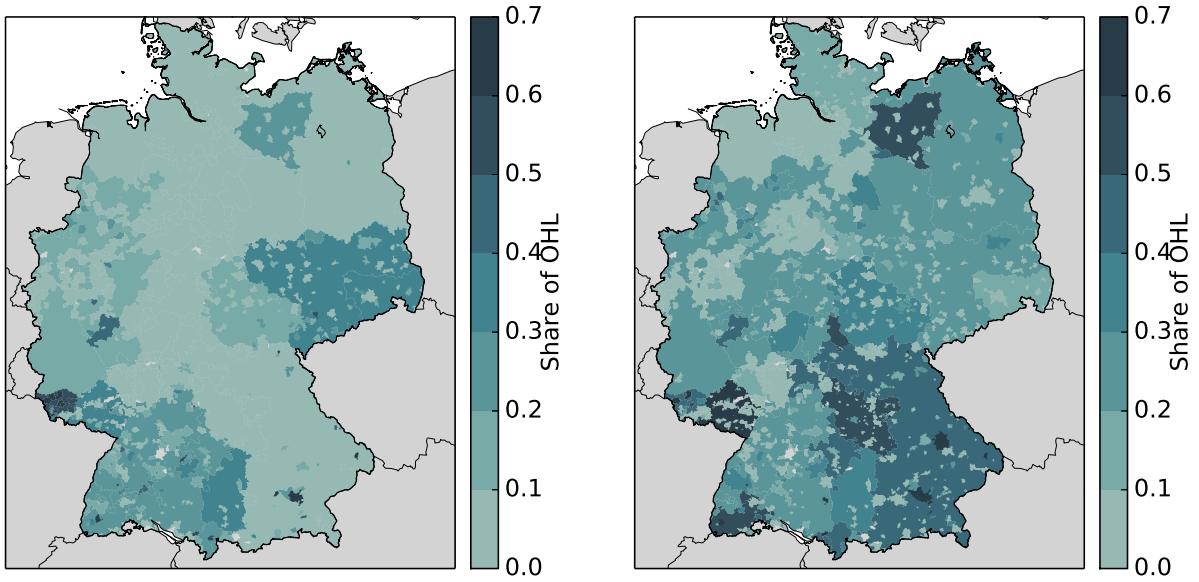

Figure 3: Share of overheadlines (OHLs) in the low voltage grid (left) and the medium voltage grid (right) of the distribution grid; based on reporting of DGOs; gray-colored domains indicate lacking information.

In general, the share of OHLs decreases the lower the voltage level. The largest number of end-customers (especially in densely populated areas) are commonly connected to the low voltage grid via buried cables. However, the share of OHLs can regionally differ quite significantly (compare Fig. 3), with some domains in the low- and medium voltage grid level being characterized by up to 60 to 70% of OHLs, whereas there are other operators of almost 0 to 19% share. This indicates an operator-specifically varying degree of vulnerability of the grid to extreme weather events.

2.4 Reasons for Grid Interruptions

In Europe and North America, weather events are a main contributor to situations of a loss of supply of customers (*Ward*, 2013a). In the US, weather impacts were responsible for more than 50% of outages (affecting more than 50,000 customers) between 1984 and 2006 (*Hines et al.*, 2009). In Europe, the majority of customer disconnections occurred in the distribution networks and were related to storms that caused trees or other debris to damage the distribution infrastructure (*Ward*, 2013a). Only the most severe storms caused direct damages to the transmission networks (*Ward*, 2013b). OHL structures of the distribution grid are in general more prone to wind-blown debris due to their – in comparison to transmission networks – lower design heights.

In Germany, grid operators are legally obliged to annually report grid interruptions. These reports establish a basis for calculating the so-called System Average Interruption

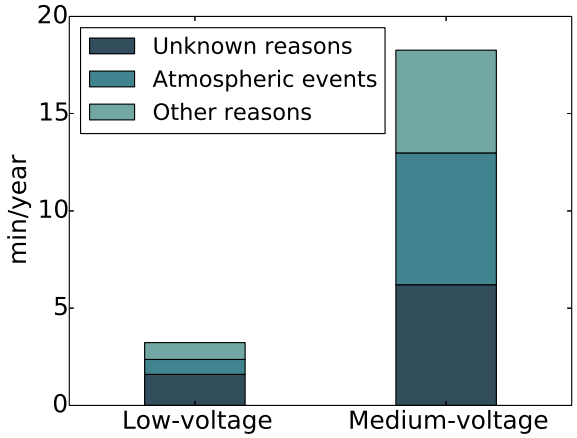

Figure 4: Comparison of the annual mean outage duration per customer in the low voltage level and the medium voltage level differentiated by its triggers in the period from 2004 to 2015, based on the evaluation of the availability statistics (*Forum Netztechnik/Netzbetrieb*, 2017).

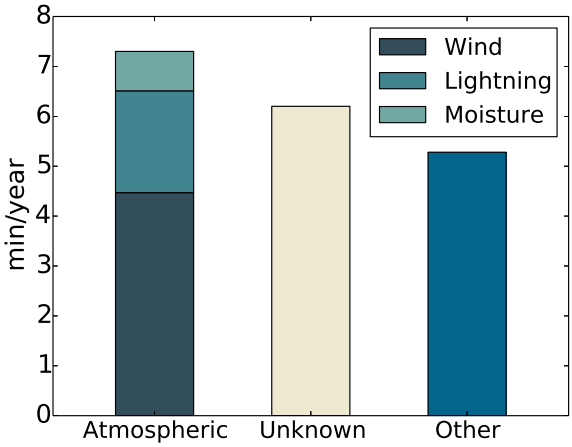

Figure 5: Annual mean outage duration per customer in the medium voltage level between 2004 to 2015 differentiated by its trigger, based on the evaluation of the incident statistics (*Forum Netztechnik/Netzbetrieb*, 2017).

Duration Index (SAIDI), which provides information on electricity outages. On average, each customer in Germany was disconnected from the grid between around 12 to 22 min/a between 2006 and 2017 (*Bundesnetzagentur*, 2018). In general, the quality of the security of supply in Germany is very high in comparison to other European countries *Bundesnetzagentur* (2015), however, a large contribution towards the inter-annual variability of outage times relates to extreme weather events, such as storms.

An analysis for the period 2004 to 2006 with special focus on Germany indicates that atmospheric impacts contributed around 40% towards those outages for which a reason of its interruption is known[1] (*Schubert et al.*, 2008). However, to the author's knowledge there is no study which investigates atmospherically induced electricity outages in the years after 2006. And, further, there is no publication which disaggregates the reasons of atmospheric impacts into its individual subcategories, such as wind/storms, icing, flooding. Therefore, a more comprehensive analysis on the reasons for grid interruptions was conducted, based on a database on grid-interruptions for the period 2004 to 2015 (Dataset: *Forum Netztechnik/Netzbetrieb*, 2017).

The analyzed dataset is based on two different survey statistics: The so-called *availability statistics* (in German: Verfügbarkeitssstatisitik) and the *incident statistics* (in German: Störungsstatistik). The availability statistics collects data on the availability

[1]For about a third of the outage duration, there was no clear reason identifiable.

of electricity by final electricity customers in the low- and medium voltage grid. The incident statistics evaluates the reasons for grid interruption down to the medium voltage level in a comparably more detailed manner. Both statistics are consistently based on at least 75% of the total grid lengths (*Forum Netztechnik/Netzbetrieb*, 2017). Therefore, they can be considered as representative for the outage statistics in the whole system. This is further stressed by the fact that the annual average SAIDI coefficients calculated from these statistics (*Forum Netztechnik/Netzbetrieb*, 2017) closely match the coefficients as published by the respective regulatory authority in charge (*Bundesnetzagentur*, 2018). The advantage of the analyzed incident statistics over the published data by the Bundesnetzagentur is its facilitation of a disaggregated analysis of the atmospheric reasons that led to an outage. However, since the incident statistics is only conducted down to the medium voltage level, this disaggregation cannot be conducted with respect to the low voltage grid.

This does not constitute a major issue, since the evaluation of the availability statistics reveals that the majority of outage duration times relates to interruptions of the medium voltage level (compare Fig. 4). Moreover, the evaluation showed atmospheric events to be the largest contributor to customer disconnections in the medium voltage grid (~ 39%). The incident statistics enables to further disaggregate the category *atmospheric event* (compare Fig. 5). The results illustrate that within the category of atmospheric events, wind is the main contributor to disconnections (~ 60%).

It is challenging to robustly project future reasons for electricity outages- Since the climatic conditions in Germany are projected to change, the probabilities of the occurrence of events potentially triggering electricity outages may also be modified. Therefore, past reasons for grid interruptions are not necessarily an indicator for future reasons for grid interruptions.

Nevertheless, expert assessments provide some guidance. For the electricity transmission and distribution sector, the increased occurrence of storms and increases in air temperature was identified as the biggest risks associated with climate change (*European Commission*, 2013; *Rademaekers et al.*, 2011). These assumptions are supported by the conclusions drawn from expert interviews with actors of the energy sector in Germany (*Gößling-Reisemann et al.*, 2012). According to that, potential future impacts on the OHLs due to wind and ice formation as well as the impacts of increased summer heat waves on the availability of cooling water are considered of being the most relevant climatic influences.

Increased ambient air temperatures especially influence the operation of thermal power plants. The transportation of fuels (usually hard coal) towards power plants could be impaired when climate change leads to lower river levels during summer periods (*Groth*

et al., 2018; *Behrens et al.*, 2017): For Germany, electricity prices have been estimated to increase by 1% if water levels fall by 1% (*McDermott* and *Nilsen*, 2011). In addition, increased river temperature during summer restricts the availability of cooling reservoirs and, hence, influences the efficiency of the generation of electricity: electricity prices in Germany were estimated to increase by 1% for each degree that water temperatures exceed 25°C (*McDermott* and *Nilsen*, 2011). Similar qualitative effects were shown by *Pechan* and *Eisenack* (2014). However, the aspect of cooling water availability is considered manageable by installing cooling towers to reduce the need for cooling water (*Gößling-Reisemann et al.*, 2012). In conclusion: High ambient temperatures have the potential to increase electricity prices over a limited period of time, but they hardly cause interruptions of electricity supply.

2.5 Windthrow

In the past, the majority of customer disconnections occurred in the distribution networks and were related to storms causing trees to damage the distribution infrastructure. Therefore, changes in the local climatic conditions that influence the windthrow probability of trees may influence the occurrence of customer disconnections.

Wind acting on the cross-sectional area of a tree may cause the tree's stem to bend and leads to a shift of weight of the crone and the trunk to the lee side of the tree. If the applied wind forces are rather moderate, the tree springs back towards its original position as soon as the wind force decreases. During gusty wind conditions, elliptic oscillations of the crone of the tree can be observed, due to the eccentricity of the crown (*Mitscherlich*, 1981). In case the wind-induced momentum acting on the tree exceeds the tree's root anchorage in the soil, roots on the luv site of the tree start to rupture, while the roots on the lee site of the tree get kinked. In particular on wet and skeletal poor soils, the whole root bale – depending on the root structure of the tree – may either turn as a hemisphere in the soil or may be lifted as a flat disk. In a preliminary phase of the latter process, it can be observed that the root plate lifts and lowers in accordance with the bending of the trunk (*Mitscherlich*, 1981).

An extraordinarily strong gust may cause stem and crone to be bended as far to the lee side, that the turning momentum (related to its excentered weight and the wind force applied; compare the right arrow in Fig. 6) exceeds the frictional resistance of the root bale and the tensile and supporting forces of the roots in the soil (the left arrow in Fig. 6). In consequence, the tree overturns. In case the applied wind force exceeds the stem's strength but does not exceed the roots' anchorage in the soil, the stem breaks. Hence, a tree's root anchorage and its trunk strength determine whether wind causes uprooting, trunk breakage or no damage. Both, stem breakage and uprooting, is commonly referred

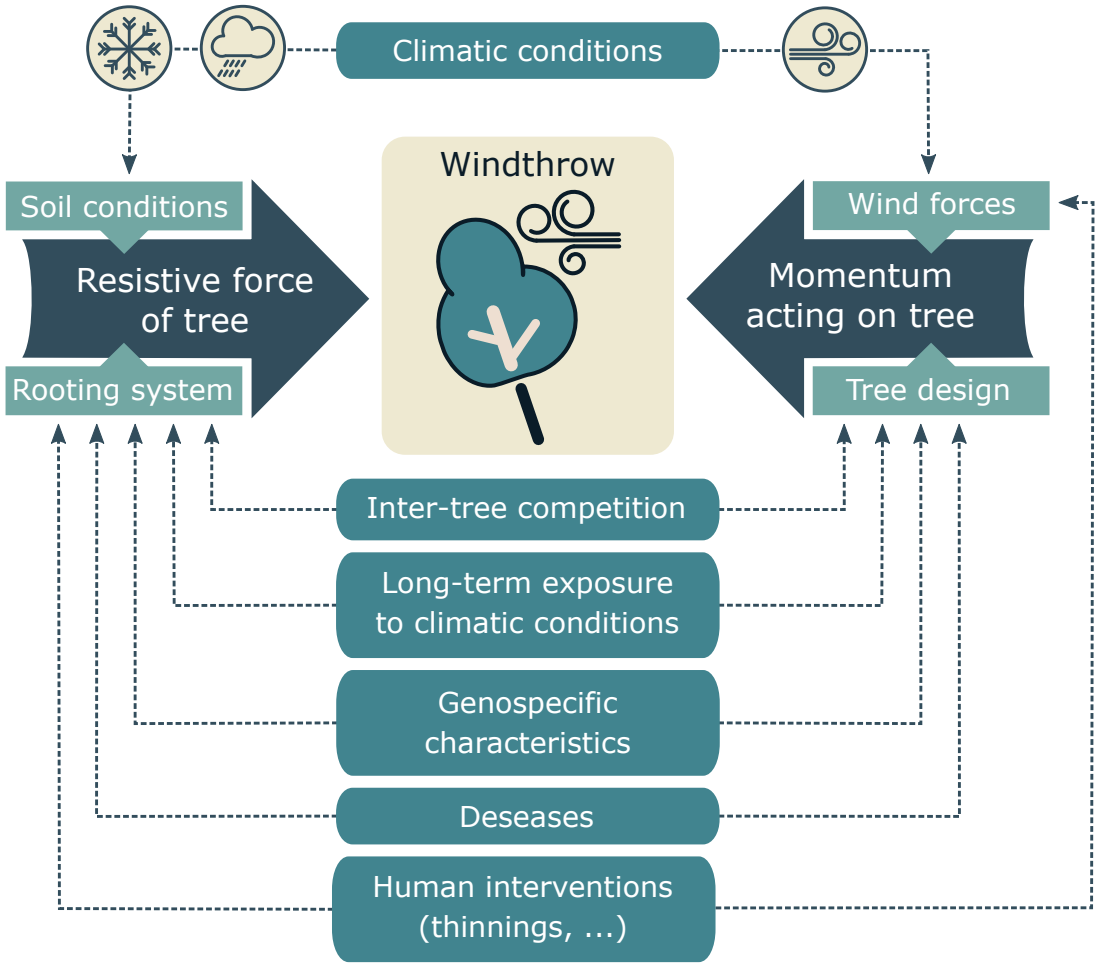

Figure 6: Schematic sketch of factors that determine a tree's windthrow risk. Changes in the climatic conditions may either impact the wind-induced momentum acting on the tree, or influence the resistive forces of the tree that determine the maximum turning moment the tree may withstand without being overturned.

to as windthrow (e.g. *Gardiner et al.*, 2008; *Klaus et al.*, 2011).

The probability that a tree is overthrown by wind is determine by a variety of factors as schematically visualized in Fig. 6. A tree's genospecific characteristics determine its resistive forces (root anchorage and stem strength) and influence the wind-induced forces applied to the tree: Its resistive forces are determined, for example, by the depth of the rooting system and the ratio of tree height to stem diameter; the applied forces are influenced for example by its crown characteristics and stem height. However, these tree characteristics are only to a certain extent species-specific. In addition, a tree's mechanistic stability mirrors its long-term exposure to climatic conditions and inter-tree competition (*Perera et al.*, 2015): Isolatedly growing trees commonly develop large crowns and adapt their crowns as well as stem thickness and roots to the local wind conditions (*Perera et al.*, 2015). Stand-growing trees, which are partially sheltered by neighboring

trees, are commonly characterized by lower mechanical stability, since they compete for light and soil resources (*Perera et al.*, 2015). Furthermore, diseases as well as human interventions (e.g. thinnings of a forest, ruptures of the rooting systems with heavy forest vehicles etc.) impact on the predisposition to windthrow.

Moreover, climatic conditions determine the windthrow likelihood of a tree. Beyond the wind conditions, soil moisture and soil temperature impact the resistive forces of the root bale within the soil. Heavy rainfall during or prior to storm events lead to increased soil moisture levels, and were observed to increase the predisposition of trees to windthrow (*Usbeck et al.*, 2010; *Panferov et al.*, 2010, 2009; *Dobbertin*, 2002). *Dobbertin* (2002) found that the probability of windthrow during winter storm Vivian was twice as high for a tree standing on water logged soils compared to stands on non-water logged soils. This observation was confirmed by tree pulling experiments (*Kamimura et al.*, 2012) and by studies investigating windthrow during winter storm Kyrill in North-Western Germany (*Klaus et al.*, 2011). Besides the moisture content, the physical state of the soil moisture (frozen or non-frozen) substantially influences soil stability: The sensitivity to storm damage has been modeled to decrease by 30% during frozen soil conditions (*Lagergren et al.*, 2012).

2.6 Climate Variables influencing Windthrow

The conditions for windthrow were identified being influenced by the climate variables wind speed, soil moisture and the state of the soil. The following subsections outline how these variables have evolved in the past and summarize the knowledge on their evolution in the forthcoming decades (compare Subsec. 2.6.1, 2.6.2 and 2.6.3).

2.6.1 Extreme Wind Speeds

Since windthrow is determined by the maximum turning moment acting on a tree, the occurrence of extreme wind speeds is the main contributor to the windthrow risk of trees. For Germany, extreme wind speeds are significantly determined by the strength and the track of cyclones originating from the Northern Atlantic (*Pinto* and *Reyers*, 2016). Cyclones develop in regions with large temperature gradients, either due to differences in solar heating between lower and higher latitudes or due to the differences in heat uptake between land and ocean surfaces. Conditions for cyclone development are especially favorable over the Northern Atlantic. Since climate change is projected to lead to altered global and regional temperature distributions, both the track and the strength of these cyclones are expected to be affected by climate change (*Pinto* and *Reyers*, 2016).

There are different methods to estimate past changes in the occurrence of extreme wind

speeds. Due to the mentioned mechanism of cyclone formation, a majority of studies on trends of extreme wind speeds focus on the North Atlantic, the North Sea and/or the Baltic Sea[2], instead of having a local focus on Germany. In the context of trends in the occurrence of cyclones, it is important to consider that cyclone activity is subjected to large multi-decadal variability (*Feser et al.*, 2015). Any trend in the data is superimposed by this internal variability. Therefore, the comparably short period of comprehensive wind data collection (of roughly 50 years) aggravates robust conclusions (*Pinto* and *Reyers*, 2016).

Feser et al. (2015) reviewed available literature on long-term storm trends in the past. The authors differentiate between approaches based on station measurements of wind speeds[3] and on reanalysis data. The findings are ambiguous: A majority of measurement-based studies indicates a decrease in the storm activity for central Europe and the Northern Sea, and about the same number of studies show an increase, a decrease or no trend for the Baltic Sea region. Contrarily, reanalysis-based studies identify no net or a positive trend for the three named regions. One root for these contrary findings are methodological differences (*Pinto* and *Reyers*, 2016). In addition, a trend analysis of measurements at several stations in Germany did not indicate any significant trends (*Hofherr* and *Kunz*, 2010). In conclusion, there is no clear historical trend to observe for Germany (*Pinto* and *Reyers*, 2016).

Feser et al. (2015) also reviewed available literature on future long-term storm trends, based on Global or Regional Climate Models (GCM and RCM): The reviewed articles do not indicate a clear trend with respect to the occurrence rate of storms for the Baltic Sea and central Europe. However, with respect to storm intensity, almost all reviewed articles diagnose an intensification of future storms for the mentioned geographic area, irrespective of the model types considered in the analysis (GCM or RCM). With special focus on Germany, *Rauthe et al.* (2010) showed an increase in the occurrence of extreme wind speeds (of 10-year return period) in the North and North-West, and decreases in the South-West of the country. However, the latter study is based on only two different RCMs, driven by the same GCM.

2.6.2 Soil Moisture

The resistive forces of a tree are, among others, determined by the anchorage of the roots in the soil. In addition to the soil type, soil moisture may significantly determine the

[2]For a detailed overview of studies, please consult *Feser et al.* (2015).

[3]Most of the reviewed studies are based on pressure-based extreme-wind-proxies, to avoid that outcomes are distorted by potential inhomogeneities in wind time series or land-use changes (*Feser et al.*, 2015). In contrast to these methods, direct wind measurements are often viewed as too inconsistent to be directly employed as a proxy for extreme wind speeds (*Pinto* and *Reyers*, 2016).

resistive forces of the roots to windthrow.

Due to the absence of studies focusing on past and future trends of soil moisture content in those soil layers relevant for root anchorage, changes in precipitation or evaporation as a consequence of climate change may serve as an indicator for the influence of climatic changes on the resistive forces of trees. With respect to precipitation sums over Germany during the summer months, *Zolina et al.* (2008) identified slight, but insignificant decreases for the past decades. During winter months, for many regions a significant increase in the precipitation sums was identified (*Zolina et al.*, 2008). Moreover, trends for heavy precipitation events were found to increase significantly for large parts of Germany (*Moberg* and *Jones*, 2005). In the near future, extreme precipitation events (90th percentile of daily precipitation sums) as well as precipitation sums in general are projected to increase all over the country during winter (*Pfeifer et al.*, 2015; *Feldmann et al.*, 2013). However, in the near-term (e.g. 2031 to 2060) robust climate change signals are identified for a limited number of regions only, while the robustness with respect to the long-term (by the end of the 21st century) is much more substantial (*Pfeifer et al.*, 2015).

These increased levels of winter precipitation, as already observed and projected for common scenarios of climate change, increase soil moisture and, therefore, have an overall increasing influence on the likelihood of windthrow.

2.6.3 Soil Frost

To the author's knowledge, there is no study investigating recent or future changes in soil frost days in Germany in a comprehensive manner. Further, soil temperatures are no standard output variable stored in climate data archives (e.g. the archives of the Earth System Grid Federation (ESGF)), and can, therefore, only be studied via proxy indicators. Hence, as an indicator towards trends in soil temperature, the following paragraphs mainly refer to studies investigating atmospheric temperatures.

Only a few studies exist regarding past trends of the extreme characteristics of atmospheric temperatures (*Deutschländer* and *Mächel*, 2016). A study regionally focusing on the Rhine basin in Western Germany found for the period from 1958 to 2000, a reduction in the number of days with temperatures below 0°C at the majority of the temperature stations (*Hundecha* and *Bárdossy*, 2005). Overall, there is a positive trend towards less extreme minimum temperatures, which also indicates a decrease of the number of days with temperatures below 0°C (*Deutschländer* and *Mächel*, 2016). By the end of the 21st century, the number of frost days was projected to substantially decrease in comparison to the reference period (1971 to 2000): Depending on the considered greenhouse gas emissions scenario, for Northern Europe the likely decrease was estimated to amount between 26 to 83 days (*Jacob et al.*, 2014).

These findings result in longer periods of unfrozen soils, during which the root anchorage is reduced (*Schindler et al.*, 2012). The importance of this phenomenon is amplified by the fact that the periods of decreasing shares of frozen soils overlap with the periods of clustered appearances of wind extremes during autumn and winter.

2.7 Conclusions

An analysis of available literature and statistics on the reasons for customer disconnections from the electricity grid was conducted. The results showed that, in the past, most customer disconnections occurred on the medium voltage level of the distribution grid; while there are hardly any documented interruptions of the transmission grid. This is related to the fact that the largest contributor to customer disconnections are atmospheric events. Further, the results of the analysis identify wind as the main reason for customer disconnections in the past. However, usually wind does not directly damage the constructions, but causes trees to fall on the structures. Since the transmission networks are characterized by a significantly higher design height than the distribution networks, the former hardly experience any windthrow-related disconnection. Therefore, the analysis conducted in Ch. 4 focuses on atmospherically-induced outages of the electricity *distribution* networks.

As indicated, windthrow – the overturning or breakage of a tree due to extraordinarily strong gusts – constituted the main contributor to atmospherically-induced customer disconnections in Germany. But due to climate change, the probabilities of the occurrence of events having the potential to trigger electricity outages may also be modified. Expert assessments identifying the increased occurrence of storms as one of the biggest risks associated with the electricity transmission and distribution sector, indicate that windthrow constitutes a major threat also under conditions of climate change.

Consequently, the influence of climate change on the windthrow risk of trees was explored: increasing occurrences of extreme wind speeds, increasing soil moisture content as well as reduced shares of days experiencing frozen soil conditions increase the likelihood of windthrow. However, windthrow threatens the security of electricity supply only in those cases where the grid infrastructure is designed as OHLs. Therefore, the share of OHLs was identified as a factor of vulnerability of the electricity system. In the medium voltage level, identified as the part of the grid most often hit by supply interruptions, the share of OHLs varies substantially between the different operators.

3 Influence of Climate Change on Windthrow

The previous section underlined that the majority of weather-induced customer outages relates to wind. In most cases the windthrow of trees damages the grid infrastructure. Consequently, potential changes in the climatic conditions that determine a tree's exposure to windthrow-facilitating weather conditions influence the occurrence of future electricity grid outages.

The first part of this chapter introduces modeling approaches to quantify windthrow-related damages and discusses their advantages and disadvantages in the context of their application to climate model simulations (compare Sec. 3.1). In Sec. 3.2 an index capturing the meteorological conditions for windthrow is developed. Thereafter, it is investigated how windthrow is projected to change according to an ensemble of state-of-the-art RCM simulations of different scenario intensity (compare Sec. 3.4). The final section discusses the results and highlights conclusions that can be drawn from these findings (compare Sec. 3.5).

3.1 Introduction

The probability that a tree is overthrown by wind is determine by a variety of factors (compare Sec. 2.5). An experimental approach to estimate and regionally compare the stability of trees is realized through tree-pulling experiments. However, robust results require a very large sample size of experiments, comprising each possible combination of the relevant determinants (*Nicoll et al.*, 2006). For reasons of practicability and financial resources, experiments are usually limited to small-scale studies intending to investigate specific research questions (*Nicoll et al.*, 2006; *Kamimura et al.*, 2012).

Different approaches on how to determine windthrow resulting from extreme wind speeds have been proposed. Basically, it can be distinguish between methods that are based on absolute thresholds and relative thresholds of wind speeds. One of the simplest absolute-threshold-based approaches relies on the categories defined by *World Meteorological Organization (WMO)* (2011). According to these categories wind speeds of 24.5 to 28.4 m/s (10 Bft) bear the potential to uproot trees. Stronger wind speed is expected to lead to widespread storm damages, while trees are expected to withstand values below the given range. An approach purely based on an absolute threshold might be considered too simplified, since it only focuses on the exposure of trees to wind (neglecting other important climatic factors), and does not consider site- or species-specific predispositions to windthrow.

In general, approaches based on an absolute wind speed threshold do not take into account that a tree's stability also mirrors its long-term exposure to climatic conditions

and inter-tree competition (*Perera et al.*, 2015). Consequently, some researchers promote approaches based on relative instead of absolute wind speed thresholds (e.g. *Klaus et al.*, 2011). In addition, absolute approaches are not suitable for an application in the context of RCMs simulations of extreme wind events, since (i) the spread in the reproduction of extreme wind speeds can be very pronounced among different RCMs (*Outten* and *Esau*, 2013), and (ii) some RCMs underestimate extreme wind speeds compared to observations (*Rauthe et al.*, 2010). Consequently, the application of an index based on an absolute wind speed threshold is prone to distorted results.

Alternatively, storm loss models making use of a relative thresholds of wind speed have been suggested. They build upon the assumption that damage occurs, once a certain percentile value of historically observed extreme wind speed is exceeded. Moreover, these models commonly assume increased probabilities of windthrow the more the wind speed threshold is exceeded. Both characteristics are captured by storm loss models, as employed for example by *Jönsson et al.* (2013) or *Klawa* and *Ulbrich* (2003), who assume damage to cubicly increase with increasing wind speed. Accordingly, the function for storm losses L^i during a singular event i with wind speed v_i reads:

$$L^i \propto \left(\frac{v_i - v_{perc}}{v_{perc}} \right)^3 \text{ (for } v_i \geq v_{perc}), \tag{1}$$

with v_{perc} constituting a certain percentile value of maximum wind speed.

There are basically two arguments for the application of a cubic function (*Klawa* and *Ulbrich*, 2003): Firstly, energy density is proportional to the cube of the wind speed. Secondly, empirical evidence by insurance companies, showing that storm losses increase with the cube of the maximum wind speed. However, it remains to be proven that the second argument also holds in the context of windthrow of trees.

A related approach specifically addressing storm damages of trees is presented by *Lagergren et al.* (2012), whose model is designed for the application within a dynamic vegetation model: Storm losses are determined based on a damage function of the form as presented in Eq. 1. In addition, the vulnerability to windthrow (V) is included as a mathematical factor. Moreover, the factor $E^i_{\text{frozen soil}}$ reflecting the state of the soil (frozen or non-frozen soil) is included . Hence, the loss function reads:

$$L^i \propto V \cdot \left(\frac{v_i - v_{perc}}{v_{perc}} \right)^3 \cdot E^i_{\text{frozen soil}} \tag{2}$$

This approach is based on the logic that the severity of the impacts of extreme weather events strongly depends on the level of *exposure* and *vulnerability* (*Cardona et al.*, 2012). In the context of this dissertation, exposure refers to the extent a tree or forest is exposed to adverse weather conditions, while vulnerability refers to the predisposition of trees to

suffer from windthrow when impacted by an extreme weather event.

The latter approach considers the physical state of the soil (frozen or non-frozen), but does not include the implications of soil moisture on windthrow. *Braden et al.* (2013) propose a simplified index design to incorporate soil moisture: Windthrow is assumed to occur once a certain threshold of wind speed and soil moisture is exceeded simultaneously. For wind speed – in analogy to the latter index designs – the 99^{th} percentile of daily maximum wind speed (over a certain reference period) is chosen as a threshold. For soil moisture, the threshold is exceeded once the sum of winter precipitation (precipitation following October 1st) amounts to more than 150 mm. This design features the following disadvantages: (1) It does not incorporate damage increase with increasing wind speed once the threshold is exceeded; (2) The precipitation indicator for soil moisture is rather simplistic since regional differences in the ability of the soil to absorb water and infiltration or evaporation of precipitation are not considered; (3) This type of index design does not account for differences in the predisposition to windthrow of different tree species and different soil types. Nevertheless, it is one example, where soil moisture is included into an indicator to estimate the risk for windthrow under climate change.

Another approach includes soil moisture into the damage function based on a quantity named *relative extractable water*[4] (e.g. *Panferov et al.*, 2009, 2010). However, the authors state the lack of published data on a critical level of soil moisture in the context of windthrow of trees, being the reason why the authors make use of a threshold based on optimal water content. This model is applied in a coupled modeling approach of a turbulence model and a soil-vegetation-atmosphere-transfer model. In consequence, it requires many local information. Therefore, its application is usually limited to a small geographic domain where such information are available.

In summary, the preceding paragraphs highlighted that climatic conditions crucially determine the windthrow probability of trees. It was shown that storm loss functions based on relative thresholds of wind speed are superior to absolute approaches, especially in the context of climate model simulations. Approaches including soil moisture and soil temperature into the storm loss function were introduced and discussed.

[4]Relative extractable water refers to the amount of soil water available to the plant.

3.2 Methodology

Based on the approaches and findings of the literature introduced in the previous section, this section develops and refines a methodology to assess and compare windthrow probabilities. In order to investigate the conditions for windthrow under future climate conditions, this thesis makes use of regional climate simulations by regional climate models (RCMs). These models numerically solve differential equations, which describe the fundamental laws of nature, in a three-dimensional grid space. Due to its comparably high spatial resolution, the application of RCM-simulations is advantageous over resorting to general circulation model (GCM) simulations, in the sense that RCMs better resolve physical processes of relevance to the climate for a specific region – which is Germany in the context of this thesis.

In general, RCMs are forced by large-scale climate information and simulate the climate over a restricted area, the model domain. This procedure is referred to as dynamical downscaling (*Warner*, 2010). The forcing data are usually provided by a GCM or retrospective reanalysis data. Projections of future climate change are assessed with RCMs downscaling GCM output that was simulated under certain socio-economic greenhouse gas emission scenarios, so called representative concentration pathways (RCPs) (*Moss et al.*, 2010). In addition, historical climate simulations under historical greenhouse gas conditions are conducted to deduce climate change signals.

Future evolutions of climate conditions as simulated by climate models are subjected to uncertainty. These uncertainties can be assessed by considering the climate projections of an ensemble of simulations (*Knutti et al.*, 2009). To systematically investigate uncertainties, coordinated experiments have been designed to perform climate simulations under standardized and comparable conditions. As such, the European branch of the WCRP initiative CORDEX (EURO-CORDEX) was established. In this framework, multi-model simulation ensembles with regional focus on Europe are compiled (*Jacob et al.*, 2014; *Giorgi et al.*, 2009). Detailed information on the ensemble used in the context of this dissertation is provided in Sec. 3.3.

The outcomes of the climate simulations are required for the application of the windthrow index proposed in this section. However, the development of this indicator necessitates preliminary work on soil temperature and moisture, since both variables are not provided as standard model output from RCMs via the data portals of the ESGF.

To this end, in Subsec. 3.2.1 the methodology how soil temperatures were approximated from atmospheric temperatures is described. Based on precipitation and evaporation, Subsec. 3.2.2 elaborates on a proxy for the soil moisture content in those soil layers relevant for root anchorage. Thereafter, Subsec. 3.2.3 proposes a windthrow index, based on a measure indicating the exposure to adverse climate conditions, as well as a

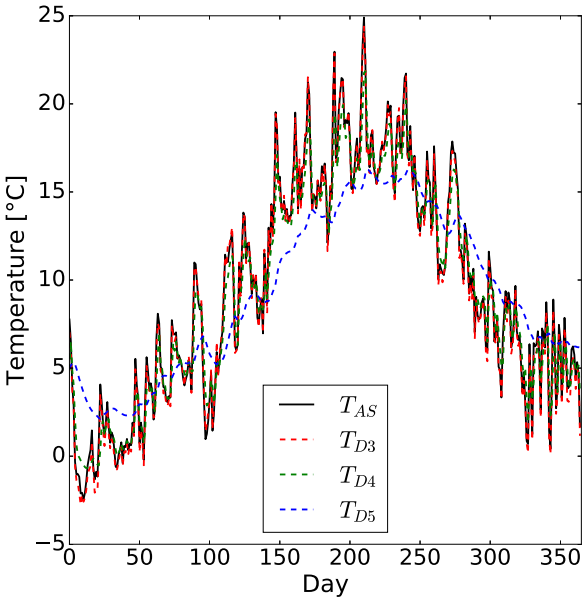

Figure 7: Atmospheric temperature (T_{AS}) and temperature of the three upper soil layers (T_{D3}, T_{D4}, T_{D5}) of the first realization of the historical run of GCM MPI-ESM downscaled with REMO2009. Model results are visualized for an arbitrary grid point (11.21°E, 51.44°N) during an arbitrary year (1990).

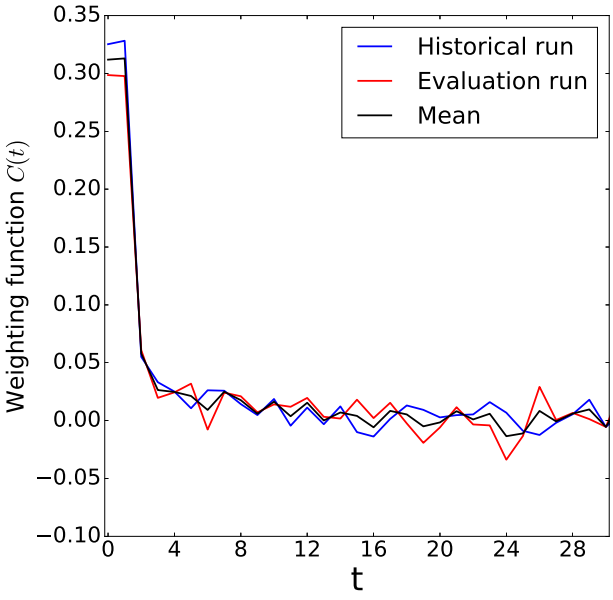

Figure 8: Weighting function C at an arbitrary grid point (11.21°E, 51.44°N), calculated for the *historical* run (blue) and the ERA-Interim driven *evaluation* run (red) based on atmospheric- and soil temperature for the period 1990-2015: The black line represents the mean of the two weighting functions.

measure indicating the vulnerability to windthrow. Finally, the suggested methodological approach is validated (compare Subsec. 3.2.4) and the applied robustness criterion is introduced (compare Subsec. 3.2.5).

3.2.1 Soil Temperature Proxy

As indicated, soil temperature data are not routinely available. To bypass this circumstance, RCM output of REMO (REgional MOdel) (*Jacob*, 2001; *Jacob* and *Podzun*, 1997) was used to establish a soil temperature proxy based on variables which are consistently available for all RCM simulations over the EURO-CORDEX domain. The validity of this approach builds upon the assumptions that, firstly, a proxy that correctly represents the soil temperature at a certain depth in REMO also correctly reproduces the soil temperature in another climate model, and secondly, that REMO correctly follows the physical processes that drive soil temperature.

In REMO, the soil is implemented as a five layer scheme; their thickness from top to bottom are 0.065m (D3), 0.254m (D4), 0.913m (D5), 2.902m (D), 5.700m (DCL) (*Kotlarski*, 2007). Fig. 7 illustrates the relationship between atmospheric temperature (T_{AS})

and the three upper soil layers (T_{D3}, T_{D4}, T_{D5}) for an arbitrarily chosen grid point. It can be seen that the most upper soil layer (T_{D3}) closely reproduces the atmospheric temperature signal close to the surface (T_{AS}), while the temperature of the lower layer (T_{D5}) features a much lower degree of variability and temporally lags behind the atmospheric signal. Since the upper 60 cm of soil are considered as the most important for root stability (*Peltola et al.*, 1999b), this work regards the state of the second soil layer (T_{D4}) as the one which determines root stability. Therefore, the proposed temperature proxy is calibrated to follow the temperature signal of this soil layer.

The temperature of a soil is determined by heat fluxes from its neighboring soil layers. Heat fluxes in the soil are guided by two soil properties, thermal conductivity and heat capacity (*Liang et al.*, 2014). The thermal conductivity refers to the ability of the soil to conduct heat. The heat capacity determines how much the soil temperature changes if a certain amount of heat is added. Both parameters, heat capacity and heat conductivity, significantly depend on soil moisture (*Abu-Hamdeh*, 2003): A higher water content increases the soil layer's heat capacity as well as the thermal conductivity. The ESGF, however, provides data on the soil water content only for the whole soil column and not for all simulations contained in the investigated ensembles of climate simulations (compare Subsec. 3.3.1). Hence, no specific information on the water content in the upper soil layer is available. Therefore, the suggested soil temperature proxy is based on atmospheric temperature only.

The proxy relies on a simple model that predicts the soil temperature from air temperatures, as proposed by *Hasfurther et al.* (1972): The authors deduce soil temperature based on the convolution of a weighting function ($C(t)$) and the atmospheric temperature records ($T_{\mathrm{atm}}(t)$) during the days prior to the day whose soil temperature is to be determined. Written in its integral form,

$$T_{\mathrm{soil}}(t) = \int_{-\infty}^{0} C(\tau) \cdot T_{\mathrm{atm}}(t-\tau)\, d\tau \tag{3}$$

it illustrates that the weighting function serves as a mechanism to linearly relate the soil temperature at time t to the atmospheric temperature records during the previous days. *Hasfurther et al.* (1972) show that the function $C(t)$ can be calculated by performing a fourier transformation (FT) on Eq. 3, followed by a rearrangement of the products and an inverse FT. When $F(\cdot)$ represents the FT, and $F^{-1}(\cdot)$ the inverse FT of the quantity in brackets, the weighting function can be calculated from:

$$C(t) = F^{-1}\left(\frac{F\left(T_{\mathrm{soil}}(t)\right)}{F\left(T_{\mathrm{atm}}(t)\right)}\right) \tag{4}$$

Based on this equation and on the time series of soil temperature and atmospheric

temperature for the *historical* run and the *evaluation* run[5] conducted with REMO2009, the weighting function $C(t)$ was calculated individually at each grid point over the EURO-CORDEX domain. The FT and inverse FT were numerically solved with NumPy, a fundamental package for scientific computing with Python that uses the efficient Fast Fourier Transform algorithm (*The SciPy Community*, 2018). By substituting the results for C into Eq. 3, the soil temperature proxy $T_{\mathrm{soil}}(t)$ can be calculated at any given time t from the time series of atmospheric temperature.

Fig. 8 illustrates the results for C at an arbitrary grid point indicating the soil temperature at time t to be predominantly described by the atmospheric temperature of the same day ($t = 0$) and the previous day ($t = 1$). The weight of the atmospheric temperature during the previous days ($t \geq 1$) is substantially less. It is worth to note, that the quantitative shape of the weighting function C is not unique to the chosen grid point, but can be observed over the entire domain (not shown).

How realistic is the soil temperature proxy to represent „real-world“ soil temperature? The analysis conducted in Appendix A.2 shows that the weighting function derived from the *historical* simulation can also be applied to determine the soil temperature of the *evaluation* simulation based on the *evaluation's* atmospheric temperature, and vice versa. This indicates that the mean of the two weighting functions calculated for each of the two simulations can be applied to any other REgional MOdel (REMO) simulation, under the assumptions listed above.

3.2.2 Soil Moisture Proxy

As true for the soil temperature, the climate data library of the ESGF does not provide a variable which reflects the soil moisture content in the individual soil layers; only data on the vertically integrated soil moisture content over the whole soil column is available (*Knist et al.*, 2017). The latter does not constitute a meaningful quantity in the context of this research, since in praticular the soil layer of 0 to 60 cm is considered most important for root anchorage (*Peltola et al.*, 1999a).

For these reasons, a proxy indicator for changes in the soil moisture content in the upper soil layer was developed. Due to the fact that soil moisture content in the layer which is relevant for root anchorage is especially governed by heavy rainfall events during or prior to storm events (*Usbeck et al.*, 2010), the water added to and withdrawn from the soil during the period prior to an extreme wind event is suggested as a reasonable

[5]The *historical* run refers to RCM simulations that are forced with the climate conditions simulated by a GCM for the period 1950 to 2005. These runs are initiated from an arbitrary state of a quasi-equilibrium control run, and will, therefore, only by chance match “really“ observed individual climate events. The *evaluation* run refers to RCM simulations that are forced by ERA-Interim reanalysis data over a historic period (often 1989 to 2008).

heuristic indicator. In a sense, this represents an expansion of the discussed concept by *Braden et al.* (2013), who use the total winter precipitation as an indicator for extreme soil moisture.

To bypass the problem of data-availability, a relationship between the soil moisture of the mesoscale Hydrologic Model (mHM) (*Samaniego et al.*, 2010; *Kumar et al.*, 2013) and the precipitation-evaporation difference is established. The mHM is characterized by two soil layers: One from 0 to 30 cm, and another from 30 to 180 cm soil depth. Since the upper 60 cm of soil are considered most important for root anchorage (*Peltola et al.*, 1999a), the relationship was established for the soil water saturation of the upper-most model soil layer, acknowledging, that the layer depth does not represent the full soil depth of importance. The relationship was calculated based on the period 1970 to 1999.

In order to establish the proxy relationship for its application for the EURO-CORDEX grid, the spatially higher-resolved mHM data was interpolated onto the coarser EURO-CORDEX grid (from ~4 km spatial resolution to ~12.5 km resolution). Thereafter, the same methodology as applied for the calculation of the soil temperature proxy was employed (compare Subsec. 3.2.1). Based on the assumption of a relationship between soil moisture and the water added to or withdrawn from the soil, it is assumed that the relative moisture content of the soil, $m(t)$, is based on the convolution of a weighting function, $D(t)$, and the water added or withdrawn from the soil W. In its integral form this reads:

$$M(t) = \int_{-\infty}^{0} D(\tau) \cdot W(t - \tau)\, d\tau \tag{5}$$

In analogy to Eq. 3, D represents a weighting function that linearly relates the moisture at time t to the water added to the system in the time steps $\tau \leq t$. Also in this case, D is calculated with the help of a fourier transformation (FT) of the moisture and water time series and its inverse:

$$D(t) = F^{-1}\left(\frac{F\left(M(t)\right)}{F\left(W(t)\right)}\right) \tag{6}$$

Based on this equation and on the time series of precipitation, evaporation and water saturation of soil for the period from 1980 to 2010, $D(t)$ was calculated individually for each grid point. Again, the FT and inverse FT were numerically solved with NumPy (*The SciPy Community*, 2018).

The weighting function $D(t)$ was calculated individually at each grid point over the EURO-CORDEX domain. Fig. 8 illustrates the results of D at two arbitrary grid points, and shows the soil temperature at time t to be predominantly described by the

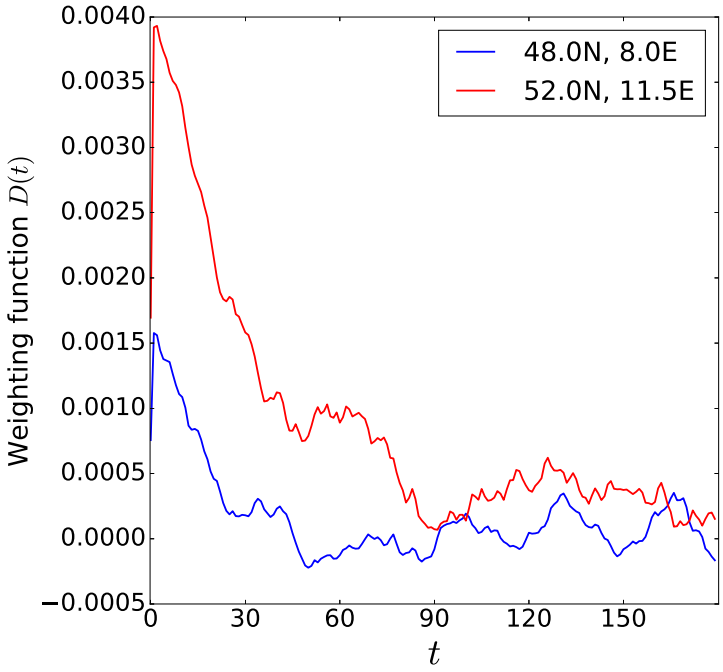

Figure 9: Weighting function $D(t)$ at two arbitrary grid points that relates the moisture at time t_1 to the water added to the system in the time steps$t < t_1$.

precipitation-evaporation-difference during the last 30 to 60 days. The weight of the atmospheric temperature during the days before is significantly less. It is worth to note, that the quantitative shape of the weighting function $D(t)$ is not unique to the chosen grid points, but can be observed over the entire domain. Therefore, for the calculation of the weighting function the precipitation-evaporation difference during the 180 days before the day for which the soil moisture proxy is to be determined was considered ($t \leq 180$). By substituting the results for D in Eq. 5, the water saturation of soil, $M(t)$, can be calculated at any given time t.

How realistic is the soil moisture proxy representing actual soil moisture? The soil moisture proxy is based on the correlation between the past precipitation-evaporation-difference, and present soil moisture content. In order to assess the quality of this technique, the proxy's skill to correctly reproduce soil moisture is analyzed in Appendix A.3. The analysis indicates that the proxy's skill to reproduce soil moisture varies regionally.

3.2.3 Design of the Windthrow Index

Windthrow losses are often expressed as the mathematical product of predisposition and exposure in the given context (compare Sec. 3.1). Hence, in analogy to the wind damage function proposed by *Lagergren et al.* (2012), the risk index I_i for windthrow during an event i is calculated from the exposure to adverse climatic conditions E^i and the

predisposition to windthrow at the very location P:

$$I_i = P \cdot (E^i_{\text{wind}} \cdot E^i_{\text{soil moisture}} \cdot E^i_{\text{soil temperature}}) \tag{7}$$

It needs to stressed that the index design does not account for certain crucial windthrow-determining variables (such as tree height), since losses also strongly depend on site-specific efforts to prevent losses and other human interventions (*Jönsson et al.*, 2013). These could for example be guided by many factors such as personal preferences, wood prices, legislation, economic considerations etc., and cannot be projected in the context of a climate model simulation. Instead, more general factors that do not depend on human preferences or managing methods are considered in the design of the windthrow index. In this regard, the index is not meant to evaluate whether a certain climatic condition actually leads to windthrow, but enables a comparison for the climatic conditions of windthrow.

Based on the literature study conducted in Sec. 3.1, the following paragraphs, firstly, refine how the individual climate variables (wind, soil moisture, soil temperature) contribute to the exposure, and secondly, illustrate how the predisposition to windthrow for application in Eq. 7 is quantified.

Exposure

In Eq. 7 the contribution of the climatic conditions to exposure is treated as the product of the individual contributions of wind speed, soil moisture and soil state during the event. With respect to **wind speed**, this thesis resorts to an approach, which models windthrow to increase cubicly beyond a relative windspeed threshold (in accordance with *Jönsson et al.* (2013) and *Lagergren et al.* (2012)):

$$E^i_{\text{wind}} = \left(\frac{v_i - v_{98}}{v_{98}}\right)^3 \tag{8}$$

The physical **state of the soil moisture** (frozen or non-frozen) has substantial influence on soil stability. Storm damage has been modeled to decrease by 30% during frozen soil conditions (*Lagergren et al.*, 2012). To reflect the fact, that storm damages are already reduced when the soil layer is partially frozen, a decrease of the exposure was implemented already between 0 and 1°C, assuming that this is the regime where parts of the upper soil are already frozen. In this regard, $E^i_{\text{soil temperature}}$ reads:

$$E^i_{\text{soil temperature}} = \begin{cases} 1 & \text{if } T^i_{soil} > 1°\text{C} \\ 0.7 + 0.3 \cdot T^i_{soil} & \text{if } 0°\text{C} < T^i_{soil} \leq 1°\text{C} \\ 0.7 & \text{if } T^i_{soil} \leq 0°\text{C} \end{cases} \tag{9}$$

Studies that determine the quantitative effects of soil moisture on the predisposition of trees to windthrow are rare (*Schindler et al.*, 2012). As indicated, no published data on a critical level of soil moisture, beyond which the predisposition of a tree to windthrow increases, exist (*Panferov et al.*, 2009, 2010). Therefore, studies taking soil moisture into account commonly apply rather arbitrary threshold values beyond which an impact on the predisposition to windthrow is assumed[6].

The soil moisture quantity considered in this dissertation is the water saturation of soil, ranging from 0 to 1 (compare Subsec. 3.2.2). In the absence of reliable research indicating a critical threshold of soil moisture, this thesis assumes windthrow damages to increase once a value of 0.6 is exceeded (in accordance with *Panferov et al.* (2009, 2010)).

Following *Kamimura et al.* (2012), one can deduce that the turning moment needed to overturn a tree can be more than halved by increasing the water content below the root plate. Therefore, this work assumes the moisture related exposure to not impact the total exposure below the chosen moisture threshold of $m_i \leq 0.6$, and to double the total exposure if $m_i = 1$. In analogy to *Panferov et al.* (2009, 2010), it is assumed that the total exposure increases linearly in between. Hence, the moisture related exposure reads:

$$E^i_{\text{moisture}} = \begin{cases} 1 & \text{if } m_i \leq 0.6 \\ 1 + \frac{m_i - 0.6}{0.4} & \text{if } m_i > 0.6 \end{cases} \tag{10}$$

Predisposition to Windthrow

In the context of this dissertation, the predisposition to windthrow is assumed to be determined by the site-specific characteristics *tree species*, *soil type* and *soil depth*. This paragraph elaborates on how these characteristics contribute to the determination of tree, soil type- and soil depth-specific vulnerability coefficients. The reason to neglect any other parameters (e.g. tree height) is that these significantly depend on the applied forest management and other human interventions, which can be driven by many factors such as personal preferences, wood prices, legislation or economic considerations and cannot be projected for the timescales considered in the context of a climate model simulation.

The predisposition-guiding factors – tree species, soil depth and soil type – cannot be discussed in an isolated manner, since the stability of a tree is not a linear function of these influencing variables, but depends on interactions between those. Nevertheless, the following paragraphs describe the effects of these variables individually, but highlight correlations to the other variables.

[6]The authors of *Panferov et al.* (2009, 2010) for example assume that damages occur beyond 0.6 of the relative extractable soil water; *Braden et al.* (2013) for example assume that damages occur beyond a winter precipitation sum (defined as precipitation after October 1st) above 150mm.

Different tree species have different genospecific characteristics, such as a specific root- and crown architecture or wood stability. Coniferous trees are characterized by a design that is more prone to windthrow than deciduous trees, as shown by several studies (*Dobbertin*, 2002; *Kropp et al.*, 2009; *Lanquaye*, 2003). During the winter storms Vivian (in February 1990) and Lothar (in December 1999), pure conifer stand and stands with more than 50% of coniferous trees were observed to be more likely damaged than others (*Dobbertin*, 2002). This was confirmed by *Schmidt et al.* (2005), who investigated the likelihood of windthrow of different tree species during Lothar. However, anchorage comparisons among species are not trivial, due to correlation to physical soil properties (*Nicoll et al.*, 2006).

The soil type is very important for tree stability under wind loads (*Dobbertin*, 2002). Its mechanical characteristics significantly influence the stability of the root plate within the soil, and set the boundary conditions for genospecific root development. These characteristics vary among soil types and can be very species dependant. For Sitka spruce, for example, tree-pulling experiments have shown 50% higher rates of windthrow for trees growing on deep peats than for trees growing on gleyed mineral soils (*Nicoll et al.*, 2006).

Most studies[7] find increased windthrow rates on soils that allow only for comparably low rooting depths (*Dobbertin*, 2002). *Nicoll et al.* (2006) found the uprooting of spruces to require 10 to 15% higher forces if the rootable soil depth amounts to more than 80 cm compared to spruces growing on a rootable soil depth below 80 cm. The rootable depth can be restricted by either solid rock or a permanent high standing water table. On shallow rootable soil depth (i.e. < 80cm), spruces commonly develop a shallow plate-like rooting system (*Mitscherlich*, 1981), which is more prone to uprooting. In order to account for the differences in the predisposition to windthrow due to species, this work relies on existing literature. *Lagergren et al.* (2012) quantitatively specify how vulnerable the trees in a cohort are to wind, neglecting factors such as other trees, patches or topography. The authors suggest species-dependent vulnerability coefficient of 1.0 for Norway spruce, 0.5 for Scots pine and 0.1 for the remaining species. These constants indicate that the vulnerability of Scots pines amounts half the vulnerability of Norway spruces. In order to disentangle the tree category *remaining species*, this thesis relies on the findings of *Kohnle* and *Gauckler* (2003), who have analyzed the vulnerability for beech, oak and other deciduous tree species by analyzing storm damages of the 1999 storm Lothar in the South-West of Germany. The study concludes a vulnerability of 16%, 20% and 6% of the

[7]Some studies identified positive correlations between soil depth and windthrow probability (e.g. *König*, 1995; *Dobbertin*, 2002). *König* (1995) argued this observation is probably due to the fact that deep soils are commonly found on soils with high clay content. High levels of precipitation prior to the occurrence of extreme wind speeds have the potential to significantly reduce the rooting stability on these cohesive soils. Therefore, a positive correlation between windthrow and soil depth in these studies is probably the result of multicolinearity of the independent variables (*König*, 1995).

Species	Soil type	Soil depth		Species Share
		<0.8m	>0.8m	
Spruce	A	1.06	0.91	25.4%
	B	1.17	1.04	
	C	1.09	0.95	
	D	0.97	0.80	
Pine	A	0.49	0.51	22.3%
	B/C/D	0.50	0.50	
Beech	A/B/C/D	0.16		15.4%
Oak	A/B/C/D	0.20		10.4%
Other	A/B/C/D	0.06		

Table 1: Determined vulnerability coefficients of different tree species depending on soil depth and soil type (A: freely draining mineral soils, B: gleyed mineral soils, C: peaty mineral soils, D: deep peats) and the share of the respective tree species in Germany (*Thünen Institut*, 2012)

respective tree species in comparison to Norway spruce.

These results provide a general intuition about vulnerability differences between different species. To further account for soil depth and soil type, this work makes use of species- and soil-specific anchorage coefficients as employed in ForestGALES (*Forestry Commission* and *Forest Research*, 2015), a hybrid mechanistic-empirical model for windthrow. For the purpose of this model, anchorage coefficients are determined for different soil depths, soil types and tree species, based on a database of tree-anchorage measurements compiled by *Nicoll et al.* (2006): Here, the product of the anchorage coefficients (c) and the weight of the bole of the tree (m) determines the critical turning moment for overturning of a tree: $M_{crit} = c \cdot m$ (*Forestry Commission* and *Forest Research*, 2015).

It is not meaningful to deduce vulnerabilities of different tree species by comparing their assigned anchorage coefficients within the ForestGALES model, since the weight of the tree's bole (m) is determined by species-specific properties, such as typical diameters and tree heights. Nevertheless, the soil depth- and soil type-dependent coefficients can be exploited to estimate deviations from the purely species-dependent vulnerability coefficients as deduced by *Kohnle* and *Gauckler* (2003) and *Lagergren et al.* (2012). Appendix A.1 illustrates how their work enables to determine vulnerability coefficients with respect to two different soil depths ($< 0.8\,m$, $> 0.8\,m$) and four different soil types (A: freely draining mineral soils, B: gleyed mineral soils, C: peaty mineral soils, D: deep peats).

The soil type- and soil depth-specific vulnerability coefficients for the five species categories *spruce, pine, beech, oak* and *other* are shown in Tab. 1. Please note that the four considered species sum up to almost 75% of the forest area in Germany (compare Tab. 1) and include those species most vulnerable to windthrow.

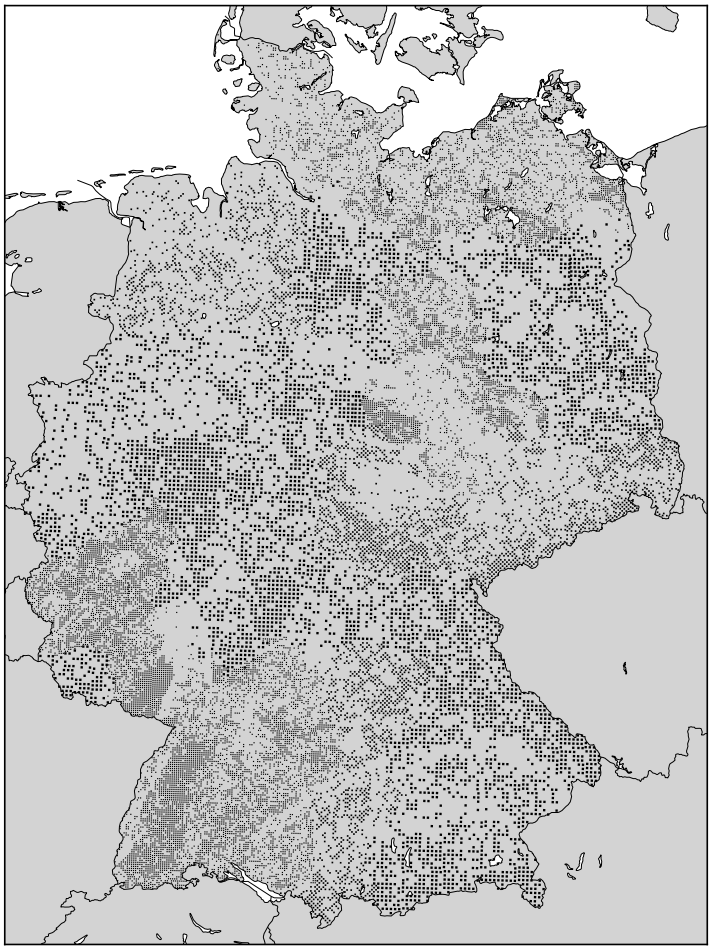

Figure 10: Resolution of latest Federal Tree Inventory (*Thünen Institut*, 2012). The applied grid has a resolution of at least 4 km x 4 km; in some federal states the grid is characterized by higher spatial resolutions.

It needs to be emphasized that the influence of differences in the rootable soil depth and soil type on vulnerability can only be included for the two coniferous species, spruce and pine, since the literature on tree-pulling experiments provide coefficients for coniferous trees only (*Forestry Commission* and *Forest Research*, 2015). Since coniferous trees are significantly more vulnerable to windthrow and dominate almost 50% of the German forest area (compare Tab. 1), this limitation is not assumed to have a pronounced influence on the results.

Finally, an average predisposition to windthrow was calculated at the spatial resolution of at least 4 x 4 km resolution, triggered by the resolution of the Federal Tree Inventory (compare Fig. 10), which is containing spatial information on the shares of tree species (*Thünen Institut*, 2012). Thus, the predisposition to windthrow P in a domain i was calculated based on the share $\lambda_i(\sigma)$ of each species σ, and the respective depth- (δ) and soil-type- (τ) dependent predisposition $p(\sigma, \tau, \delta)$:

$$P^i = \sum_{\sigma} \lambda_i(\sigma) \cdot p(\sigma, \tau_i, \delta_i)$$

3.2.4 Validation

Before applying the suggested methodology, its validity is to be investigated. In order to quantify how realistic the index represents actual conditions for windthrow, it is to be investigated whether the index based on the ensemble of RCM simulations matches with an index based on observational data. To this end, a comparison to ERA-Interim reanalysis was conducted. Moreover, it is to be tested whether the suggested windthrow index is able to capture the likelihood of windthrow of observed individual historical windthrow events. In this regard, the windthrow index was tested against observed damage during winter storm Kyrill.

How realistic is the index representing actual conditions for windthrow? In Fig. 11 the results of the calculated windthrow index for the median of the EURO-CORDEX ensemble of the historical reference simulation (23 member, compare Sec. 3.3) are compared to the calculated windthrow index based on ERA-Interim. The comparison quantifies how well the simulated climate matches with observed conditions for windthrow: It can be observed that both indices substantially differ. The following paragraphs illustrate that the previous observation relates to the differences of the upper (low probability) tails of the wind speed probability distribution of the reanalysis data and the climate simulation ensemble.

The windthrow index is largely determined by the wind climate, as only those events feed into the calculation which exceed the 98$^{\text{th}}$ percentile of historical wind speed[8]. Therefore, the exposure to adverse wind conditions

$$E_{\text{wind}} = \sum_{i} \left((v_i - v_{98}) / v_{98} \right)^3 \forall v_i > v_{98}$$

between the historical simulation of the EURO-CORDEX simulation ensemble and ERA-Interim was compared. Fig. 12 illustrates pronounced deviations between the EURO-CORDEX simulation ensemble and ERA-Interim. In most parts of Southern Germany, the simulation ensemble substantially underestimates the exposure to adverse wind conditions, while in most parts of Northern Germany, the ensemble substantially overestimates the exposure to adverse wind conditions. The reason for these differences relates to the formulation of exposure in the index design, which is substantially influenced by events of very low probability. For the illustration of this argument, the probability distribution

[8]Note that the differences between the indices are primarily due to the exposure to adverse climatic conditions E, since the predisposition P is identical for both index calculations.

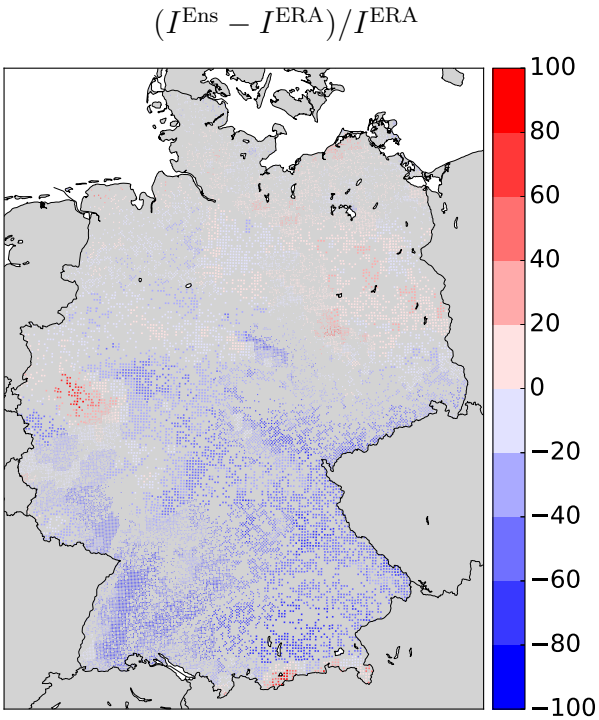

Figure 11: Relative difference of the windthrow index (I, compare Eq. 7) between the median of the EURO-CORDEX ensemble (I^{Ens}) and ERA-Interim (I^{ERA}): $(I^{\mathrm{Ens}} - I^{\mathrm{ERA}})/I^{\mathrm{ERA}}$. The index resolution is determined by the resolution of the predisposition to windthrow (compare Fig. 10).

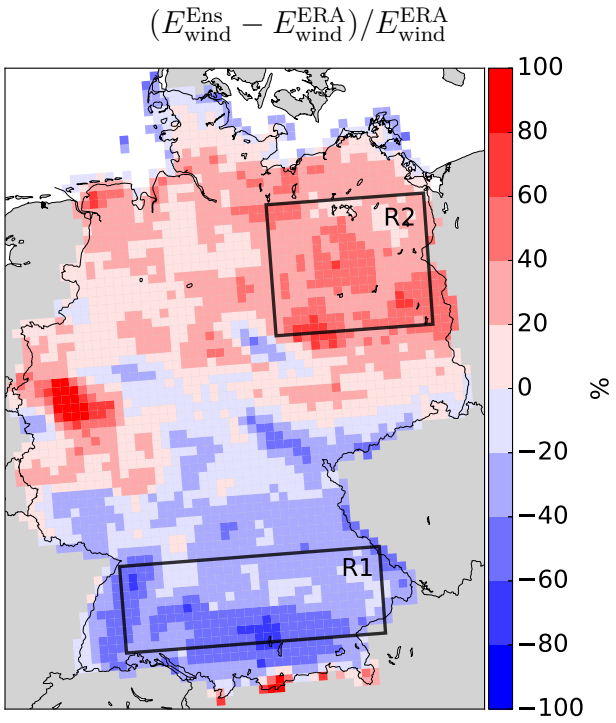

Figure 12: Relative difference of the exposure to adverse wind conditions (E_{wind}, compare Eq. 8) between the median of the EURO-CORDEX ensemble ($E^{\mathrm{Ens}}_{\mathrm{wind}}$) and ERA-Interim ($E^{\mathrm{ERA}}_{\mathrm{wind}}$). Detailed information on the ensemble is provided in Tab. 2.

($P(\Delta v)$) of wind speeds exceeding the 98th percentile of maximum daily wind speeds ($\Delta v = (v - v_{98})/v_{98}$) for two chosen case study areas (R1 and R2; highlighted in Fig. 12) are compared (Fig. 13). At first sight, the two probability distribution of the two areas (R1 and R2) do not substantially deviate from each other and appear to behave according to typical extreme value distributions (such as the Poisson distribution). However, the tails (compare zooms in the upper sub-figures of Fig. 13) reveal decisive differences. The lower sub-figures of Fig. 13 illustrate that these differences in the upper tails of the probability distribution exert substantial influence on the exposure due to its cubic shape ($E_{\mathrm{wind}} = (\Delta v)^3 \cdot P(\Delta v)$), and, thus, cause the observed differences in the exposure between ERA-Interim and the ensemble. In case of the area R1, the deviations in the upper tails lead to a windthrow index value of the reanalysis data which is substantially higher than the ensemble's index, while for area R2 the opposite is the case.

The conducted analysis illustrates that single events of extraordinary strong wind speeds bear the potential to dominate the outcomes of the index calculation. This is

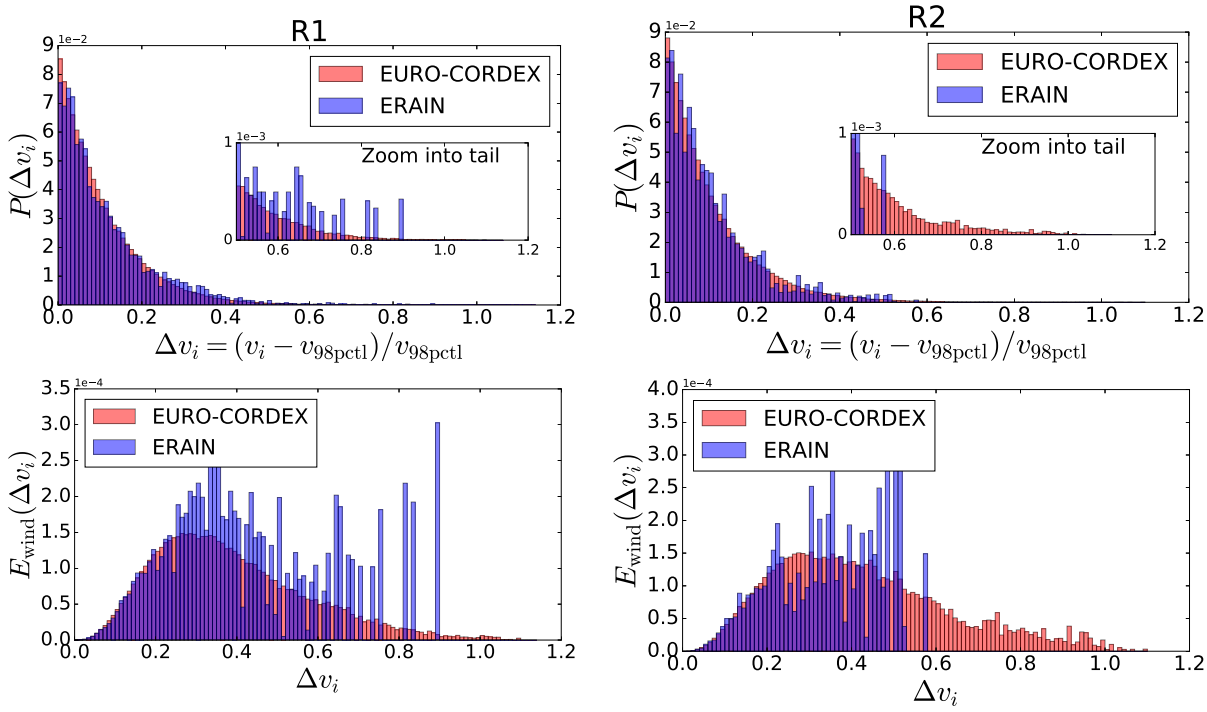

Figure 13: Explanation on the differences between the exposure to adverse climatic conditions based on the EURO-CORDEX simulation ensemble (detailed information can be found in Tab. 2) and ERA-Interim in the two case areas R1 and R2 (compare Fig. 12). Top figures show the probability distribution beyond 98th percentile of wind speeds. The bottom figures show the related exposure (E_{wind}). The graphs illustrate that small deviations in the upper tails of the probability distributions can substantially affect exposure.

even the case when a period of 30 years – typically considered as being representative for climatic conditions (*World Meteorological Organization (WMO)*, 2019) – is considered. This is due to the fact that even during such long-terms period some regions can experience an extreme wind event with a return periods of more than 30 years, while others do not. It needs to be stressed that the ensemble comprises 23 different simulations of the *historical* climate, which means that each individual simulation is representative for the historical climate conditions but are not forced by any actually observed historical climate data. Hence, during the 30 year simulation period, some simulations experience wind events with return periods beyond 30 years, while others do not. Therefore, the windthrow index of the EURO-CORDEX simulation ensemble is based on a smoother probability distribution in the upper (low probability) tail compared to the ERA-Interim based index.

In consequence, it remains unclear whether the period analyzed by the ERA-Interim data simply experiences an overproportional high occurrence of events of high return periods in case study area R2, and an overproportional low occurrence in R1, or if the ensemble fails to correctly simulate historical extreme wind statistics. Overall, the observed differences of the windthrow indices aggravates an interpretation of considering

the ensemble median of the historical scenario as representative for observed historical climate conditions (with respect to extreme wind statistics).

Is the suggested windthrow index able to capture the probability of windthrow occurrences of observed individual historical windthrow events?

Validating whether a windthrow index correctly reproduces tree damages occurring during specific climatic events is inherently difficult, as it requires a variety of information: (a) comprehensive surveys on the damage, (b) data on the prevailing climatic conditions, and (c) knowledge on the characteristics of the forest during the event (*Hale et al.*, 2015). Such information are only seldom or insufficiently accessible. Validating the proposed index is even more difficult, since information being crucial for windthrow risk (e.g. tree height or forest management schemes) are not included in the index design due to the fact that such information are neither available nor are potential future changes predictable. The index can rather be interpreted as an indicator for windthrow-facilitating conditions.

Despite these difficulties, the capability of the developed index was tested against the windthrow documented during winter storm Kyrill (occurring in January 2007). Windthrow during Kyrill was comprehensively documented for selected geographical areas in North Rhine-Westphalia (*Franken et al.*, 2013). The prevailing weather conditions during the storm can be deduced from meteorological observations. The forest inventory (*Thünen Institut*, 2012) adds information on the characteristics of the forest (with respect to the tree species).

Based on these information, the windthrow index was determined for January 18th, 2007 (the day when the majority of windthrow damage occurred during Kyrill), in order to validate the actually observed windthrow to the windthrow conditions according to the windthrow index. The index was calculated based on three RCM simulations dynamically downscaling the ERA-Interim reanalysis (compare Figs. 14 a-c). Only for these three RCM simulations the four necessary climate variables are accessible through the ESGF for a period of at least 30 years (which is required to deduce the 98th percentile of maximum daily wind speeds).

Figs. 14 (a-c) illustrate that the calculated windthrow index largely overlaps with the areas for which damages have been documented in the course of Kyrill in North Rhine-Westphalia. However, the RCA4 simulation reproduces a comparably weak index signal. In addition to the damages in North Rhine-Westphalia, the windthrow indices calculated based on REMO and RACMO indicate windthrow of almost similar severity as in North Rhine-Westphalia for also other parts of Germany, such as the Harz, the Thuringian Forest, Saxony-Anhalt, Saxony and the Bavarian Forest. Since no comprehensive documentation of windthrow were conducted for these areas, it is difficult to evaluate whether the index outcome for these areas reflects the conditions for windthrow

during Kyrill. However, news reports on the occurrence of electricity grid interruptions in these regions indicate the occurrence of windthrow also in these regions: 150,000 customers were affected by windthrow-induced grid interruptions in Brandenburg, Saxony and Saxony-Anhalt (*N-tv*, 2007); further outages of unspecified scale occurred in Bavaria (*Leuschner*, 2007), and the Thuringian Forest (*Süddeutsche Zeitung*, 2010). However, as damages have not been documented by authorities and media coverage has been less comprehensive, it is reasonable to assume that windthrow in these regions was less pronounced than in North-Rhine Westphalia.

In this context, it needs to be recalled that the index is not designed to reproduce damage, but to capture the likelihood for damage under identical boundary conditions (i.e. that the same management techniques were applied and the same tree heights prevailed). Further, deviations of the calculated index from observed windthrow could also relate to the fact that a dynamical downscaling of ERA-Interim does not necessarily reproduce the same dynamics as observed.

Despite these limitations, the illustrated results indicate that the proposed windthrow index has the potential to correctly reproduce windthrow damage. For a more refined validation, it would be helpful to compare the index to other storm events with documented damages. However, due to data availability this is currently out of the scope of this thesis.

3.2.5 Robustness test

For each of the two EURO-CORDEX simulation ensembles (RCP4.5 and RCP8.5), the median climate signal of the windthrow index was determined. Choosing median instead of mean values ensures outliers to not impact the results too strongly. The robustness of this climate change signal was tested with a two-step robustness test (*Pfeifer et al.*, 2015; *Jacob et al.*, 2014; *Tobin et al.*, 2014). Accordingly, robustness is defined as a combination of model agreement and the significance of the individual projections, as further elaborated on in the next paragraph.

Firstly, the model agreement is tested by checking whether a certain specified number of climate projections of the ensemble members agree on the direction of the climate signal. In the context of (small) climate model simulation ensembles a threshold of 66% of the simulations is commonly employed (*Pfeifer et al.*, 2015; *Jacob et al.*, 2014; *Tobin et al.*, 2014). This – in comparison to other disciplines – relatively low threshold criterion relates to the small number of ensemble members, as already the deviation of a few simulations causes test failure in case a more strict threshold was applied (*Pfeifer et al.*, 2015). Secondly, the climate change signal of every ensemble member is tested for significance by applying the so-called U-test, often also referred to as *Wilcoxon-Mann-Whitney* test

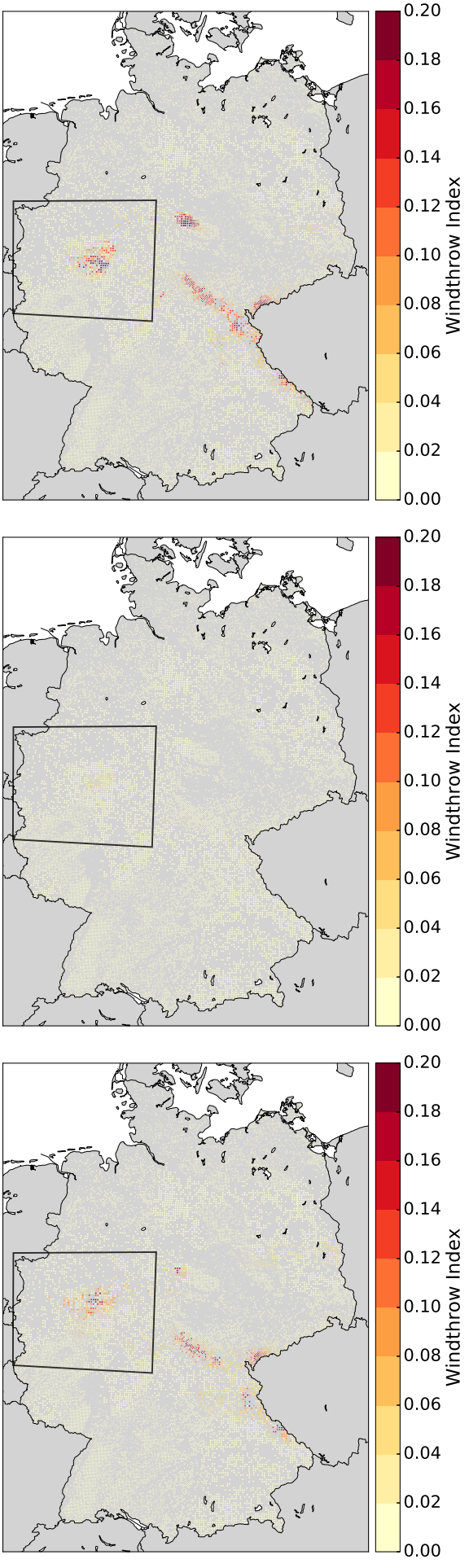

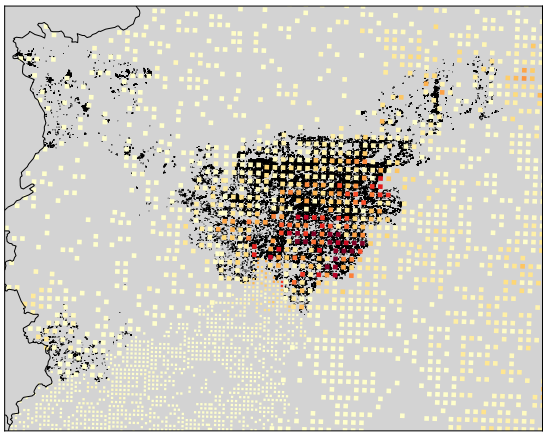

(a) Windthrow index based on RACMO22E downcaling of ERA-Interim: Germany (left) and zoomed into Kyrill hot spot (right) on January 18th, 2007.

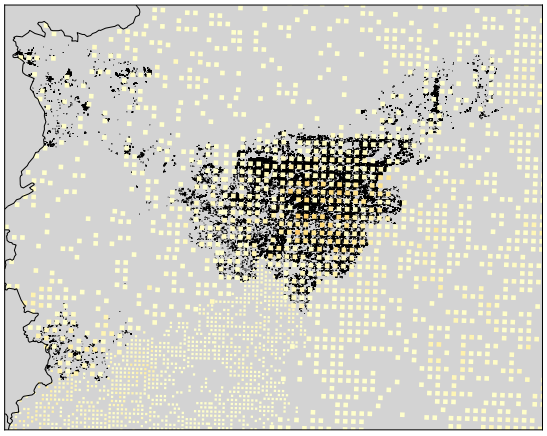

(b) Windthrow index based on RCA4 downcaling of ERA-Interim: Germany (left) and zoomed into Kyrill hot spot (right) on January 18th, 2007.

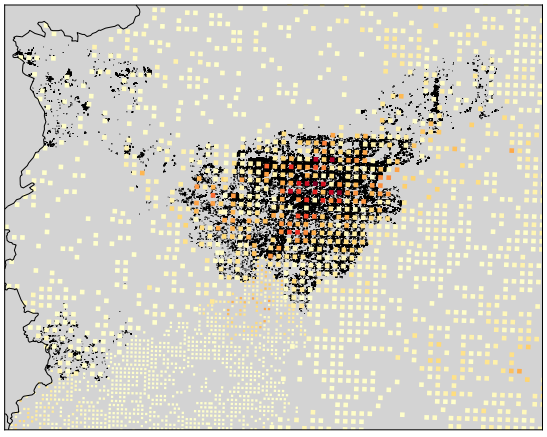

(c) Windthrow index based on REMO2009 downcaling of ERA-Interim: Germany (left) and zoomed into Kyrill hot spot (right) on January 18th, 2007.

Figure 14: Documented windthrow during winter storm Kyrill (black) versus the results of the windthrow index calculation based on three different RCMs forced by ERA-Interim.

(*Pfeifer et al.*, 2015). This statistical test checks, whether two samples are either drawn from the same population, or significantly deviate from one another (*Mann* and *Whitney*, 1947). In analogy to *Pfeifer et al.* (2015) and *Jacob et al.* (2014), a significance level of 85% was used.

Hence, in this work a climate change signal is considered robust, when 66% of the ensemble members agree on the direction of change with a significance level of 85%. With respect to robustness, two issues need to be considered: Firstly, significance levels of a climate change signal between a mid-21st century period (2040 to 2069) and a historical period (1970 to 1999) are in general smaller in comparison to analyses that investigate periods at the end of the 21st century. The robustness tests conducted by *Pfeifer et al.* (2015) for example illustrate (for the specific case of the 95th percentile of daily winter precipitation) that only in a few regions a robust climate signal is identified for the period 2031 to 2060, while – in contrast – robustness is determined over a majority of regions in a later period (2061 to 2090). Secondly, it needs to be mentioned that this thesis investigates climate extremes, which – by definition – occurr rather seldom: In the proposed windthrow index design only events beyond the 98th percentile of daily maximum wind speeds contribute to the calculation of the index. Therefore, the sample of data in a 30 year time series comprises only about 220 events per grid box. This comparably small sample leads to higher uncertainties and reduced levels of robustness.

3.3 Data

Future climate conditions as simulated by climate models are subjected to uncertainty. As outlined in Sec. 3.2, the EURO-CORDEX initiative compiles multi-model simulation ensembles with regional focus on Europe (*Jacob et al.*, 2014), to assess and quantify uncertainties. The climate projections analyzed in the context of this chapter are based on the two representative concentration pathway RCP4.5 and RCP8.5. These refer to socio-economic scenarios characterized by an anthropogenic radiative forcing of 4.5 W/m^2 and 8.5 W/m^2 by the end of the 21$^{\text{st}}$century (*van Vuuren et al.*, 2011). These forcings relate to concentration of 650 ppm and 1370 ppm of CO_2-equivalents, respectively. While the anthropogenic radiative forcing of the two scenarios does not differ substantially at the beginning of the century, they substantially differ from each other in the analyzed period (2040 to 2069) on the order of about 1 to 3 W/m^2(*van Vuuren et al.*, 2011).

In Subsec. 3.3.1 the EURO-CORDEX ensemble and further climate data employed for the analysis are described. In Subsec. 3.3.2 information on the sources of information for tree species and soils are provided.

3.3.1 Climate data and climate change information

In the context of this thesis 40 RCM simulations, covering two different RCPs, were accounted for the index calculation (compare Tab. 2). All RCP8.5 and RCP4.5 EURO-CORDEX simulations available at the instant of ensemble composition (September 2018) were considered (23 RCP8.5 members, 17 RCP4.5 members).

The RCP8.5 ensemble comprises 7 different RCMs (10 different RCM versions) which are forced by 8 different GCMs (11 different realizations). The RCP4.5 based ensemble comprises 6 different RCMs (7 different RCM versions) which are forced by 5 different GCMs (9 different realizations). For each ensemble member (listed in Tab. 2), the 2 m temperature, precipitation, evaporation and maximum wind speeds at 10 m height on a daily temporal resolution were retrieved from the ESGF. The spatial resolution of the RCM simulations is roughly 12.5 km (0.11°).

In order to conduct the proxy calculation of soil temperatures (compare Subsec. 3.2.1), the soil temperature of the second soil layer (T_{D4}) of the historical and the evaluation experiments of REMO2009 (realization 1) were retrieved directly from the modeling center (Climate Service Center Germany (GERICS)). For the validation of the index against observational records, ERA-Interim reanalysis from the European Centre for Medium-Range Weather Forecasts (ECMWF) is used (*Dee et al.*, 2011).

For the comparison of the index to observed windthrow during Kyrill, RCM simulations downscaling ERA-Interim reanalysis of three different RCMs (KNMI-RACMO, RCA4, REMO2009) were retrieved from the ESGF. The documented forest damages

RCP4.5	RCP8.5	Driving GCM (realization)	RCM (version)
x	x	EC-EARTH (1)	KNMI-RACMO (1)
x	x	HadGEM2 (1)	KNMI-RACMO (2)
x	x	EC-EARTH (12)	KNMI-RACMO (1)
x	x	CNRM-CM5 (1)	CCLM4-8-17 (1)
x	x	EC-EARTH (12)	CCLM4-8-17 (1)
x	x	HadGEM2 (1)	CCLM4-8-17 (1)
x	x	MPI-ESM (1)	CCLM4-8-17 (1)
x	x	MPI-ESM (1)	REMO2009 (1)
x	x	MPI-ESM (2)	REMO2009 (1)
x	x	CNRM-CM5 (1)	RCA4 (1)
x	x	EC-EARTH (12)	RCA4 (1)
x	x	IPSL-CM5A (1)	RCA4 (1)
x	x	HadGEM2 (1)	RCA4 (1)
x	x	MPI-ESM (1)	RCA4 (1a)
x	x	IPSL-CM5A (1)	WRF331F (1)
x	x	EC-EARTH (3)	DMI-HIRHAM5 (1)
x	x	NCC-NorESM1 (1)	DMI-HIRHAM5 (2)
	x	HadGEM2 (1)	DMI-HIRHAM5 (1)
	x	CanESM2 (1)	REMO2015 (1)
	x	MIROC5 (1)	REMO2015 (1)
	x	EC-EARTH (12)	REMO2015 (1)
	x	CNRM-CM5 (1)	REMO2015 (1)
	x	HadGEM2 (1)	REMO2015 (1)

Table 2: Overview of the RCM climate simulations over the EURO-CORDEX domain employed in this study. The crosses ('x') in the first and second column indicate the simulations considered in the RCP4.5 and the RCP8.5 ensemble.

caused by Kyrill (*Franken et al.*, 2013) were provided by the federal state office for forest and wood of North-Rhine Westphalia (*Landesbetrieb Wald und Holz NRW*).

3.3.2 Tree species and soil data

The quantification of the predisposition of windthrow was based on information of tree species and soil. In Germany, the share of tree species at a certain location is regularly documented in Federal Tree Inventories. The latest inventory from 2012 is provided by *Thünen Institut* (2012). Herein, Germany's forests are subdivided into more than 20,000 quadratic domains of 150 m lateral length (*Bundesministerium für Ernährung und Landwirtschaft BMEL*, 2019). The applied grid has a resolution of at least 4 km x 4 km; some federal states have chosen to apply higher grid resolutions (compare Fig. 10). For each of these domains, the Federal Tree Inventory distinguishes between six different coniferous and 19 deciduous species. These species were allocated to the five

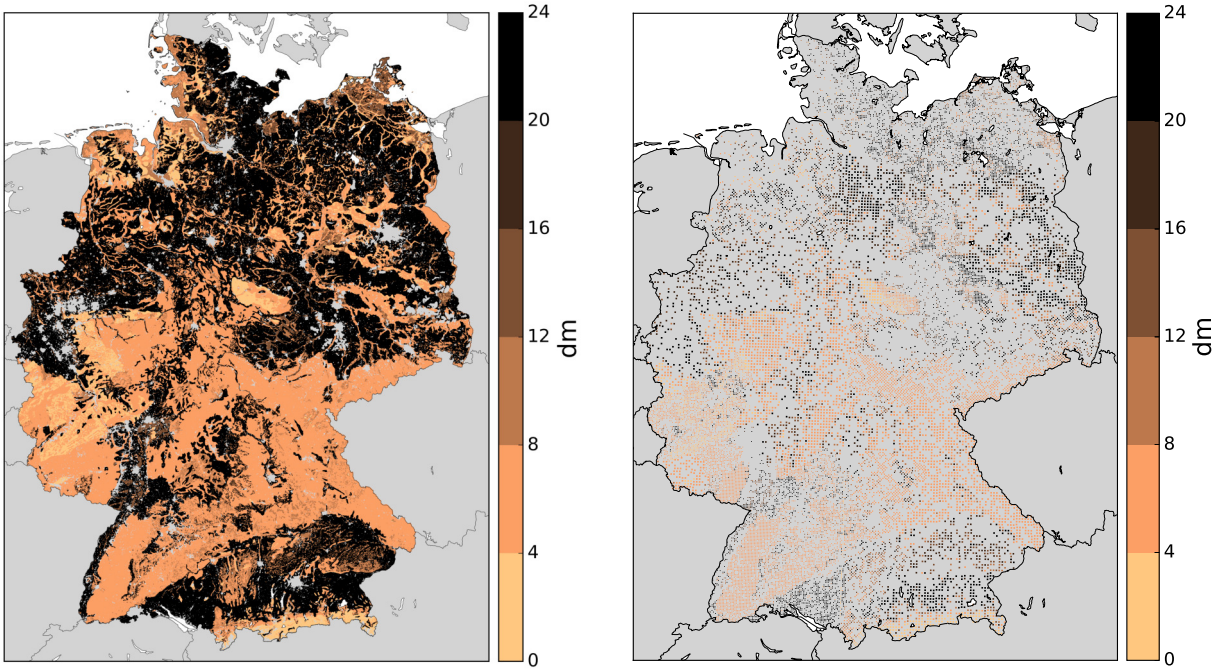

Figure 15: Rootable soil depth (German: *Physiologische Gründigkeit*) on 1:250,000 spatial resolution (left), and on the resolution (4 km x 4 km) of the latest Federal Tree Inventory (right) .

tree categories vulnerability coefficients were estimated for (compare Subsec. 3.2.3).

For most parts of Germany, soil type classifications on a resolution of 1:200,000 (BUEK200) from the webportal of the Federal Institute for Geosciences and Natural Resources were employed (*Bundesanstalt für Geowissenschaften und Rohstoffe*, 2015). In total, Germany is subdivided into 55 different BUEK200 domains; for five of these domains (CC6318, CC6326, CC7126, CC8734, CC8726) data were not accessible (as of 28.03.2018). In order to cover these areas, a coarser datasat at the resolution of 1:1,000,000 (BUEK1000) was used (*Stegger* and *Vinnemann*, 2013).

Tree vulnerability coefficients differentiate between four different soil types (A: freely-draining mineral soils, B: gleyed mineral soils, C: peaty mineral soils, D: deep peats). Therefore, the dominant soil types according to the subdivision into the four different soil types was determined for each domain of the Federal Tree Inventory (compare Appendix A.4).

Information on soil depth were collected from the *Federal Institute for Geosciences and Natural Resources*. These are resolved at a scale of 1:250,000 (*BGR*, 2015). Analogous to the soil type classification, the mean soil depth was determined for each domain of the Federal Tree Inventory. Fig. 15 illustrates the differences between the original data set on 1:250,000 resolution compared to the processed data set on the resolution of the Federal Tree Inventory.

3.4 Results

The following subsections illustrate the results of the application of the developed windthrow index methodology. The given climate change signals are based on the climate during the period 2040 to 2069 compared to the climate during the reference period 1970 to 1999.

In the subsections 3.4.1, 3.4.2 and 3.4.3 relative changes in the occurrence of extreme wind speeds, soil temperature conditions, and the water saturation of soil are analyzed. The geographically varying predisposition to windthrow calculated based on species, soil type and -depth is illustrated in Subsec. 3.4.4. In Subsec. 3.4.5 results for the windthrow index calculations are shown, and the individual contribution of wind, moisture and temperature with respect to the climate change signals is illustrated.

3.4.1 Wind climate

Climate change induced alterations in the conditions of extreme wind speeds can be a main source for a decreased or increased occurrence of windthrow. Fig. 16 illustrates the ensemble median of the 98^{th} percentile of maximum daily wind in the historical reference simulation period covering 1970 to 1999. In the Figs. 17 (a) and (b) the ensemble median change of the occurrence of extreme wind speed are illustrated for the RCP4.5 and RCP8.5 scenario . The shown results fail the robustness test (compare Subsec. 3.2.5) for (almost) all grid points. Multi-decadal variability of cyclone activity (compare Subsec. 2.6.1) could constitute the main reason for low levels of robustness. These findings substantiate the challenge to project robust regional climate change signals of the occurrence of extreme wind speed.

According to the ensemble median of the RCP4.5 scenario, occurrences of events with extreme wind speed are projected to increase over Baden-Württemberg, Rhineland-Palatinate, Hesse, the North of Bavaria and the West of Schleswig-Holstein, primarily in the range of 2 to 10%. Decreases on the same order of magnitude are projected, for example, for some southern parts of Bavaria, Saxony-Anhalt and Saxony. In case of the RCP8.5 scenario, increases of up to between 10 to 18% are simulated in the North-East of Bavaria, Thuringia and the North Sea-shore of Schleswig-Holstein. Overall, the shown results illustrate a spatially heterogeneous climate change signal of the occurrence of extreme wind speeds, mostly characterized by low levels of robustness.

3.4.2 Soil Temperature Proxy

Soil frost increases the tree root stability during stormy conditions. Hence, a decrease of soil frost conditions due to climate change leads to more favorable conditions for

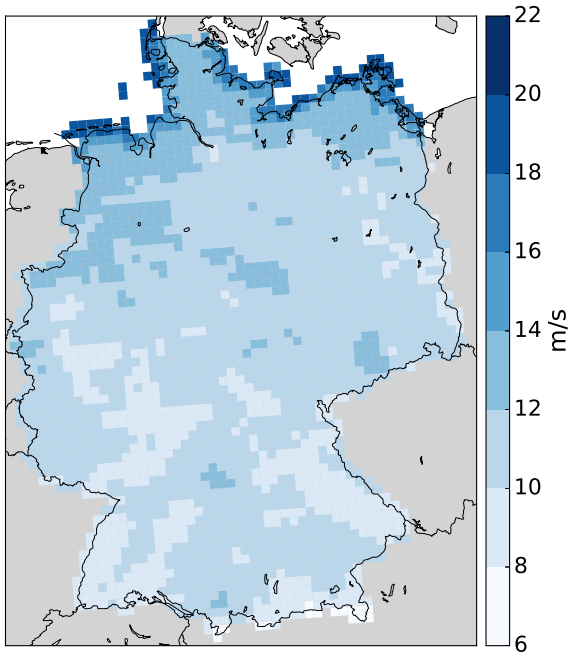

Figure 16: Ensemble median 98th percentile of maximum daily wind in the historical reference simulation for the years 1970 to 1999.

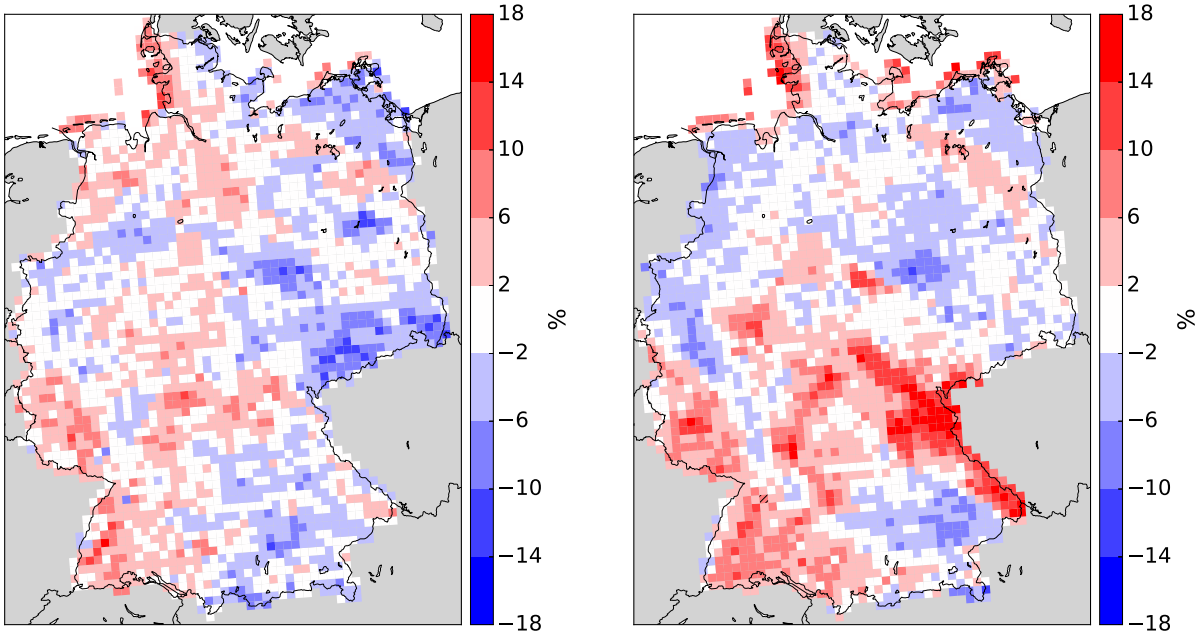

(a) RCP4.5 (b) RCP8.5

Figure 17: Relative changes in the occurrence of extreme wind speeds (98th percentile) comparing the ensemble median of the RCP4.5 (a) and RCP8.5 (b) scenario (for the years 2040 to 2069) to the ensemble median of the historical reference (for the years 1970 to 1999). Hatched areas indicates robustness (66% agreement, 85% significance; Note: criterion is fulfilled at one grid point of RCP8.5 only).

windthrow. The temperature of the upper soil layer was approximated from the atmospheric temperature of the respective climate simulation (compare Subsec. 3.2.1). During the historical reference period, soil frost is simulated to occur predominantly over mid-range mountain areas (roughly in the range of 15 to 30% of days with frozen soil conditions annually) and the German Alps (up to 40 to 50%) (compare Fig. 18). The shares in the remaining parts of Southern Germany mostly amount to between 10 to 20%; while for the majority of the North-West of Germany a ratio between 5 to 10% can be observed; the North-East is to a large extent characterized by a ratio of 10 to 15% over the year.

Figs. 19 (a) and (b) quantify the absolute change of days with frozen soil for the RCP4.5 and RCP8.5 scenario by the middle of the 21st century (2040 to 2069) in comparison to the reference period (1970 to 1999)[9]. The results reveal for both RCP scenarios an absolute decrease in the share of days with frozen soil; most pronounced over those regions characterized by comparably high shares of frozen soil states in the reference period (mid-range mountain areas and the German Alps). For RCP4.5 scenario, absolute decreases in those regions are mostly on the order of 6 to 10%. In case of the RCP8.5 scenario, absolute decreases are slightly higher in the range of 8 to 12%.

Decreasing shares of frozen soil states lead to increasing occurrences of soil temperature conditions favoring windthrow. However, only those soil conditions are of relevance for windthrow which coincide with (sufficiently) strong wind speeds. Therefore, and due to the fact that storm conditions primarily occur during the autumn and winter seasons (compare Subsec. 2.6.1), the share of storm events which occur during frozen soil conditions is likely to show a more pronounced climate change signal, than the share of days with frozen soil conditions over the course of a year.

This is verified by the illustration of the proportion of extreme wind conditions that occur during frozen soil conditions Ishown in Figs. 21 a and b). In the mid-range mountain areas and in Southern and Eastern Germany in general, frozen soil states during events with extreme wind conditions are reduced more markedly, than the annual average of frozen soil states (Figs. 19 a and b). While for the RCP4.5 (RCP8.5) scenario, the decrease of frozen soil states (in the mid-range mountain areas) amounts to a maximum of 12% (14%), the absolute decrease of simultaneous occurrences of extreme wind events with frozen soil states amounts up to 30% (30%).

The share of grid points characterized by robust climate change signals of soil state conditions during extreme wind events is notably smaller in comparison to the state of

[9]In this context, the chosen representation in absolute terms is chosen instead of a relative representation, since the historical basis of frozen soil shares regionally varies substantially (compare Fig. 18). In consequence, a pronounced relative reduction at a grid point of insignificant historical share of frozen soil days (e.g. close to the North Sea) very likely does not substantially influence windthrow.

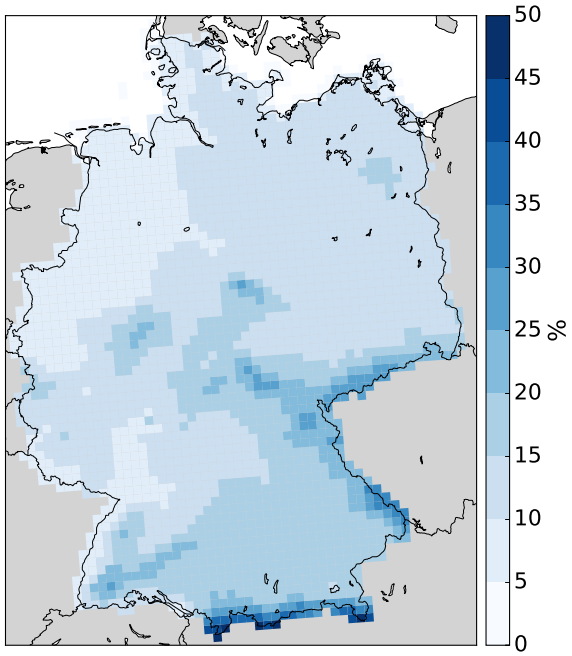

Figure 18: Ensemble median share of days with frozen soil state in the *historical* reference simulation for the years 1970 to 1999.

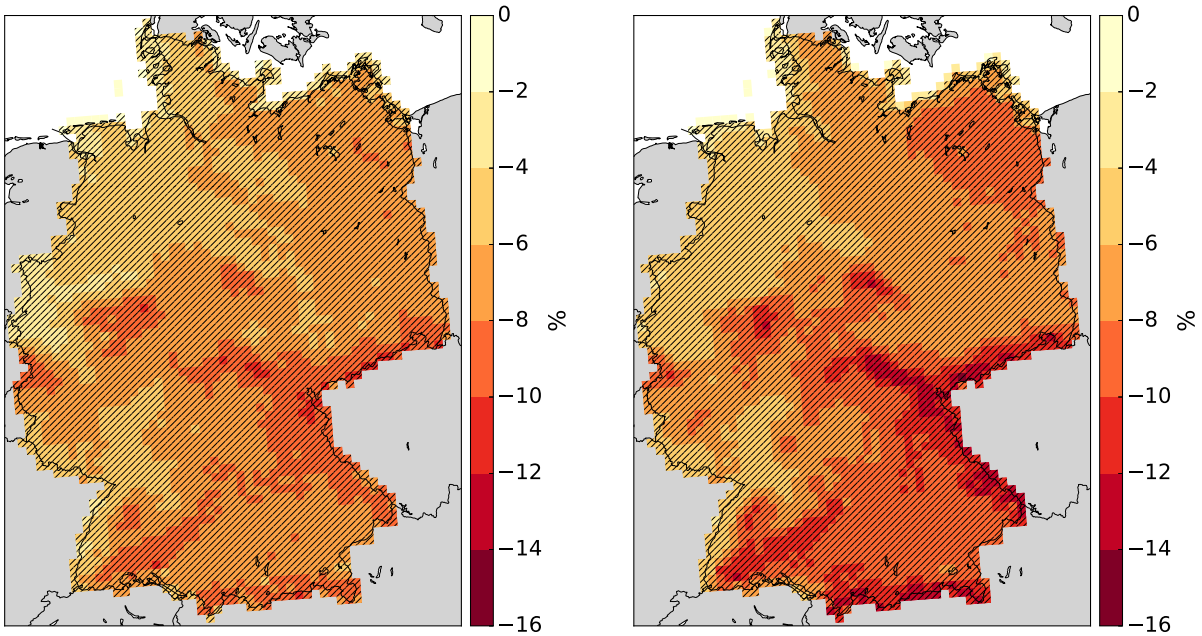

(a) RCP4.5 (b) RCP8.5

Figure 19: Absolute reduction of the share of days with frozen soil state comparing the ensemble median of the RCP4.5 (a) and RCP8.5 (b) scenario (for the years 2040 to 2069) to the ensemble median of the *historical* reference (for the years 1970 to 1999). Hatched areas indicate robustness (66% agreement, 85% significance).

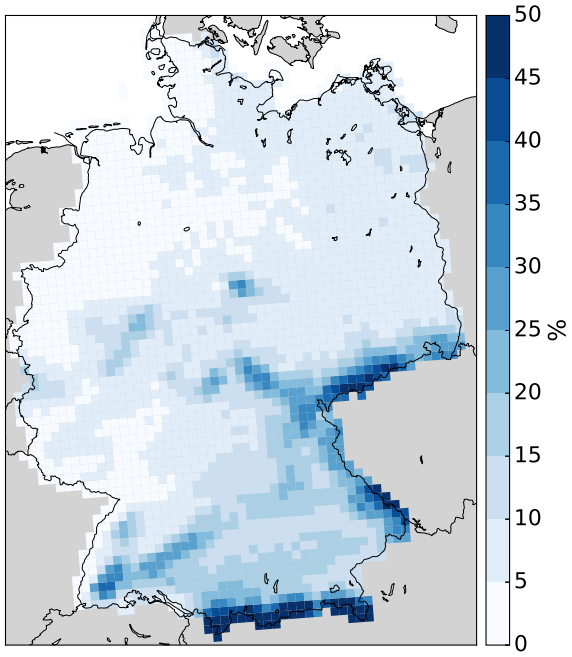

Figure 20: Ensemble median share of wind events with frozen soil state in the historical reference simulation for the years 1970 to 1999.

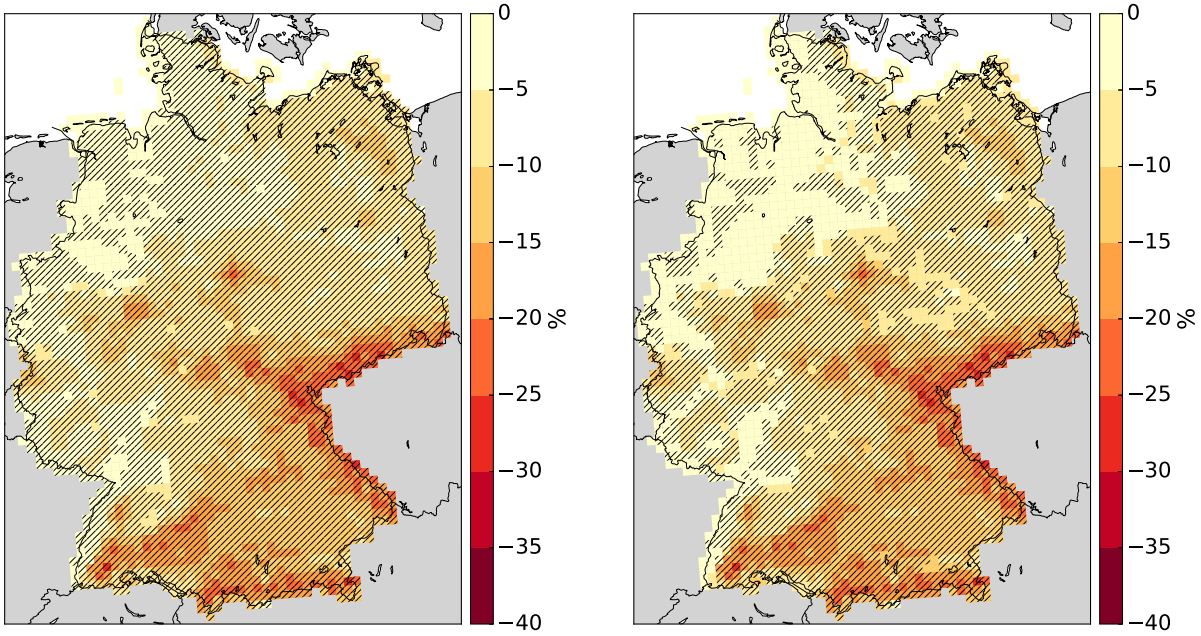

(a) RCP4.5 (b) RCP8.5

Figure 21: Absolute reduction of the share of wind events with frozen soil state comparing the ensemble median of the RCP 4.5 scenario (for the years 2040 to 2069) to the ensemble median of the historical reference (for the years 1970 to 1999). Hatched areas indicate robustness (66% agreement, 85% significance).

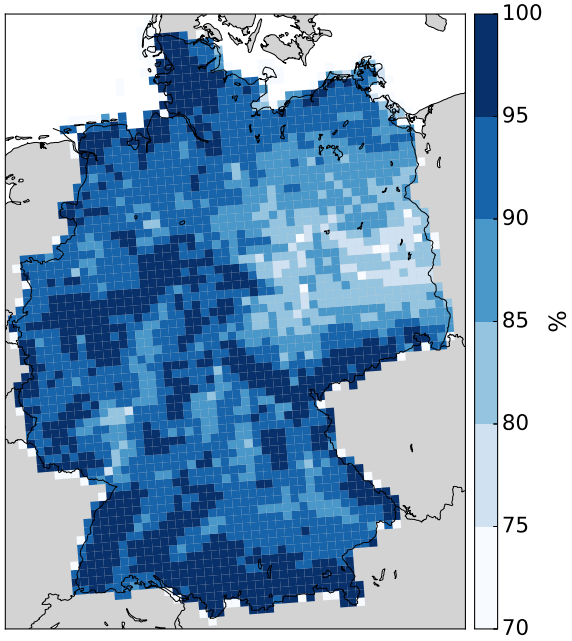

Figure 22: Ensemble median water saturation of soil during conditions of extreme wind events in the historical reference simulation for the years 1970 to 1999.

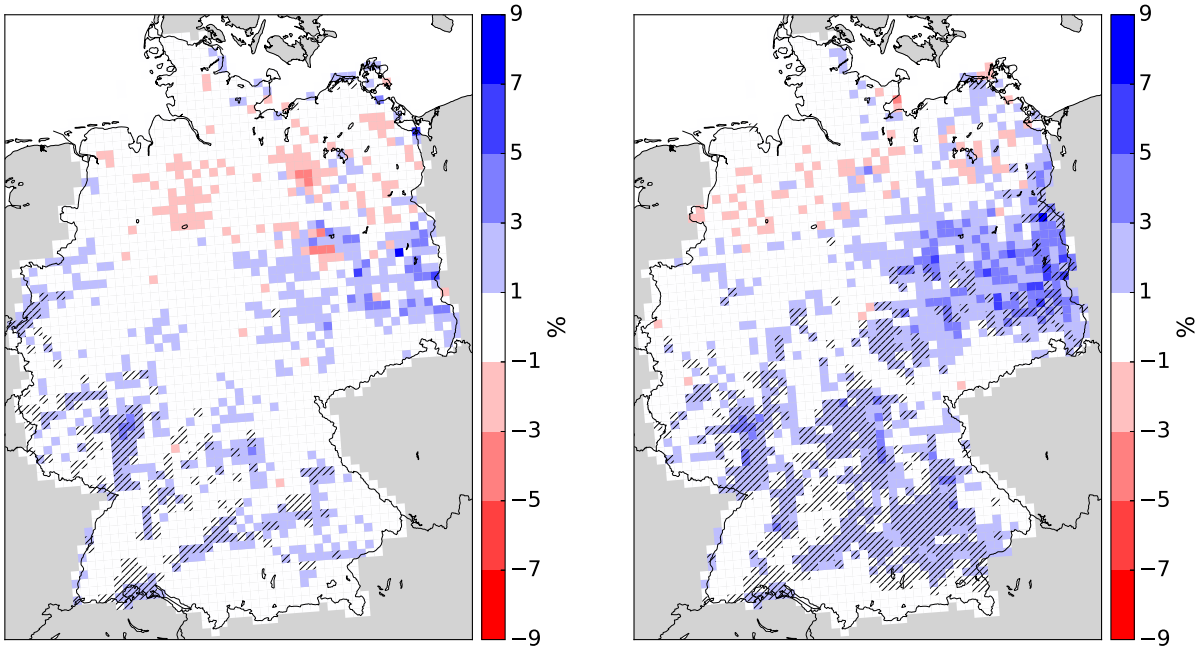

(a) RCP4.5 (b) RCP8.5

Figure 23: Relative changes of the water saturation of soil during extreme wind events comparing the ensemble median of the RCP scenarios (for the years 2040 to 2069) to the ensemble median of the historical reference (for the years 1970 to 1999). Hatched areas indicate robustness (66% agreement, 85% significance).

the soil over the course of the full 30-year period. This can be explained, by a reduced sample size, when the events of extreme wind conditions are analyzed only (especially at grid points of rather weak climate change signals).

As a remark: in comparison to the results of the predisposition of trees to windthrow (see Subsec. 3.4.4), the projected reductions of frozen soil conditions experience most pronounced absolute changes over those regions characterized by a comparably high predisposition to windthrow (e.g. most mid-range mountain areas). Consequently, increasing soil temperatures have an amplifying effect on windthrow in particular in these vulnerable regions.

3.4.3 Soil Moisture Proxy

High shares of soil moisture lead to decreasing tree root stability during stormy conditions. Hence, an increase in the soil water content due to climate change may lead to an increase of windthrow probability. As elaborated in Subsec. 3.2.2, the soil moisture of the upper soil layer was approximated from a relationship between the water saturation of the soil (modeled by an hydrological model) and the precipitation-evaporation difference.

During the historical reference period, the upper-most soil layer (0 to 30 cm) was found to be rather saturated with water during conditions of extreme winds (compare Fig. 22). Over most regions, the ensemble median water saturation of soil amounts between 90 to 100%. However, especially over the East of Germany, soil moisture content is less, amounting just 70% at some locations.

According to climate projections, soil moisture is projected to slightly increase over certain regions such as the East and South of Germany during conditions of extreme wind speed (compare Fig. 23). Both climate projection scenarios (RCP4.5 and RCP8.5) indicate increases of soil moisture, mostly on the order of 1 to 3%; however, in case of the RCP8.5, these can amount up to 9% at some grid points over Eastern Germany. Decreasing soil moisture content during extreme wind conditions on the order of 1 to 3% are projected only rarely over the North and North-East of Germany.

3.4.4 Predisposition to Windthrow

Besides the meteorological conditions during a storm, the vulnerability of a tree to be adversely affected by these conditions determines whether windthrow occurs or not. In the context of this thesis, the predisposition to windthrow was determined based on the site-specific characteristics *tree species*, *soil type* and *soil depth* (compare Subsec. 3.2.3). As shown, the major determinant for the resulting predisposition is the tree species, while the soil type and the soil depth are rather second-order influencing factors. Accordingly, the calculated predispositions (compare Fig. 24) particularly reflects the distribution

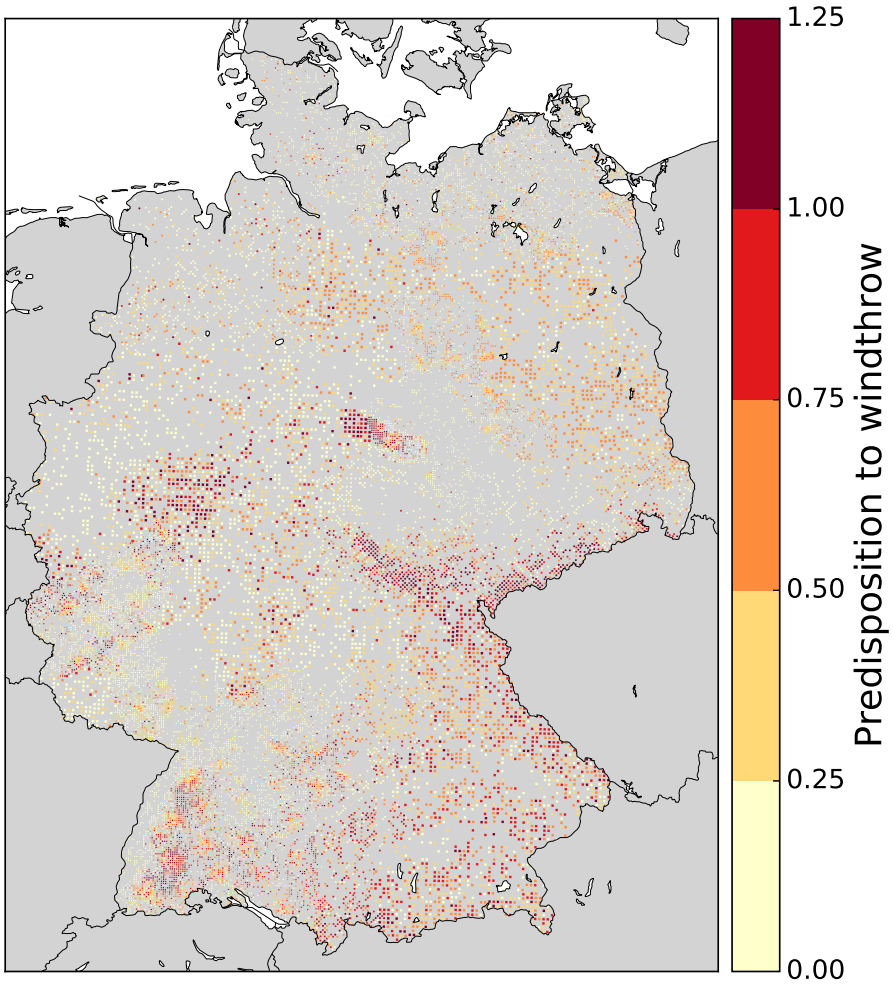

Figure 24: Vulnerability coefficients (predisposition to windthrow) of tree populations over Germany (compare Subsec. 3.2.3) visualized on the spatial resolution of at least 4 x 4 km (in some federal states the Federal Tree Inventory is conducted on a higher resolutions, compare Subsec. 3.3.2).

of vulnerable tree species. Hence, comparably high values of around 0.75 to 1.25 are observed for areas with high shares of spruce tree populations, which are primarily located in the mid-range mountain areas (such as the Blackforest, the Harz and the Ore mountain ranges). Values around 0.25 to 0.75 (determined e.g. over the Northern lowlands) either indicate high shares of pines or a mixture of spruce, pine and less vulnerable tree species; while values below 0.25 (e.g. over the Saarland, North-Rhine-Westphalia and Schleswig-Holstein) result from high shares of tree species less vulnerable to windthrow, such as beach and oak.

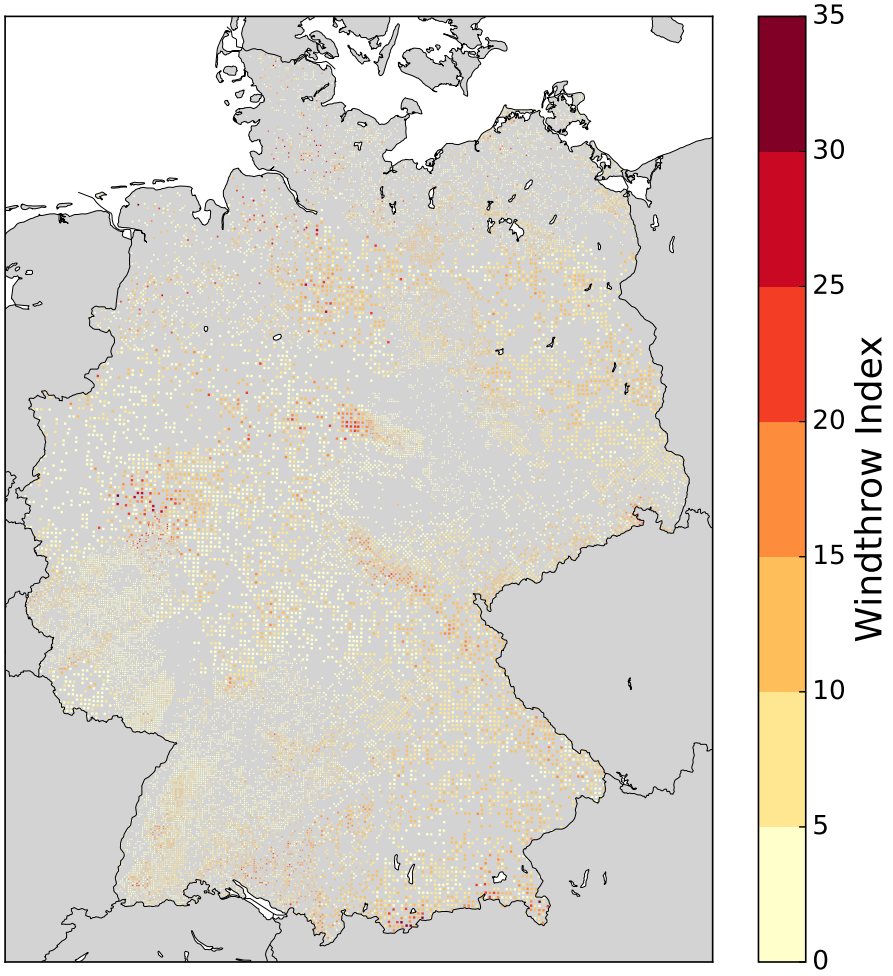

Figure 25: EURO-CORDEX ensemble median windthrow index of the *historical* reference simulation for the period 1970 to 1999.

3.4.5 Windthrow Index

The climate variables *maximum daily wind speed*, *soil temperature* and *soil moisture* determine the potentially windthrow-favoring conditions to which trees are exposed. In combination with the predisposition to windthrow, these variables determine the proposed windthrow index calculation (compare 3.2.3). The result of the windthrow index calculation for the reference period is illustrated in Fig. 25.

The (dimensionless) scale of the shown index results does not translate into physical windthrow of trees. This is primarily because variables largely determined by management schemes and crucial for windthrow probability (e.g. tree heights and thinnings) are not reflected in the design of the index (compare Subsec. 2.6.1). Hence, the proposed windthrow index enables a comparison for the climatic conditions of windthrow, instead of real physical windthrow of trees.

The index results for the historical reference climate mirror the spatial characteristics

of the predisposition to windthrow to some extent. Therefore, the index calculated for the reference climate period is characterized by comparably high values over many parts of the mid-range mountain areas and close to the Alpes as well as over parts of North and North-East Germany. Regarding the two climate change scenarios (RCP8.5 and RCP4.5), Figs. 26 (a) and (b) indicate substantial increases of up to a doubling of the windthrow index (in comparison to the reference climate) over most Southern parts of Germany and over some areas in the vicinity to the North and Baltic Sea. Most areas over the remaining North of Germany are characterized by a less pronounced increase, indifferent changes or even small decreases.

Deviations between the two climate change scenarios (compare Figs. 26 a and b) manifest most obviously in the share of grid points that satisfy the robustness criterion. In case of the RCP4.5 scenario, only few areas over the South of Germany indicate robust increases (e.g. over Baden-Württemberg and over a few locations of Bavaria). In contrast, the RCP8.5 scenario indicates markedly larger areas of robust increases over these areas. In addition, robust increases are present over the Sauerland, the Ore mountain range areas, and the Palatine Forest. These robust increases are largely on the order of 40 to 70%. In case of the RCP4.5 scenario, robust decreases are projected only for a few isolated areas in the North of Germany, while for the RCP8.5 scenario some robust decreases (on the order of -10 to -25%) are present over the North of Saxony-Anhalt.

In order to illustrate the individual contribution of the considered climate variables to the windthrow index, the climate change signals of the individual variables (i.e. relative changes of the windthrow index[10]) were analyzed. Figs. 26 (c) and (d) illustrate the results of the windthrow index, neglecting the influence of moisture and soil temperature on windthrow. Comparing the windthrow index accounting for all variables (Figs. 26 a and b) to the index results accounting for the variable wind only (Figs. 26 c and d) illustrates that the inclusion of soil moisture and soil temperature in the index design led to a pronounced increase of the windthrow index over most areas. This is true for both climate change scenarios. The effect of soil moisture and soil temperature is most pronounced over some of the mid-range mountain areas in the South of Germany and the Sauerland. Besides the impact on the strength of the climate change signal, the consideration of soil moisture and temperature led to a substantial increase of robustness.

Analogous, the contributions of soil temperature and soil moisture to the calculated windthrow index were determined. Their individual contributions were calculated based on the differences in the climate change signal between, firstly, an index that considers for

[10]The advantage of this representation over the representation of the absolute value is, firstly, that it better visualizes differences between the RCP scenarios and the historical reference period, and secondly, that the climate signal can be illustrated on the spatial resolution of the climate simulations, which most readers are probably more used to.

all variables (wind, soil moisture and temperature) and, secondly, an index that neglects the influence of either soil moisture or soil temperature. Note, that due to the non-linearity of the proposed index calculation method, the sum of the determined individual contributions (wind: Figs. 26 c,d; soil temperature: Figs. 27 a,b; and soil moisture: Figs. 28 a,b) does not necessarily equal the total windthrow index (Figs. 26 a,b).

The results show that soil temperature changes either contribute to an increase of the windthrow index or do not show a substantial influence (compare Figs. 27 a,b). Maximum absolute contributions to the increase of the climate change signal amount to 40 to 55%, which are predominantly observed over the North-East of Bavaria and the Ore mountain range areas, but also over the Sauerland and other areas in the South of Germany. Comparing the two climate change scenarios does not reveal a systematic difference[11]. As hypothesized in Subsec. 3.4.2, the soil temperature contribution to the windthrow index quantitatively largely follows the absolute reduction of the share of wind events with frozen soil state (compare Fig. 21). However, the observed difference between the two climate change scenarios that was observed with respect to the absolute reduction of the share of wind events with frozen soil state are not reflected in the soil temperature contribution to the windthrow index.

Soil moisture changes contribute to increases of the windthrow index over most regions on the order of 10 - 25% (compare Figs. 28 a,b). However, a much higher regional heterogeneity can be observed, with several grid points being characterized by a negative contribution of soil moisture content (mostly located in close proximity to grid points of positive contribution to the windthrow index). This spatial variation does not match the more uniform characteristic of the ensemble median relative change of soil moisture during events of extreme wind speed (compare Figs. 23 a,b). This can be explained by the cubicly shaped influence of wind speed into the calculation of the windthrow index (compare Eq. 8), which causes the total contribution of soil moisture towards the calculated windthrow index to be dominated by the soil moisture conditions during individual storm events of very high return periods (compare Subsec. 3.2.4). Related to this, there exists no pronounced systematic qualitative difference between the two climate change scenarios, except that the number of grid points with negative contributions is slightly higher in case of the RCP4.5 scenario.

[11]This statement is also valid for a reduced and more sensitively subdivided range of the colorbar (not shown in this dissertation). Therefore, the range of the colorbar is chosen consistently with Fig. 26, in order to facilitate comparability of the dimensions of the individual contributions to the windthrow index.

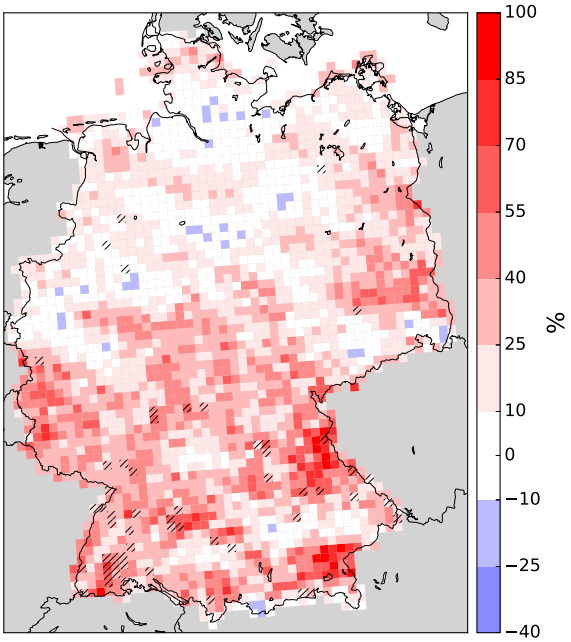

(b) RCP4.5, all climate variables

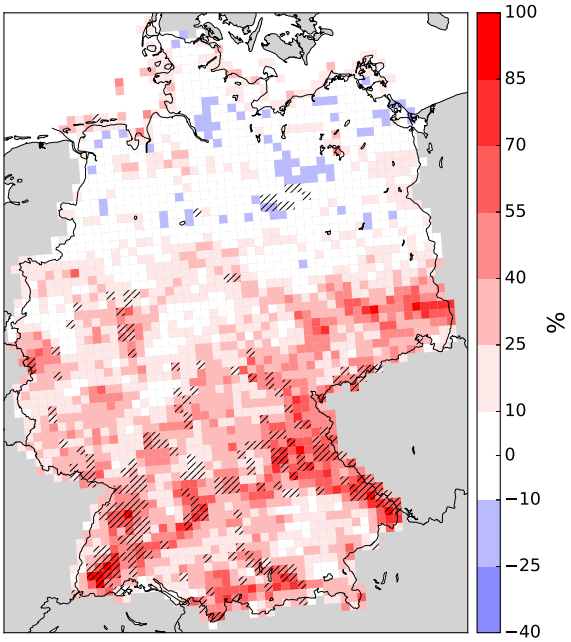

(a) RCP8.5, all climate variables

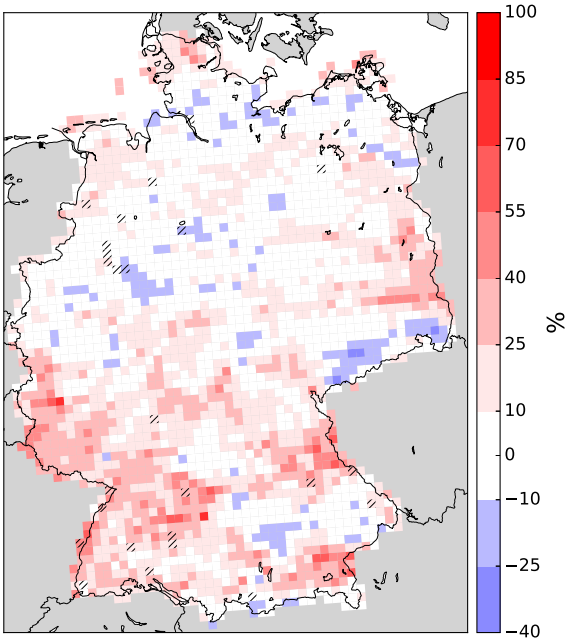

(d) RCP4.5, wind only

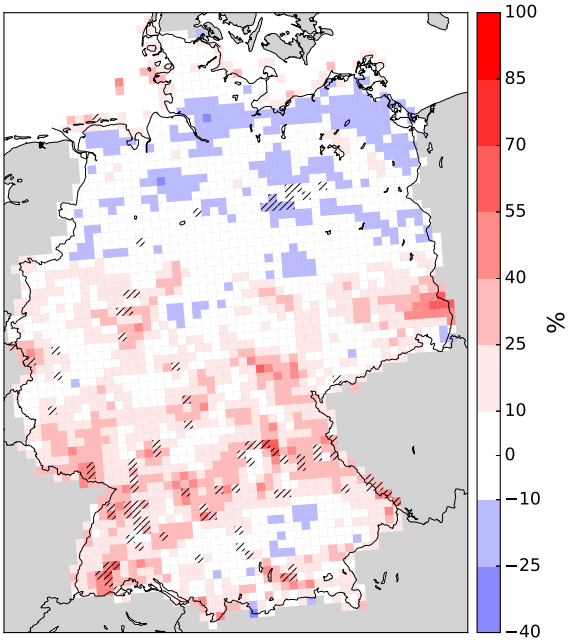

(c) RCP8.5, wind only

Figure 26: Median climate signal considering wind, soil moisture and soil temperature in the calculation of the windthrow index for the EURO-CORDEX ensemble of RCP4.5 (a) and RCP8.5 (b), in contrast to the median climate change signal considering only wind in the calculation of the windthrow index for RCP4.5 (c) and RCP8.5 (d). Hatching indicates robustness (66% agreement, 85% significance).

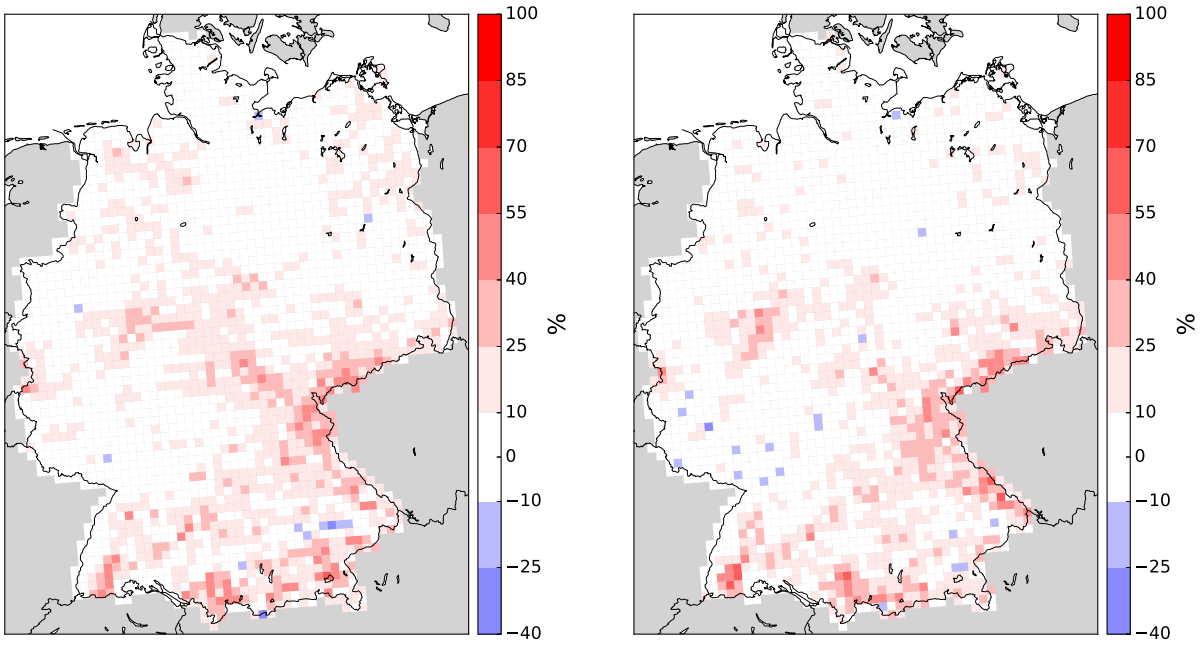

(a) RCP4.5 (b) RCP8.5

Figure 27: Absolute contribution of soil temperature to the median climate signal in the calculation of the windthrow index for the EURO-CORDEX ensemble of RCP4.5 (a) and RCP8.5 (b).

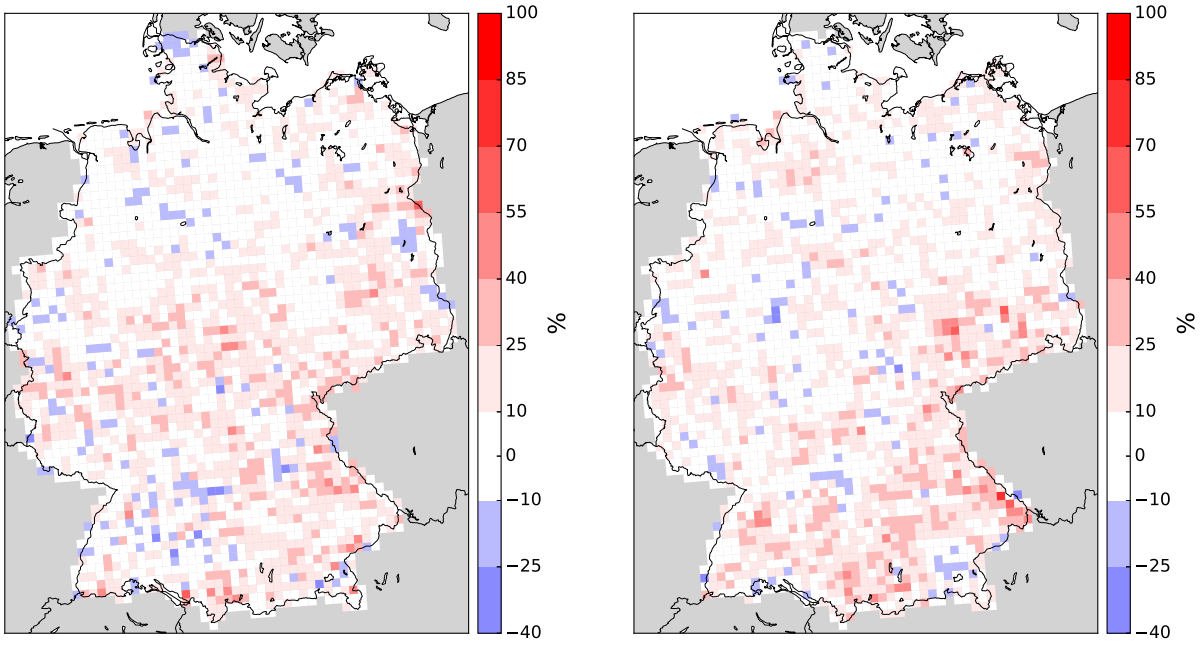

(a) RCP4.5 (b) RCP8.5

Figure 28: Absolute contribution of soil moisture to the median climate signal in the calculation of the windthrow index for the EURO-CORDEX ensemble of RCP4.5 (a) and RCP8.5 (b).

3.5 Discussion and Conclusions

In the past, the majority of customer disconnections was related to windthrow causing damage to the distribution grid infrastructure. Windthrow refers to the overturning or breakage of a tree, usually caused by extraordinary strong gusts. The conditions influencing the probability for windthrow were analyzed and an index reflecting these influencing variables was developed. To this end, a concept capturing the exposure to adverse (i.e. windthrow-facilitating) climatic conditions was introduced. In addition, the predisposition of a tree to windthrow was determined based on tree species, soil depth and soil type information. The product of exposure and predisposition determines the final windthrow index. A comparison of the damages documented during winter storm Kyrill to the results of the windthrow index on that day strongly indicates the ability to reproduce spatial differences of the windthrow likelihood during specific storm events.

For the historical reference period (1970 to 1999), it was shown that the windthrow index to some extent qualitatively mirrors the spatial characteristics of the predisposition to windthrow, with highest index values occurring in the mid-range mountain areas (e.g. the Black Forest, the Sauerland, the Harz and the Ore mountain range areas and parts of Bavaria). However, the identified differences between the windthrow index results of an ERA-Interim based calculation and a calculation based on the climate simulation ensemble (for the historical reference period) aggravates an interpretation of considering the ensemble median of the historical scenario representative for observed historical climate conditions. Nevertheless, assuming that any systematic bias is present in historical as well well as future climate simulations, the interpretation of relative climate change signals is not constrained by the previous finding.

Regarding the two analyzed climate change scenarios (RCP8.5 and RCP4.5), increases of up to a doubling of the windthrow index were calculated over most Southern parts of Germany and over some areas in the vicinity to the North and Baltic Sea (comparing the climate in 2040 to 2069 to the historical reference climate). Most areas over the remaining North of Germany are characterized by a less pronounced increase, indifferent changes or even small decreases. Deviations between the two climate change scenarios manifest most obviously in the share of grid points that satisfy the robustness criterion. In case of the RCP4.5 scenario, only few areas over the South of Germany indicate robust increases, while in case of the RCP8.5 scenario markedly larger areas of robust increases over these areas are found. The fact that robustness is identified only for a small share of areas indicates the substantial uncertainty with respect to the climate change signal of the windthrow index.

The analysis of the individual contributions of wind, soil temperature and soil moisture towards the windthrow index highlighted wind to be the major determinant of the index,

but also indicated the significance to include soil moisture and temperature into the index design. Largely independent of the considered climate change scenario, projected changes in soil temperature cause a maximum absolute contribution to the projected increase of the windthrow index on the order of 25 to 40%. Also soil moisture changes contribute to windthrow index increases for most areas (on the order of 10 to 25%). Besides their impact on the strength of the climate change signal, the consideration of soil moisture and temperature led to a substantial increase of robustness.

In order to correctly interpret these outcomes, the limitations concerning the methodological approach and data need to be taken into account. Firstly, it is a very complex endeavor to determine the predisposition to windthrow. The main reason for this is the large variety of influencing factors, and the difficulty to robustly distinguish between the individual contributions of the variables and the contributions based on interactions between these. The rareness of windthrow events plus the sparse documentation of windthrow damages aggravates the statistical basis needed to determine and disentangle influencing factors.

Secondly, the index design does not account for certain variables crucially determining windthrow (e.g. tree height), because these variables substantially depend on the forest management scheme and other human interventions, which are not simulated in the context of a climate model simulation. Instead, the windthrow index is meant to reflect more general factors that do not depend on human preferences or management methods. In consequence, the outcome of the index calculation is not capable to assess whether windthrow actually occurs or not, but enables a comparison for the climatic conditions of windthrow. Moreover, it needs to be stressed, that the percentile-based approach can be regarded as a strong assumption. Though backed by data on insured damages and used by other studies, it has not been empirically proven in the context of windthrow.

In addition, the projected climate change signals and their robustness depend on the composition of the climate model ensemble: The ensembles used are ensembles of opportunity, with all model simulations available for a certain climate change scenario being included. Though, the compilation of the climate model ensembles are subjected to efforts to systematically structure the matrix of simulations (as done by the modeling groups contributing to EURO-CORDEX), a certain model (or a model family) could be overrepresented (*Pfeifer et al.*, 2015). Hence, any potentially associated systematic problem may either cause an artificial increase of robustness or it makes underrepresented (but correct) signals appear as putative wrong outliers. However, in the absence of a commonly-accepted alternative ensemble compilation methodology, such as model selection (*McSweeney et al.*, 2012), ensembles of opportunity are a widely preferred methodology.

Furthermore, the domain-specific predisposition to windthrow was calculated from information on the distribution of tree species, soil types and soil depth. While soil depth and soil type do not strongly vary on climate timescales, the distribution of tree species may indeed respond to climate change. This feedback was not considered in the methodology, since the distribution of tree species is mainly determined by the forest management: If climate change makes certain tree species economically unattractive, forest managers may decide to adapt their species selection to increase profitability. These adaption measures cannot be robustly projected.

Despite the listed limitations with respect to methodology and data, the information on regional differences in windthrow likelihood can provide decisive knowledge on how to adapt forest management to altered climatic conditions. Potential response opportunities are for example planting less vulnerable tree species, apply forest management techniques less sensitive to the tree rooting systems, refraining from rigorous clearings or resort to mixed forests instead of monocultures.

Hence, this chapter's findings can contribute to forest-management specific considerations which focus on the economic revenues of forest owners. However, embedded in the context of this thesis, the results of this chapter should in particular feed into the efforts of distribution grid operators to prevent interruptions of the electricity grid. In regions with comparably high windthrow index, efforts to prevent interruptions, such as regular clearings of the power-line corridors, more redundant network architectures or other measures may become economically reasonable. Whether such measures are cost-efficient also depends on the economic losses resulting from distribution grid interruptions. These are addressed in the following chapter.

4 Economic Value of Electricity Distribution Networks

As elaborated on in Sec. 2.2, the German electricity distribution grid is in the process of being significantly altered to respond to challenges linked to the energy transition. In consequence, considerable investments are required to adapt the electricity networks. In addition, further adaptation may be required to account for changing climatic conditions, as elaborated on in depth in the previous chapter of this thesis.

From a social planner perspective, these two issues should be taken into account conjointly, as it is probably more cost-efficient to combine the current need for extension requirements related to the energy transition with the need to adapt the grid to potentially altered climatic conditions as part of the standard maintenance-renewal cycle. In consequence, the level of grid reliability should reflect the actual economic risks associated with an interruption of the grid.

The previous chapter investigated how climate change alters the conditions for the windthrow of trees, which is one of the main reasons for atmospherically-induced grid interruptions (compare Ch. 2). In order to conduct a proper risk evaluation, not only the probabilities of occurrence need to be considered, but also the economic value actually at stake due to an interruption of the grid has to be quantified, which is addressed in this chapter of the thesis[12].

4.1 Introduction

A quantity named *Value of Lost Load (VoLL)* measuring a consumer's willingness to pay for avoided electricity outages has been proposed as one guiding variable to determine optimal economic levels of supply security (*Welle* and *Zwaan*, 2007). However, the *VoLL* quantifies the economic benefit of a unit of delivered electricity, whereas it does not quantify the benefit of a securely functioning distribution grid and does not put these benefit in relation to the infrastructural requirements necessary for a secure delivery. In response to these two deficits, this thesis proposes to expand the *VoLL* concept, by incorporating, (i) information on the amount of electricity consumed from the grid, in order to quantify the total benefit of a securely functioning grid, and (ii), information on the infrastructure which is needed to generate that economic benefit. To the author's best knowledge, there is no methodology yet that combines these streams of information into one measure. By proposing a concept named *Value of Lost Grid (VoLG)*, this part of the dissertation closes this methodological gap.

[12]Note that an intermediate version of the content of this chapter has been published in the context of a working paper (*Stankoweit et al.*, 2017).

In a general sense, the proposed methodology contributes to an economic assessment of all events potentially triggering electricity outages within the distribution grids, in the sense that it enables a comparison of the economic importance of different distribution grid domains. The outcomes of this approach may support for example network quality considerations: grids of high relative economic value generation should be – from an purely economic perspective – comparably more resilient to potential outage events. Therefore, the central aim of this chapter is to apply the sketched methodology to Germany in order to quantify differences in the electricity distribution grid's economic importance, and to investigate the limitations and the expressive power of the proposed methodology.

For the calculation of the *VoLL*, on which the *VoLG* quantification is based, various approaches have been suggested; these can be grouped into direct and indirect methods (*Schröder* and *Kuckshinrichs*, 2015). Direct approaches are for example survey studies that inquire how much people would be willing to pay for an uninterrupted supply (e.g. *Praktiknjo*, 2014), or blackout studies which deduce economic losses from past blackout-events[13] (e.g. *Schubert et al.*, 2013). This thesis resorts to an indirect method, namely the production function approach, which is based on a macroeconomic production function. This approach features two decisive advantages: (i) it relies on easily accessible and mostly freely available macroeconomic data; and (ii) it enables to calculate *VoLLs* on a relatively high spatial resolution (limited only by the resolution of the collection of macroeconomic data by statistical offices). The approach has frequently been applied to determine *VoLLs* on different scales of spatial resolution for various countries: *Bliem* (2005) determined *VoLLs* on NUTS 2 resolution (federal states) in Austria; *de Nooij et al.* (2007) and *de Nooij et al.* (2009) on NUTS 3 resolution (the so-called COROP regions) and on the spatially higher resolved municipality level in The Netherlands; *Tol* (2007) and *Leahy* and *Tol* (2011) determine *VoLLs* for the electricity market of the Republic of Ireland and Northern Ireland; *Linares* and *Rey* (2013) for the Spanish NUTS 2 regions; and *Zachariadis* and *Poullikkas* (2012) for the electricity market of Cyprus. For Germany, *Röpke* (2013) determined country-wide *VoLLs* for five industries plus the households sector; *Growitsch et al.* (2014) calculated *VoLLs* for 15 industries and the private sector on NUTS 2 resolution (16 federal states), whereas *Piaszeck et al.* (2014) and *Wolf* and *Wenzel* (2015) further refined the spatial resolution to the around 400 NUTS 3 regions (counties) and four industries plus the household sector.

This thesis applies a *VoLL* estimation on NUTS 3 resolution as conducted by the latter two mentioned studies (*Piaszeck et al.* (2014) and *Wolf* and *Wenzel* (2015)) as a tool to quantify the total economic value annually generated due to the secure functioning of the

[13]For a more complete list on direct approaches and recently conducted studies, as well as the advantages and disadvantages of these approaches, I refer to *Schröder* and *Kuckshinrichs* (2015).

distribution grid infrastructures. The *VoLG* calculation requires to combine macroeconomic data and structural grid data[14]. Hence, a harmonization of the spatial resolution of data sets is conducted, since the two sets do not relate to the same geographic reference domains. Geographic intersections between counties (which are the reference units of macroeconomic data) and grid operators (which are the reference units of operators) are exploited to determine the *VoLL* for the electricity consumed from a certain operator's voltage level. Accordingly, the total economic value attached to the consumption of the electricity supplied by a specific voltage level is deduced. Thereafter, this economic value is related to the total grid length of that voltage level, to enable a comparison between different operators and voltage levels.

Sec. 4.2 describes how the economic value of a grid was quantified and related to the infrastructure installed, and refers to the limitations inherent in the applied approaches. Sec. 4.3 provides information on the data sources used. In Sec. 4.4, it is shown that the *VoLG* may vary significantly between different *distribution grid operators (DGOs)* by more than an order of magnitude even within one and the same voltage level; the difference in the relative economic importance between the low and the medium voltage level is quantified, and domains whose electricity infrastructure is of comparable higher economic relevance are identified. Further, uncertainties induced by the suggested methodology are quantified. The results are concluded and discussed in Sec. 4.5.

[14]For example the total electricity consumption from each voltage level of a certain distribution grid operator.

4.2 Methodology

In this section, a methodology is developed to quantify the economic value of an electricity distribution grid and relate it to the infrastructure needed to generate that value. To this end, the *VoLL* is, firstly, calculated on county resolution for five different sectors (Subsec. 4.2.1) based on macroeconomic data. The subsequent subsection elaborates on how to derive the *VoLL* with respect to each *DGO* (Subsec. 4.2.2). Finally, the *VoLG* concept is proposed as a measure to express a grid infrastructure's relative economic value (Subsec. 4.2.3)

4.2.1 Value of Lost Load on County Resolution

This part of the thesis aims at analyzing differences in the economic value at highest possible spatial resolution. As already indicated in the introductory section to this chapter, the *VoLL* can be determined via direct and indirect methods. However, the application of any direct approach is infeasible, either due to a lack of comprehensive data (needed for blackout studies) or because they are very costly and time-consuming (willingness to pay survey). Therefore, an indirect method is used, namely the production function approach, which is based on a macroeconomic production function. For the *VoLL* calculation, this thesis largely follows the methodology as applied by *Piaszeck et al.* (2014) and *Wolf* and *Wenzel* (2015), apart from deviations in certain assumptions, and the application of updated data.

In a first step, the *VoLL* is determined county-wise for each sector. This study differentiates between the four economic sectors *Agriculture*, *Construction*, *Manufacturing & Mining* and *Services*, and the *Household* sector[15]. In line with the literature (e.g. *Growitsch et al.*, 2014; *de Nooij et al.*, 2007, 2009; *Leahy* and *Tol*, 2011), the production function approach is chosen, making use of a Leontieff production function, which is characterized by zero substitutability of electricity with any of the other input factors. In other words, a direct linear relationship between production and electricity use is presumed. Based on these thoughts, the *VoLL* of a sector s in a county c can be determined from the ratio of the gross value added by the respective sector s in the respective county c, $\mathrm{GVA}(s,c)$, and the electricity consumed, $\mathrm{EC}(s,c)$, by the respective sector:

$$\mathrm{VoLL}(s,c) = \frac{\mathrm{GVA}(s,c)}{\mathrm{EC}(s,c)} \tag{11}$$

The applied approach features certain limitations worth mentioning. Since production functions are commonly applied to estimate production on the timescale of a year, the

[15]The applied differentiation is determined by the aggregation level of data as collected by statistical offices.

capability to precisely estimate outage costs resulting from interruptions of a few hours to days might be limited (*Leahy* and *Tol*, 2011). Further, it has been noted that the simplifying assumptions underlying the production function approach may lead to over- as well as underestimations of the real costs of an electricity outage (*de Nooij et al.*, 2009): An overestimation could result from the fact that backup generators, catching-up effects (e.g. the compensation of a delayed production through overtime or stock-keeping) and adaptive responses to a blackout are not taken into account (*Piaszeck et al.*, 2014). However, *Wolf* and *Wenzel* (2015) argue that for the purposes of cross-regional comparisons this constitutes only a minor problem. An underestimation could be caused by production processes very sensitive to outages, such that a short outage leads to a comparably long interruption until processes can be restarted. The unequal distribution of such sensible sectors across counties may lead to biases reducing the validity of interregional comparisons (*Piaszeck et al.*, 2014). Moreover, the linearity assumption inherent in the Leontieff production function seems reasonable for energy-intensive production processes, whereas it might underestimate substitution options for the construction sector and other labour-intensive services (*Piaszeck et al.*, 2014). However, it has been argued that this does not induce a significant bias, due to the fact that keeping up productivity during an outage requires significant reorganisational efforts and costs (*Piaszeck et al.*, 2014).

For most sectors, the application of Eq. 11 is rather straightforward: The gross value added by a sector and the electricity consumed are calculated from macroeconomic statistics, and the ratio of the two determines the *VoLL*. However, determining the household sector's *VoLL* is contingent upon estimations of the value of electricity-dependent leisure activities. This issue is approached applying microeconomic theory, according to which total labor supply is determined from each individual maximizing its personal utility resulting from work and leisure (*Becker*, 1965). When each individual can freely allocate its time between work and leisure, the situation can be interpreted as an optimization problem, whose optimal solution is that each individual allocates its time such that marginal benefits from work equal marginal benefits from leisure. Based on these considerations and due to a lack of information on marginal wages, average net wages per hour were suggested to be used as a proxy of leisure-induced gross value added (e.g. *de Nooij et al.*, 2007; *Growitsch et al.*, 2014). This approach, which is sometimes referred to as the *household income approach* (e.g. *Schröder* and *Kuckshinrichs*, 2015), is also applied in this work.

However, not all leisure activities are electricity-dependent. Therefore, the relevance of electricity for leisure needs to be estimated. Based on time use statistics (*Statistisches Bundesamt*, 2015) and a boolean decision, whether the practice of a leisure activity relies on electricity or not, *Wolf* and *Wenzel* (2015) estimate for Germany that 65% of leisure activities are electricity-dependent. In this respect, however, this thesis heuristi-

cally assumes, that 50% of leisure activities are electricity-dependent (in accordance with e.g. *Bliem*, 2005; *Growitsch et al.*, 2014; *Piaszeck et al.*, 2014), since the author views a boolean decision rather difficult[16].

The household income approach is further complicated by the difficulty to value the leisure activities of non-working persons. In line with the literature, this work assumes that the monetary value of each hour of leisure activity of a non-working person amounts half the value of an employed person (e.g. *Growitsch et al.*, 2014; *de Nooij et al.*, 2009; *Piaszeck et al.*, 2014; *Wolf* and *Wenzel*, 2015). Hence, based on the total population and the number of employed persons in a county and their average net wages, the total GVA of the household sector in the respective county was quantified, and plugged into Eq. 11 to determine the household sector's *VoLL*.

The gap between microeconomic theory and practice leads to a number of restrictions. Firstly, making use of average net wages per hour as a proxy for leisure-induced utility gains, may appear inappropriate for voluntary and involuntary unemployment (*Piaszeck et al.*, 2014). Secondly, the assumption that employees can freely decide on their optimal amount of working time does not necessarily reflect reality in a work environment of union regulation and other traditional habits (*Sanghvi*, 1982). Thirdly, the value of leisure of unemployed persons also incorporates pensioners, children and homemakers, and it may be criticized that the value of leisure for such individuals is also determined based on the wages of the working population (*Schröder* and *Kuckshinrichs*, 2015). Finally, the approach does not take into account the possibility of switching to non-electricity dependent leisure activities in case of a blackout (*Sanghvi*, 1982).

The application of the production function and the household income approach were shown to imply well-known disadvantages and limitations. Therefore, it might be necessary to once again stress that the decisive advantage of the method over any of the other ones is, that it allows an almost cost-free calculation of *VoLLs* on a high spatial resolution.

4.2.2 Value of Lost Load on Grid Operator Resolution

Determining the total economic value attached to the consumption of the electricity supplied by an operator's voltage level, requires information on the value of an average unit of electricity consumed from this voltage level. Since data on electricity consumption from the grid levels are reported by individual *DGOs*, the *VoLL* needs to relate to the same reference unit: the resolution of individual *DGOs* and voltage levels, instead of being related to individual counties.

In general, the average *VoLL* of the electricity consumed within the voltage level v of a

[16]It is for example difficult to decide whether the reading of books and magazines requires electricity, since this significantly depends on whether electric light is required or not.

DGO o, VoLL(v, o), can be calculated from the electricity consumed within the respective voltage level of the operator, and the *VoLLs* attached to each kWh of this consumption. Let EC(s, c, v, o) name the amount of electricity consumed from the voltage level v of *DGO* o by a sector s located in county c. Then the VoLL(v, o) can be determined from the sector- and county-specific *VoLLs*, VoLL(s, c) (as already calculated in the previous subsection):

$$\text{VoLL}(v, o) = \frac{\sum_{s,c} \text{VoLL}(s, c) \cdot \text{EC}(s, c, v, o)}{\sum_{s,c} \text{EC}(s, c, v, o)} \tag{12}$$

However, the amount of electricity consumed by a sector s, located in county c, consuming from voltage level v of operator o, cannot directly be inferred from readily available databases. Hence, it needs to be determined from available data on county resolution. Ideally, a bijective mapping needs to be performed, i.e. each unit of the electricity consumption, EC(s, c), of a sector s in a county c, is unambiguously assigned to a unit of electricity consumption within a specified voltage levels v of a specified *DGO* o. But a substantial proportion of electricity consumption cannot be unambiguously assigned to a certain *DGO*'s voltage level. Therefore, two different mappings are conducted: One mapping for those parts of sectoral- and county-specific electricity consumption EC(s, c) which can unambiguously be assigned to a specific voltage level v of a specific *DGO* o. And a second mapping, for the remaining consumption, which could potentially be consumed within several voltage levels and/or several *DGO*'s domains.

In the following subsections, the calculation of average *VoLL* of the household sector and the remaining sectors for each *DGO* and each voltage level is explained in detail.

Value of Lost Load of the Household Sector

The application of Eq. 12 to the household sector requires information on the electricity consumption by the households in each operator's domain. This consumption was inferred from county population statistics and geographical overlaps between operators and counties. Appendix A.5 in detail shows the first step of this process, which is to determine, how many people living in county c are supplied by which operator o. In the following, the population living in county c being supplied by operator o is abbreviated $P^{(u)a}(c, o)$. The superscript ua/a indicates whether the population can be unambiguously or ambiguously assigned from county c to operator o.

In the second step, county-specific per-capita electricity consumption by households was considered. Note, that the household sector (s = 'HH') withdraws its electricity from the low-voltage grid (v = 'LV'). Then, the electricity (un)ambiguously consumed by those households which are located in a certain county c and which are supplied by operator o, were calculated from the county-specific per-capita electricity consumption in each county,

$e_{p.c}(c)$, and the population living in county c supplied by operator o, $P^{(u)a}(c,o)$:

$$\mathrm{EC}^{(u)a}_{s='\mathrm{HH}',\, v='\mathrm{LV}'}(c,o) = \mathrm{P}^{(u)a}(c,o) \cdot e_{p.c}(c). \tag{13}$$

In the following equations, the subscripts were shortened from "s = 'HH', v = 'LV'" to "HH, LV". Based on this convention and the latter equation, the total electricity consumed by the household sector was determined from:

$$\mathrm{EC}_{\mathrm{HH,LV}}(o) = \underbrace{\sum_c \mathrm{EC}^{ua}_{\mathrm{HH,LV}}(c,o)}_{=:\mathrm{EC}^{ua}_{\mathrm{HH,LV}}(o)} + \underbrace{\mathrm{P}^a(o) \cdot \frac{\sum_c g_1(c) \cdot \mathrm{P}^a(c,o) \cdot e_{p.c}(c)}{\sum_c g_1(c) \cdot \mathrm{P}^a(c,o)}}_{=:EC^a_{\mathrm{HH,LV}}(o)} \tag{14}$$

Note that $\mathrm{P}^a(o)$ is defined as $(\mathrm{P}(o) - \sum_c \mathrm{P}^{ua}(o,c))$, and represents the number of people supplied by operator o not unambiguously assigned to any county. The weighting factor $g_1(c)$ is determined by the ratio between the number of people living in county c which are not unambiguously assigned to any operator o, and the sum of all people living in county c which are ambiguously assigned to any operator:

$$g_1(c) = \left(P(c) - \sum_o \mathrm{P}^{ua}(o,c) \right) / \left(\sum_o \mathrm{P}^a(o,c) \right)$$

There are two reasons for including this weighting factor: Firstly, the probability that a person is actually consuming its electricity from an ambiguously assigned *DGO* is much higher, if it is ambiguously assigned to few other operators only, and vice versa. The second reason is a conservation rationale; to keep the Germany-wide average *VoLL* of the household sector constant, when transforming the spatial resolution of the *VoLL* from county- to *DGO*-resolution. Without incorporating $g_1(c)$, an individual county ambiguously assigned to several *DGOs* would exert larger influence on the German average *VoLL* of the household sector then another one, which is assigned to a very small number of *DGOs* only.

Based on the *VoLL* of electricity consumption in the assigned counties (calculated from macroeconomic data), $\mathrm{VoLL}_{\mathrm{HH}}(c)$, the *VoLL* of unambiguously and ambiguously assigned electricity consumption in the domain of an operator was determined:

$$\mathrm{VoLL}^{ua}_{\mathrm{HH,LV}}(o) = \frac{\sum_c \mathrm{EC}^{ua}_{\mathrm{HH,LV}}(c,o) \cdot \mathrm{VoLL}_{\mathrm{HH}}(c)}{\sum_c \mathrm{EC}^{ua}_{\mathrm{HH,LV}}(c,o)} \tag{15}$$

$$\mathrm{VoLL}^{a}_{\mathrm{HH,LV}}(o) = \frac{\sum_c g_1(c) \cdot \mathrm{EC}^{a}_{\mathrm{HH,LV}}(c,o) \cdot \mathrm{VoLL}_{\mathrm{HH}}(c)}{\sum_c g_1(c) \cdot \mathrm{EC}^{a}_{\mathrm{HH,LV}}(c,o)} \tag{16}$$

The household sector's mean VoLL can be determined straightforwardly from the arithmetic mean of the both:

$$\overline{\mathrm{VoLL}}_{\mathrm{HH,LV}}(o) = \frac{\mathrm{EC}^{ua}_{\mathrm{HH,LV}}(o) \cdot \mathrm{VoLL}^{ua}_{\mathrm{HH,LV}}(o) + \mathrm{EC}^{a}_{\mathrm{HH,LV}}(o) \cdot \mathrm{VoLL}^{a}_{\mathrm{HH,LV}}(o)}{\mathrm{EC}_{\mathrm{HH,LV}}(o)} \tag{17}$$

Due to the partially ambiguous mapping of population from counties to operators, the average *VoLL* as determined with Eq. 17 is characterized by uncertainty. The uncertainty increases, the larger the fraction of households supplied by o whose county-affiliation is ambiguous, and the larger the spread of the individual *VoLLs* of the household sector among these ambiguously assigned counties. To quantify uncertainty, we determined the minimum and maximum values of the *VoLL* of the household sector of operator o. For this purpose, the difference between reported population supplied by a *DGO* and the unambiguously mapped population, $P(o) - \sum_c \mathrm{P}^{ua}(o,c)$, was bridged with those ambiguously mapped population, that minimizes/maximizes the *VoLL* of the ambiguously assigned electricity consumption $\mathrm{VoLL}^{a}(v,o)$. Thus, a minimum and maximum of the *VoLL* of the household sector is determined for each *DGO*.

Further, it has to be mentioned that not only the average *VoLL* but also the amount of electricity consumed by the household sector (as determined with Eq. 14) is characterized by uncertainty. This uncertainty is driven by the variability of the per-capita electricity consumption $e_{p.c.}$. Since data on the latter are available on the spatial resolution of federal states only (compare Sec. 4.3), the applied values of $e_{p.c.}$ varies only with respect to different federal states. Hence, the electricity consumption of households within the domain of a certain *DGO* is only attached with uncertainty, if the ambiguously assigned population live in different federal states. For that reason, the uncertainty of the households' electricity consumption was found to be comparably negligible in its effect on the uncertainty attached to the *VoLL* of the low-voltage level. Therefore, the uncertainty of the amount of electricity consumed by households was neglected.

Value of Lost Load of other Economic Sectors

The application of Eq. 12 to the remaining four economic sectors requires information on the electricity consumption by these sectors in each *DGO* grid. Appendix A.5 in detail shows the first step of this process, which is to unambiguously determine, which sector s in county c consumed electricity from which voltage level v of operator o. Based on this mapping, the average *VoLL* for the unambiguously mapped electricity consumption, $\mathrm{VoLL}^{ua}(v,o)$, was calculated for the four economic sectors. As for the household sector, these mappings cannot be performed purely unambiguously. Therefore, in analogy to the approach to determine the *VoLL* of households, the calculation of the average *VoLL* of the ambiguously mapped electricity consumption by the remaining economic sectors was based on how often a specific kWh is ambiguously attributed to a certain *DGO* and/or

voltage level. This was taken into account by adding a weighting factor, $g_2(s,c)$, into Eq. 12, which reflects the probability that the ambiguously mapped electricity consumption $\mathrm{EC}^a(s,c,v,o)$ is actually consumed within voltage level v of operator o:

$$\mathrm{VoLL}^a(v,o) = \frac{\sum_{s,c} g_2(s,c) \cdot \mathrm{EC}^a(s,c,v,o) \cdot \mathrm{VoLL}(s,c)}{\sum_{s,c} g_2(c) \cdot \mathrm{EC}^a(s,c,v,o)}, \tag{18}$$

The factor $g_2(s,c)$ was determined from the ratio between the amount of electricity consumed by a sector s in county c, which remains to be assigned after the unambiguous mapping ($\mathrm{EC}(v,o) - \sum_{v,o} \mathrm{EC}^{ua}(s,c,v,o)$) and the sum of all ambiguously mapped electricity consumption from the same sector and county ($\sum_{v,o} \mathrm{EC}^a(s,c,v,o)$)). Hence, $g_2(s,c)$ reads:

$$g_2(s,c) = \frac{\mathrm{EC}(v,o) - \sum_{v,o} \mathrm{EC}^{ua}(s,c,v,o)}{\sum_{v,o} \mathrm{EC}^a(s,c,v,o)}$$

The weighting factor $g_2(s,c)$ is necessary for very similar reasons for which $g_1(c)$ was added as a weighting factor when determining the average *VoLL* of the household sector via Eq. 16. Firstly, to account for the fact that the probability that a kWh is actually consumed in an (ambiguously) assigned *DGO* is much higher, if it is ambiguously assigned to few others only, and vice versa. Secondly, it is required to keep the Germany-wide average *VoLL* independent of the mapping process. Without taking $g_2(s,c)$ into account, Germany's average *VoLL* would be dependent on the number of operators and voltage levels, to which a certain sector's electricity consumption is assigned to; in that scenario, a county's sector ambiguously assigned to several voltage-levels and *DGOs* would exert larger influence on the German average *VoLL*, than another one which is assigned to a very small number of voltage-levels and *DGOs* only.

Finally, based on the *VoLL* of the unambiguously mapped electricity (as determined with Eq. 12) and ambiguously mapped electricity (as determined with Eq. 18), the mean *VoLL* for any v,o-combination was determined from the arithmetic mean:

$$\overline{\mathrm{VoLL}}(v,o) = \frac{\mathrm{VoLL}^{ua}(v,o) \cdot \mathrm{EC}^{ua}(s,c) + \mathrm{VoLL}^a(v,o) \cdot (\mathrm{EC}(v,o) - \mathrm{EC}^{ua}(v,o))}{\mathrm{EC}(v,o)},$$

with $\mathrm{EC}^{ua}(v,o) := \sum_{s,c} \mathrm{EC}^{ua}(s,c,v,o)$. As for the calculation of the mean *VoLL* of the household sector, the mean *VoLL* is characterized by uncertainty due to the partially ambiguous mapping. Analogously, minimum and maximum values of the *VoLL* of each voltage level and operator were determined.

4.2.3 Value of Lost Grid

As argued in Sec. 4.1, the *VoLL* concept does not serve as a meaningful quantity to determine optimal economic levels of supply security, as for example suggested by *Welle* and *Zwaan* (2007), since a quantitative analysis of the economic value of a grid requires information not only on the economic value generated by a unit of delivered electricity, but also on the amount of electricity consumed and the infrastructure needed to generate the respective economic value. This methodological gap motivated the introduction of a new measure, referred to as *Value of Lost Grid (VoLG)*, and which is further elaborate on in the following.

The general idea is to relate the economic value generated due to the steady supply of electricity by a certain grid infrastructure to the infrastructure needed to enable that steady supply. In a first step, the total economic value generated by a voltage level of a *DGO* can be concluded from the *VoLL* as calculated in the previous subsections: Based on the unambiguously and ambiguously assigned electricity consumption of the individual economic sectors within a certain grid domain, a minimum, mean and maximum *VoLL* was calculated for each *DGO* and for each voltage level (as outlined in Subsec. 4.2.2). Based thereon, the total value generated within a certain voltage level v of a certain operator o depends on the total amount of electricity consumed from the respective voltage level in a defined period of time, $\mathrm{EC}(v, o)$. Accordingly, the total value generated within that time horizon can be calculated from $\mathrm{VoLL}(v, o) \cdot \mathrm{EC}(v, o)$.

Next, a useful reference parameter needs to be selected, that captures the infrastructure requirements to distribute electricity, which in turn contributed to the estimated generated economic value. From those quantities which are publicly available, the total grid length of a certain voltage level as well as the necessary transformer station capacities between the voltage levels are potential meaningful proxy variables. However, as there is no objective way of combining both into one reasonable quantity, this study uses the total grid length of a certain voltage level as a reference quantity, since it, in the author's view, captures the infrastructural requirements in the most meaningful manner. Based on the minimum-, maximum- and mean-value of the *VoLL* (of a certain voltage level and a certain *DGO*), $\mathrm{VoL}L_{\mathrm{min/mean/max}}(v, o)$, the *VoLG* was determined via:

$$\mathrm{VoLG}_{\mathrm{min/mean/max}}(v, o) := \mathrm{VoLL}_{\mathrm{min/mean/max}}(v, o) \cdot \frac{\mathrm{EC}(v, o)}{L(v, o)}, \tag{19}$$

with $L(v, o)$ being the grid length of voltage level v of operator o.

In this context, two issues should be stressed. Firstly, it needs to be emphasized that the suggested approach is targeting at exploring a measure that is superior to the *VoLL* in terms of expressing and comparing the economic value of the electricity distribution grids.

Its derivation is based on heuristic considerations, namely to relate the economic value generated from the energy consumed from the grid to the infrastructural requirements needed for this value generation, and is, therefore, difficult to scientifically proof. Nevertheless, its application contributes relevant information to considerations on network architecture and grid design, which the *VoLL* is not able to reflect. Secondly, it is one of the *VoLG*'s advantages, that the required macroeconomic and structural grid data are almost entirely straightforwardly accessible from operator's reporting or statistical offices. At the same time, the simplicity of the suggested approach is disadvantageous in the sense that information on the scale below the size of individual operators remain disregarded. However, information on the sub-operator scale are not publicly available. Therefore, the suggested methodology as a proxy of the relative economic value of the electricity grid is proposed.

Having noted these issues, this paragraph continues to describe the methodological procedure. Based on the *VoLG*'s minimum and maximum values, a measure is introduced that mirrors the uncertainty induced by the partially ambiguous mapping process: A probability distribution function (pdf) of the *VoLL* of a random kWh of electricity is determined for the ambiguously assigned electricity consumption and its determined *VoLL*. As elaborated on in Appendix A.7, the pdf does not constitute a useful measure to quantify the uncertainty attached to the actual amount of electricity consumed. In consequence, this study opted for minimum and maximum values of *VoLL* and *VoLG* as a measure of uncertainty in the manner already described. In order to facilitate a quick comparison between uncertainties attached to the mean *VoLG*, the relative average deviation of minimum and maximum from the mean value were determined: $d = 1/2 \cdot (\mathrm{VoLG}_{\mathrm{max}} - \mathrm{VoLG}_{\mathrm{min}})/\mathrm{VoLG}_{\mathrm{mean}}$.

The following methodological intricacies need to be stressed: (1) It has to be noted, that in this study the electricity consumption from the transformation stations was attributed to the respective upper voltage level[17]. The reasoning for this approach is that the upper voltage level is required to transport the electricity to the substations. Hence, substations are treated as any other consumer from the respective level. (2) When calculating the *VoLG* of a certain voltage level, the electricity consumption from the respective lower voltage levels was included. This means that the value generated within the low voltage level, was added to the value of the electricity directly withdrawn from the medium voltage level. One could argue to not consider the share of electricity which is directly induced by small-scale generation units into the low voltage level, when calculating the *VoLG* for the medium voltage level. However, a stable operation of the electricity grid

[17]The electricity consumption from the substations between the low voltage and medium voltage level was for example attributed to the medium-voltage level.

as an interconnected network requires a continuous connection to the respective upper voltage levels as a buffer to balance differences between supply and demand in the lower voltage levels. Hence, an interrupted electricity transfer for example in the medium-voltage level may trigger interrupted supply in the low-voltage level, which is not only constrained to the electricity which was delivered by the medium voltage level.

4.3 Data

In order to account for the large interregional heterogeneities of the *VoLL* (compare *Growitsch et al.*, 2014; *Piaszeck et al.*, 2014; *Wolf* and *Wenzel*, 2015), this study calculated the latter at county resolution, which is the highest possible resolution achievable with available macroeconomic data. The data needed in this respect are described in Subsec. 4.3.1. Subsec. 4.3.2 refers to the data relevant to deduce *VoLGs* on the spatial resolution of individual operators.

4.3.1 VoLL on County Resolution

For Germany, *VoLLs* on county resolution were determined by *Piaszeck et al.* (2014) and *Wolf* and *Wenzel* (2015). Therefore, the data sources used in this study to calculate *VoLLs* on county resolution, are mostly in line with the data sources of the latter publications. However, this study resorts to updated data where available, deviated from certain assumption and makes use of additional datasets. To determine *VoLLs* for the five different sectors (four economic sectors plus households) on county resolution, not all necessary data are widely available. Therefore, in some cases proxy data or data from a coarser spatial resolution were employed. The following paragraphs list the applied data.

Data on the county-specific *gross value added (GVA)* by each of the four economic sectors are published in the regional statistics of the German Federal Statistical Office. Data on electricity consumption within each county are published only for the *manufacturing & mining* sector by the same authority. It has to be noted that for reasons of confidentiality or a lack of data, this data set is incomplete with respect to five counties[18]. For the remaining three sectors, the county- and sector-specific electricity consumption is approximated from national average *VoLLs* of these sectors. These national average *VoLLs* are calculated from the Germany-wide electricity consumption and the *GVA* of the respective sectors. Data on both can be deduced from the energy balance sheets of Eurostat and the national accounts of the German Federal Statistical Office respectively.

Though, data on electricity consumption are available on county resolution for the *manufacturing & mining* sector, sector-specific *VoLLs* cannot be directly calculated, since the data on the *GVA* also subsumes the energy sector, which is not included in the data on electricity consumption. Hence, the *GVA* by the energy sector is subtracted in a two-step process, as applied by *Piaszeck et al.* (2014) and *Wolf* and *Wenzel* (2015): Information on the *GVA* by the energy sector is only available on federal states's level in the national

[18]Four of these are located in Brandenburg: Oberhavel, Uckermark, Märkisch Oderland, Brandenburg an der Havel; the fifth in Lower Saxony: Wolfsburg. For the four of the counties located in Brandenburg, electricity consumption was estimated based on the average *VoLL* of the sector in Eastern Germany. Energy consumption in the fifth non-reported county, Wolfsburg, was estimated based on the *VoLL* of the Transport Equipment industry in Lower Saxony as determined by *Growitsch et al.* (2014).

accounts of the federal states (available via the Federal Statistical Office). Therefore, in a first step, the *GVA* by the energy sector is allocated to the counties within the respective federal state according to the share of energy sector employees working in a county. Employee data were purchased from the German Employment Agency. Due to the fact that some of these data were made anonymous for reasons of confidentiality, a second step is needed, in which the remaining share of the federal *GVA* is allocated to the remaining counties in proportion to the number of companies active in the sector (data can be accessed via the regional statistics of the Federal Statistical Office).

The highest available resolution of data on electricity consumption of the household sector is at federal states level via the federal states' statistical offices. At the date of data compilation, the data's reference years varied amongst the authorities, and four federal states (Bavaria, Bremen, Hesse and Saarland) did not report on electricity consumption by households individually. Of the remaining, all but two federal states report at least on 2013 electricity consumption by households (North Rhine-Westphalia reports until 2012, Rhineland-Palatinate until 2011). For these two, 2012 and 2011 values were used instead. For the four non-reporting states, electricity consumption at federal level was approximated by distributing the remaining national consumption according to population numbers and household sizes[19]: for each federal state the number of one-person-equivalent-households[20] was calculated. Data on the ratio of average electricity consumption of households of different size, were taken from the *BDEW* (2014); data on population and household size in the different federal states were deduced from the German Federal Statistical Office. Finally, household electricity consumption at county level was approximated by distributing the federal consumption amongst the counties proportionally to the county's population numbers[21].

In order to determine the value of leisure (i.e. of household electricity consumption), county-specific net wages per employee are calculated from gross average wages, which are available via the national accounting of the Federal Statistical Office. In analogy to the discussed literature (e.g. *Growitsch et al.*, 2014; *Piaszeck et al.*, 2014; *Wolf* and *Wenzel*, 2015), net wages are assumed to equal half of the gross wages. Moreover, data on the total number of working hours by the population living in a county is required, but the workforce accounts of the Federal Statistical Office only provide data on the number of working hours of all employees *working* in a county. In order to consider commuting flows, data on working hours are multiplied by the ratio of employees living in the county over

[19]In this respect, I deviate from *Piaszeck et al.* (2014) and *Wolf* and *Wenzel* (2015) which considered total population size only.

[20]This accounts for the fact that a one-person-household consumes more electricity per person then a two-person-household.

[21]Here, household sizes cannot be taken into account, since these data are unavailable on county resolution.

employees working in the county[22].

The time remaining to be devoted to leisure activities and work is estimated from data on the time needed for personal activities, such as sleeping, eating or washing (which can be found in *Statistisches Bundesamt*, 2015). Accordingly, an average German employee devotes 10.58 hrs (10:35 hrs:min) to these personal activities. Unemployed and non-working persons, pensioners, and young people aged below 16 years devote 11:29, 11:49 and 10:35 hrs:min respectively to these activities. Based on these data, I assumed that during a year, employees may devote $(24 - 10.58) \cdot 365$ hrs to leisure activities and work, whereas non-employed people may devote $(24 - 11.5) \cdot 365$ hrs on leisure activities[23].

4.3.2 VoLG on Operator Resolution

The mapping of electricity consumption from county resolution to *DGO* resolution required geo-information of counties, municipalities and *DGOs*. The shape of the *DGOs*' domains at the reference date of 01.01.2016 was purchased from a geomarketing consultancy (*Lutum + Tappert DV-Beratung GmbH*, 2016); geo-information of German counties and municipalities are available via the GADM database (*Gadm.org*, 2015); Population data on municipality resolution are available via the federal statistical offices at the reference date of 31.12.2014. In addition changes in municipality domains in the course of 2015 based on the reporting of the statistical federal offices were considered, to avoid inconsistencies related to the different reference period of county shapefiles and municipality population records.

From the *DGOs*' legal reporting obligations, the grid lengths of each voltage level, the total annual electricity consumption per voltage level, the total annual electricity withdrawal of a certain voltage level from the upstream voltage level as well as the population number supplied were deduced. The electricity consumption from each voltage level was determined from the difference between total annual electricity consumption (which usually includes the supply to lower voltage levels), and the annual electricity withdrawal of the respective lower voltage level from the upper one. The reported grid length of the low voltage grid includes house connections to the households.

Due to the large number of *DGOs* in Germany (almost 900), a basic data set of structural grid data was purchased (*Lutum + Tappert DV-Beratung GmbH*, 2016). This data set is mostly based on the operators' reporting with respect to the reference year 2012[24]. However, for this study, if available, data was updated to the most recent reporting

[22]This implies the assumption that the working hours of an employee living in a county are the same as the working hours of an employee commuting to that county.

[23]Hence, I slightly deviate from e.g. *Growitsch et al.* (2014) and *Piaszeck et al.* (2014), who used 11 hours for both groups.

[24]In some cases, the reference year of published company information was older than the date at which

period at the date of data collection (commonly: reference year 2015) for those *DGOs* which provide electricity to at least 100,000 inhabitants, plus all those operators which were non-existent at the time the GET AG data set was compiled, and if operators merged, split up or renamed.

The data of the GET AG data base, as well as those additionally collected were subjected to plausibility checks[25]. Due to inconsistencies in the reporting and non-compliance with the legal reporting obligations, data sets could not fully be compiled for all *DGOs*. The required data to determine the voltage-level specific electricity consumption were not available for 78 of the around 900 *DGOs* in total.

the data had been collected by the Get AG.

[25]For example double-checking unexpectedly high or low values of e.g per-capita electricity consumption and investigate infringements with energy conservation.

4.4 Results

The VoLG, the quantity proposed as a new measure to economically assess differences in the relative importance of the distribution grid infrastructure, is basically the ratio between the economic value of electricity consumed and the infrastructure needed to deliver that economic value. Since the fundamental assumptions and macroeconomic data gathered to determine county- and sector-specific *VoLLs* are largely in line with *Piaszeck et al.* (2014) and *Wolf* and *Wenzel* (2015), the presented outcomes are in very good agreement with the results of these authors: Firstly, national *VoLLs* for the sectors *agriculture*, *construction* and *services* of 2.22 €/kWh, 125.30 €/kWh and 12.67 €/kWh respectively are consistent with their results (which are 1.98 €/kWh, 118.15 €/kWh and 10.16 €/kWh respectively). Secondly, patterns of regional *VoLLs* on county resolution of both, the household sector as well as the county-average of all remaining other economic sectors (compare Fig. 29), quantitatively compare well with the county-resolved *VoLLs* as published in *Piaszeck et al.* (2014). Hence, these findings reinforce the authors' finding that the *VoLL* is subjected to significant interregional heterogeneities.

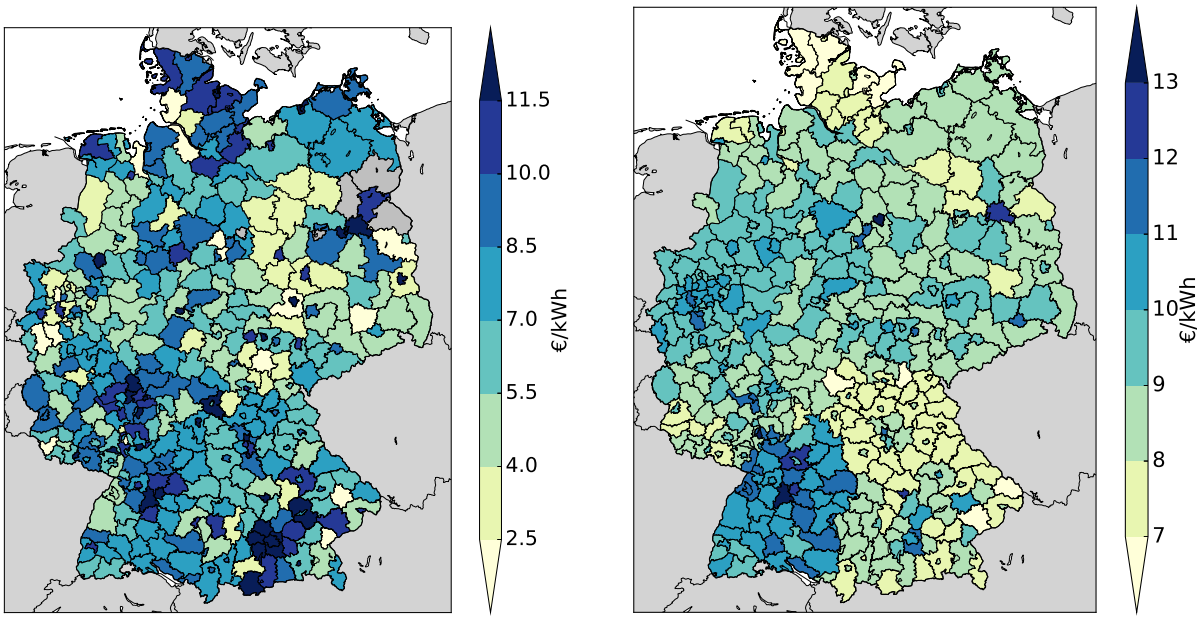

Figure 29: *Value of Lost Load (VoLL)* in €/kWh at county resolution. Left: Average *VoLL* of the four economic sectors; Right: *VoLL* of the household sector. Grey indicates a lack of data.

As already indicated, the calculation of *VoLLs* on the resolution of voltage levels and *DGOs* required a mapping of electricity consumption on county resolution to individual voltage levels and operators. As indicated, this mapping could only partially be performed unambiguously. Therefore, this paragraph briefly elaborates on the degree of how much electricity was actually unambiguously mapped, since it markedly influences how

precisely the *VoLL* can be determined on the spatial resolution of operators. Due to the fact that population data are resolved on municipality level and are, thus, available on a spatial resolution which significantly exceeds the resolution of counties[26], a very large share of the household sector's electricity consumption was unambiguously assigned: In course of the mapping process, 71.2 million inhabitants (approx. 88% of the total German population) were unambiguously assigned to a specific *DGO*. However, this share significantly varied amongst the operators[27]. The household sector significantly contributes to the electricity consumption from the low voltage grid and accounts for a markedly 73.4%-share of electricity consumption from the low voltage level[28]. This high share of unambiguous mapping was not observed for the medium voltage grid. In total, only 7.2% of total electricity consumption consumed from the medium voltage level was ambiguously mapped[29].

Having introduced the relative average deviation d of minimum and maximum *VoLG* from the mean *VoLG* (see Subsec. 4.2.3) implies the advantage, that mean *VoLGs* can be more easily illustrated in conjunction with the uncertainty attached to the mean value, as illustrated in Fig. 30 and Fig. 31 for the low and medium voltage grid respectively. There are a few general observations which can be drawn from these figures. Firstly, the difference in the scaling of the colorcode signals at first sight that in general the *VoLGs* in the medium voltage level is significantly above the *VoLGs* in the low voltage level. Secondly, the variability of the colors indicates a pronounced interregional heterogeneity of *VoLGs* for both voltage levels. Thirdly, the uncertainty of the *VoLG* is more pronounced in the medium than in the low voltage level. The following paragraphs focus on these three observations in more detail:

Since the higher voltage levels in general have higher capacities to transport electricity, the *VoLG* in the medium voltage level was anticipated to be higher than in the low voltage level. The lower box plot in Fig. 32 specifies this general observation and illustrates the difference between the *VoLG* in the low and medium voltage level; Accordingly, the median *VoLG* of the low voltage grid of 1.43 million €/km/yr is markedly below the median *VoLG* of the medium voltage grid of 4.68 million €/km/yr. The upper box plot in Fig. 32 reveals, that this does not root in the differences of the *VoLL*, whose relation is exactly opposite: the *VoLL* of electricity directly consumed from the medium voltage grid is substantially lower than electricity withdrawn from the low-voltage grid. Therefore, one

[26] Germany is subdivided into around 400 counties or around 11300 municipalities.

[27] Sorted by the share of unambiguously assigned population, the central 90% of operators are characterized by an assignment ratio ranging from 56% to 100%.

[28] According to my calculations, the household sector consumes between 50.0% and 95,3% (range given for the central 90% of operators) of electricity from the low-voltage grid of an individual *DGO*.

[29] Again, this ratio experiencing a significant variation from 0.00% to 56.10% for the central 90% of operators.

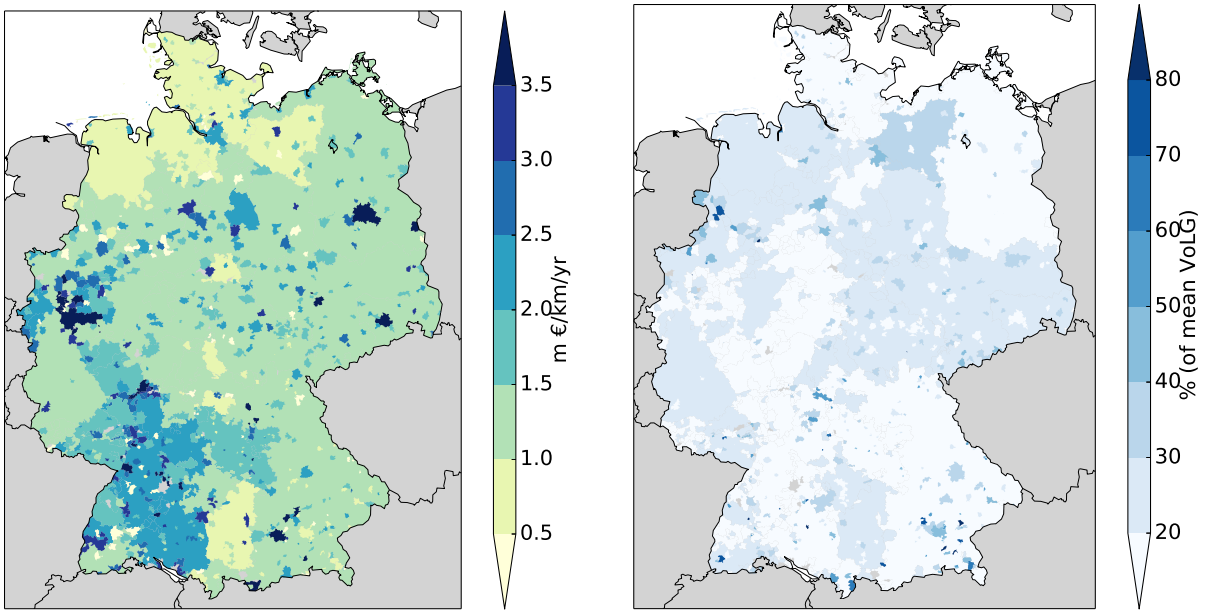

Figure 30: Low voltage grid: *Value of Lost Grid (VoLG)* in million €/km/yr within individual distribution grid domains (left), and the uncertainty attached to it (right) expressed as the relative average deviation d of minimum and maximum *VoLG* from the mean *VoLG* in each grid domain ($d = 1/2 \cdot (\mathrm{VoLG}_{max} - \mathrm{VoLG}_{min})/\mathrm{VoLG}_{mean}$). Hatched gray-colored domains indicate lacking data.

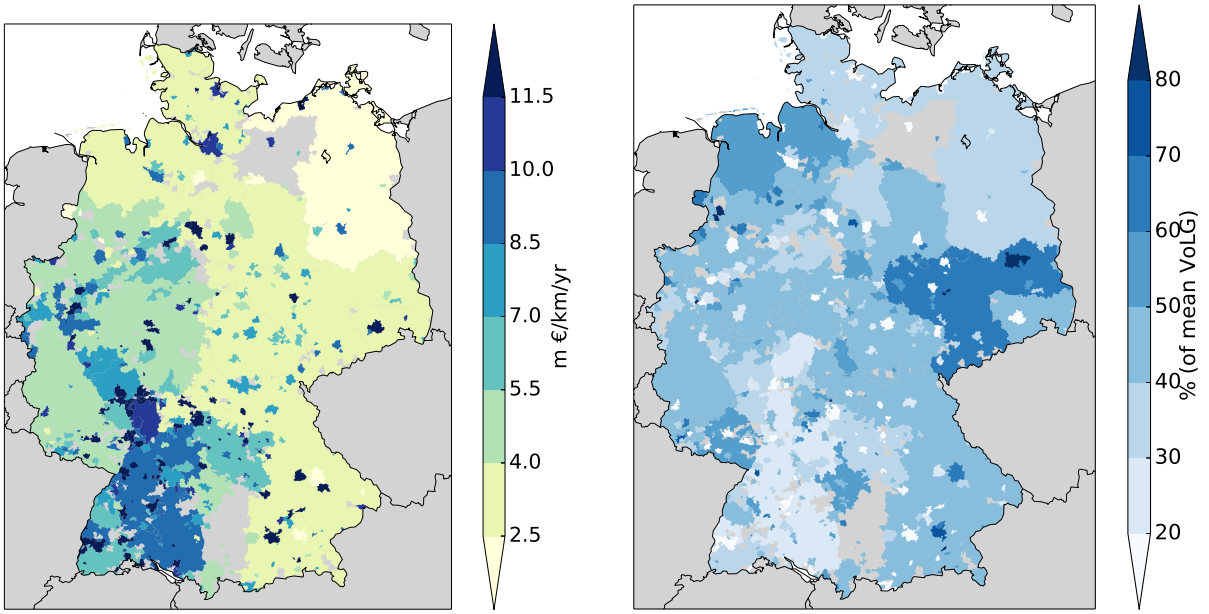

Figure 31: Medium voltage grid: *Value of Lost Grid (VoLG)*) in million €/km/yr within individual distribution grid domains (left), and the uncertainty attached to it (right) expressed as the relative average deviation d of minimum and maximum *VoLG* from the mean *VoLG* in each grid domain ($d = 1/2 \cdot (\mathrm{VoLG}_{max} - \mathrm{VoLG}_{min})/\mathrm{VoLG}_{mean}$). Hatched gray-colored domains indicate lacking data.

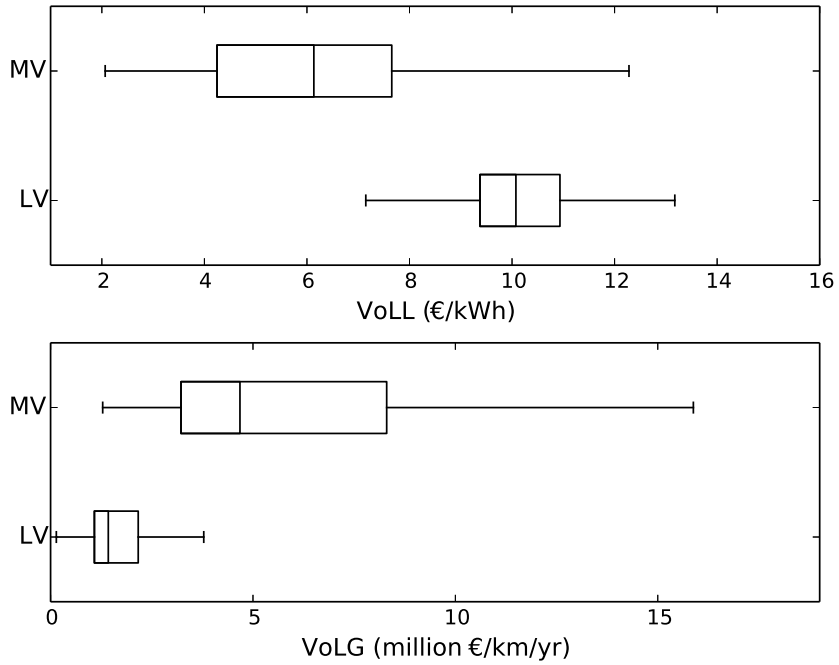

Figure 32: Box-and-Whisker plots (excluding outliers) of average *VoLLs* (top) and *VoLGs* (bottom) for the low voltage (LV) and medium voltage (MV) grid. The central box indicates the *VoLL*/ *VoLG* range of the central 50% of the total electricity consumption of the respective voltage level.

may conclude that the difference between the two voltage levels with respect to the *VoLG* results from a high ratio of electricity consumption to grid length, which is moderated by a countervailing characteristic of the *VoLL*.

With respect to the regional variability of the *VoLG*, Fig. 30 and Fig. 31 illustrate, that the South-West and certain Western parts of Germany are characterized by comparably high *VoLGs* in both analyzed voltage levels. Moreover, many smaller operators have considerable high *VoLGs*. Comparing results on the *VoLG* to data illustrating the ratio of electricity used per voltage level over area of the *DGO*'s domain (kWh/km^2), illustrate a positive correlation between the two quantities (not displayed in this work). Moreover, comparing the interquartile range (IQR) of *VoLLs* and *VoLGs* in Fig. 32 illustrates that the interregional heterogeneity of the *VoLG* is markedly higher than heterogeneity of the *VoLL*[30]. In addition, the *IQR* of the *VoLGs* is markedly more pronounced in the medium voltage level then in the low voltage level. Hence, the interregional heterogeneity in the medium voltage grid is significantly higher.

Comparing Fig. 30 and Fig. 31 illustrates that the uncertainty attached to the *VoLGs* in the medium voltage level is comparably larger compared to the low voltage

[30]The *IQR* of *VoLLs* is 15.7% of median low voltage *VoLL* and 55.5% of median medium voltage *VoLL*, whereas the *IQR* is 76% of median low voltage *VoLG* and 109% of median medium voltage *VoLG*.

level. This is rooted in the fact, that the mapping process, as described in Subsec. 4.2.2, was less unambiguous for the low voltage level than for the medium voltage level. Hence, information deduced from the *VoLG* calculations of the medium voltage grid is more uncertain, than the conclusions that can be drawn from the *VoLGs* calculated for the low voltage grid. However, due to the fact that mean *VoLGs* in the medium voltage grid may differ up to an order of magnitude (compare lower box plot in Fig. 32), a comparison between operators is still meaningful, especially having in mind, that the uncertainty measure introduced is based on the maximum possible deviation from the determined mean value.

4.5 Discussion and Conclusions

This chapter of the dissertation resorted to an established economic concept (the *VoLL* methodology) as a starting point to investigate differences in the economic value of the electricity distribution grid infrastructure, in order to facilitate cost-efficient decision making with regard to grid extension requirements and altering climatic conditions.

Based on macroeconomic data, the *VoLL* was determined on the spatial resolution of German counties for five different sectors. However, a quantitative analysis of the relative economic value of an electricity grid requires information not only on the economic value generated by a unit of delivered electricity consumed from the respective grid. In response this thesis suggests the *VoLG* concept, which is characterized by the idea to relate the economic value generated due to the steady supply of electricity by a certain grid infrastructure, to the infrastructure needed to enable that steady supply. Based on this approach, the total economic value associated with the electricity consumed from a *DGO*'s voltage level was determined (including a measure indicating the uncertainty attached) and related to the grid length of the respective voltage level.

In principle, the results allow an operator- and voltage level-specific analysis of the relative economic value of the respective grid infrastructure. With regard to the statistical distribution of *VoLGs* in the two analyzed voltage levels, also a few general conclusions can be drawn. Firstly, the ratio of the economic importance of the medium- to the low voltage grid was quantified: the median *VoLG* of the medium voltage grid is more than a three times higher than the median *VoLG* of the low voltage grid.

Secondly, comparing the statistical distribution of *VoLLs* to the distribution of *VoLGs* showed that the interregional heterogeneity of *VoLGs* is substantially higher on both voltage levels compared to the heterogeneity of *VoLLs*. Moreover, in particular the medium voltage grid is characterized by large variations in the *VoLG*. Domains of comparably high *VoLG* are especially associated with those *DGOs*, characterized by a high ratio of electricity consumption to domain area, which is often found in rather densely populated domains. Apparently, in these domains, less infrastructure is needed to supply a comparably high amount of electricity to consumers. Examples of these domains are most operators in charge of geographically rather small network domains and few larger operators in the South-West and West of Germany.

Thirdly, the uncertainty attached to operator- and voltage level-specific *VoLGs* (resulting from the partly ambiguous mapping of sectoral electricity consumption from county- to operator- and voltage level-resolution) was shown to be especially pronounced with respect to the medium voltage level. Nonetheless, in many cases a comparison between operators still provides meaningful insights, since (i) differences between the operator-specific mean *VoLGs* in the medium voltage grid in many cases exceed the uncertainty

attached to the individual *VoLGs* and (ii) having in mind that the uncertainty measure introduced was based on the maximum possible deviation from the determined mean value.

In a general sense, these outcomes contribute to an economic assessment of all events potentially triggering electricity outages within the distribution grids: In domains with high relative economic value generation of the grid infrastructure, there is – from an economic perspective – an argument to opt for a relatively safer design of the infrastructure compared to domains with less relative economic importance of the infrastructure (if outage probabilities were uniform). Hence, this study's results can contribute to the design planning of expansions in the distribution grid with respect to resilience and redundancy, and can provide guidance with respect to decision making on maintenance and retrofitting measures. Further, regulators that currently control expenditures by *DGOs* primarily for efficiency (*Welle* and *Zwaan*, 2007; *Ward*, 2013a) may consider whether operators have proper incentives to invest such that the relative economic importance is incorporated in their decision making.

The author does not expect the observed heterogeneity of relative economic importance of the distribution grid infrastructure to be unique for Germany. Hence, contingent upon data availability, a transfer of the suggested methodology to other countries can help identify differences in the relative economic importance of electricity distribution infrastructures.

Finally, some remarks for the proper interpretation of this chapter's findings need to be reemphasized. One needs to be aware of the limitations arising from the assumptions inherent in the production function- and household income approach, as discussed in Subsec. 4.2.1. It has to be stressed that an economic evaluation can only be part of an overall analysis which should certainly incorporate ethical and political considerations, such as the potential implications when areas of less relative economic importance whose inhabitants already feel socially and economically disadvantaged are treated differently (in terms of outage security of the grid) from those areas of high economic importance. Moreover, it has to be emphasized that the suggested approach is targeting at exploring a measure that is superior to the *VoLL* in expressing and comparing the economic value of the electricity distribution grids. Its derivation is based on heuristic considerations and is, therefore, difficult to scientifically proof. Nevertheless, its interpretation contributes relevant additional information to considerations on network architecture and grid design, which the *VoLL* concept is not able to do.

Furthermore, this chapter's results cannot replace a more regionally detailed analysis, since within the domain of an individual *DGO*, the relative economic importance of the operational reliability of each infrastructure unit may again vary significantly. Therefore,

an assessment of the economic importance for each individual infrastructure unit may guide decision making in a more precise manner. However, an analysis of this kind would require information on *VoLLs* and structural grid data on a significantly increased spatial resolution, which are either not publicly available or not collected by statistical offices.

Finally, this chapters findings cannot help answering the question whether the current resilience and redundancy of the grid well reflects the economic risks it is exposed to, since risk, as employed in the context of this thesis, is not determined by the implications only. To this end the following chapter relates the identified differences in the economic importance of the electricity distribution grid of this chapter to the findings of climate change induced alterations of windthrow likelihood of 3, in order to derive conclusions on the risks related to climate change on the electricity distribution networks.

5 Risk of Windthrow-induced Network Outages

As stressed in Ch. 1, risk can be represented as the likelihood of the occurrence of hazardous events multiplied by the impacts if these events occur (*IPCC*, 2014). Therefore, the likelihood of a network interruption as well as its monetary implications should be taken into account in the context of analyzing the risk on the electricity distribution grid associated with climate change. In the following paragraphs, the results for the two principal chapters of this thesis (Ch. 3 and Ch. 4) are integrated into one quantity measuring risk.

Methodologically, this chapter basically depends on the definition of risk as the product of likelihood times impact. The results of the windthrow index (compare Ch. 3) were interpreted as windthrow likelihood, while the results of the VoLG calculation (compare Ch. 4) provide operator-specific information on the economic impact of an interruption of a certain grid infrastructure. Hence, the risk measure was determined from the product of the VoLG and the windthrow index.

The Figs. 33 and 34 illustrate the resulting risk of the two analyzed scenarios (RCP4.5 and RCP8.5) for the period 2040 to 2069. Due to the sketched methodological limitations (see next paragraph), the results allow for interregional comparisons only and cannot be translated into meaningful monetary units. The results highlight regions of comparably high risk to be primarily located in the mid-range mountain areas of North-Rhine Westphalia, Baden-Württemberg and Bavaria. Interestingly, the Harz and the Thuringian-Franconian mid-range mountain areas, which were identified to be characterized by the most pronounced windthrow likelihood, are not highlighted to be at risk, due to the comparably low relative economic importance of the grid infrastructure in these regions.

The results do not reveal substantial differences with respect to the two analyzed RCPs. This relates, firstly, to the fact that one of the two streams feeding into the risk calculation, the VoLG, is RCP-invariant, and secondly, the fact that the relative inter-regional differences of the windthrow index are less substantial than the relative inter-regional differences of the VoLG. In consequence, the differences in risk between the two RCP scenarios are mostly not substantial enough to be captured by the relatively coarse scale of the color bar.

Since the introduced risk measure is based on the results of the two subsequent chapters, it features also the listed limitations with respect to the methodological approaches and data these were based upon. The most important with respect to the windthrow index are: (i) the potentially limited representativeness of the ensemble for the historical reference period and the comparably low levels of robustness of the climate signal; and (ii) the fact that the proposed methodology is not able to quantitatively determine the likelihood for grid outages, due to a lack of data and methodology needed to translate

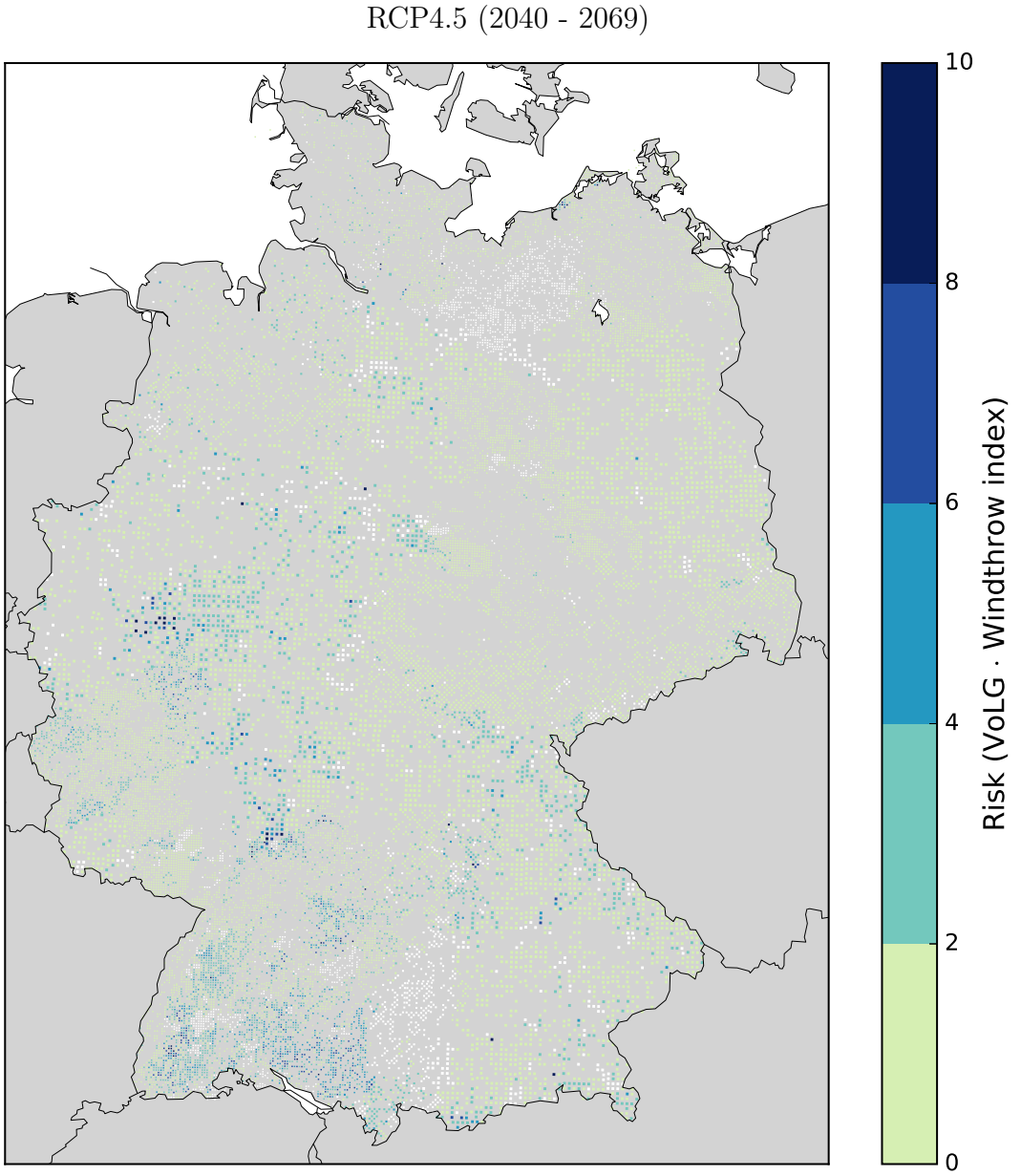

Figure 33: Risk related to windthrow-induced outages of the medium voltage level of the electricity distribution networks: Risk values are calculated as the product of VoLG and the windthrow index determined for the climate change scenario rcp4.5 for the period 2040 to 2069. Values are normalized to the illustrated range. The results are shown on the resolution of the Federal Tree Inventory (at least 4 km x 4 km). White colored regions indicate lacking data to quantify the VoLG.

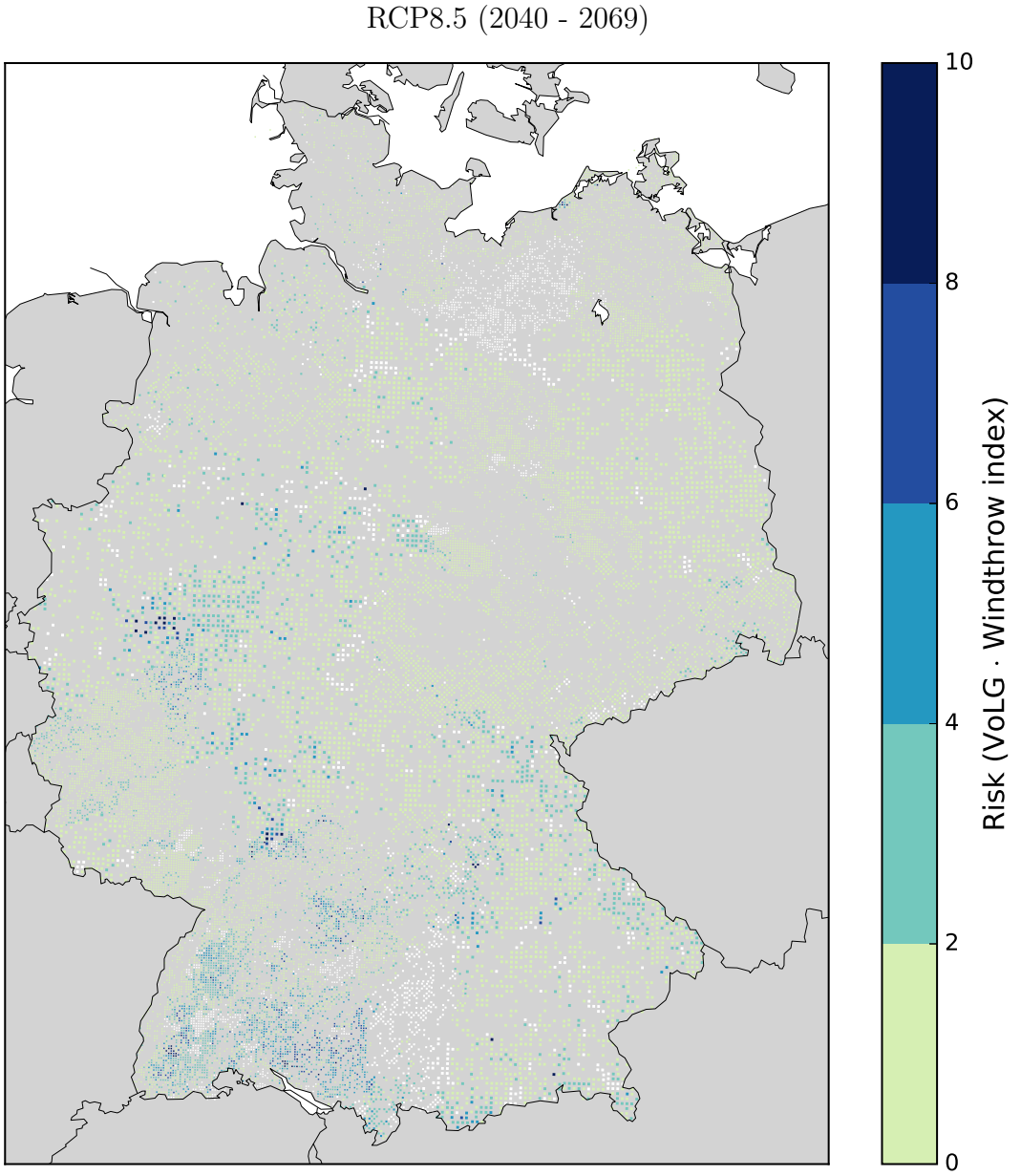

Figure 34: Risk related to windthrow-induced outages of the medium voltage level of the electricity distribution networks: Risk values are calculated as the product of VoLG and the windthrow index determined for the climate change scenario rcp8.5 for the period 2040 to 2069. Values are normalized to the illustrated range. The results are shown on the resolution of the Federal Tree Inventory (at least 4 km x 4 km). White colored regions indicate lacking data to quantify the VoLG.

windthrow of trees into outages of the electricity grid. The most important limitation with respect to the VoLG methodology is the fact that within the domain of an individual DGO, the economic importance of the operational reliability of each infrastructure unit may again substantially vary.

In addition, the integration of the two streams of information implies that projections of *future* conditions for windthrow are blended with the *current* economic importance of the electricity distribution network. The absence of future projections of the design of electricity distribution networks, the longevity of electricity infrastructure and the slow processes of adaptations and expansions of these infrastructure are certainly arguments in favor of the conducted integration. Nevertheless, the reader should be aware of this time gap between the two consolidated quantities.

Despite these limitations, the geographical heterogeneity of economic risks provides important guidance to identify regions or operators subjected to over-proportionally high economic risks associated with windthrow-induced outages of the electricity distribution network. Thus, the results can contribute to the planning of the expansion of the distribution grid with respect to resilience and redundancy towards these outages. However, concrete response measures to these findings should be based on a more locally focused analysis. The sketched results provide the basis to this end, as they facilitate identifying regions of comparably high risk, where it is most promising to resort to an additional analysis accounting for local features of the grid. The outlook at the end of Ch. 6 further elaborates on these thoughts.

6 Conclusions and Outlook

The German electricity grid is in transition in response to the challenges linked to an increasing share of renewable electricity generation. The necessary adaptation- and extension measures in the forthcoming years are substantial especially with respect to the distribution grid infrastructure. Beyond these challenges in the context of the energy transition, the grid infrastructure has to cope with implications related to anthropogenic climate change. Therefore, this dissertation argues that it is probably more cost-efficient to combine the current need for extension requirements related to the energy transition with the need to adapt the grid to climate change.

The risk associated with climate change impacts on the electricity grid infrastructure was suggested as a guiding quantity to determine cost-efficient future grid expansion and adaptation pathways. In this respect, intermediate research questions were posed (compare Ch. 1) along the definition of risk formulated in the field of quantitative risk analysis, where risk is defined as the likelihood of the occurrence of hazardous events multiplied by the impacts if these events occur. Consequently, the two principal parts of this thesis aimed at, firstly, contributing to the determination of the likelihoods of windthrow damage to grid infrastructure (see Ch. 3) and, secondly, quantifying the resulting economic consequences of a grid interruption (see Ch. 4). In the following, the overall conclusions are set specifically into the context of the initial research questions.

Which atmospheric events trigger grid interruptions?
Identifying the relevant atmospheric events leading to grid interruptions is crucial, firstly, for the identification of climate variables influencing the occurrence of these events, and secondly, for the identification of the grid infrastructure units which are affected by these events.

Therefore, an analysis of available literature and statistics on the reasons for customer disconnections was conducted. It showed that historically windthrow constituted the main contributor to atmospherically-induced customer disconnections in Germany. In the majority of these cases, wind causes trees to fall on the grid structures. But since the climatic conditions in Germany are projected to change, the likelihood of the occurrence of events triggering electricity outages gets modified. It is challenging to robustly project future reasons for electricity outages, as past reasons for grid interruptions are not necessarily a reliable indicator for future reasons for grid interruptions. However, expert assessments identifying the increased occurrence of storms as one of the biggest risks associated with the electricity transmission and distribution sector, indicate that windthrow is going to constitute a major threat also under changed climatic conditions. In conclusion, this motivates the focus on the influence of climate change on windthrow in Ch. 3.

Moreover, the analysis of outage data indicated most incidents to occur on the medium voltage level of the distribution grid infrastructure. Since the overheadlines of the transmission networks run at substantially higher altitudes than the distribution networks, they hardly experience any windthrow-related disconnections. In conclusion, the focus of the analysis in Ch. 4 was set on the economic consequences of outages for the electricity *distribution* networks.

How does climate change impact the likelihood for grid outages?

Due to the decades-long lifetimes of investments in the electricity grid infrastructure, these structures should be adapted to the climate conditions prevailing during its lifetime. Therefore, a windthrow index was developed to investigate how the climatic conditions for windthrow in the period 2040 to 2069 differ from historical climate conditions (1970 to 1999). Beyond the wind climate, also other local climatic conditions (i.e. soil moisture and soil temperature) were considered in the index design.

For the historical reference period (1970 to 1999), the windthrow index was most pronounced in the German mid-range mountain areas (e.g. the Black Forest, the Sauerland, the Harz and the Ore mountain ranges and parts of Bavaria). However, due to the differences between the index results of an ERA-Interim based calculation and a calculation based on the climate simulation ensemble (for the historical reference period), it remains unclear whether the ensemble median of the reference simulations can be considered representative for observed historical climate conditions. The reason for these differences was shown to relate to the formulation of exposure in the index design, which grants substantial influence to events of very low probability. Nevertheless, assuming any systematic bias to be present in historical as well well as future climate simulations, the interpretation of relative climate change signals is not constrained by this finding.

With respect to the two analyzed climate change scenarios (RCP8.5 and RCP4.5), increases of up to a doubling of the windthrow index (in comparison to the reference climate) were calculated over most Southern parts of Germany and over some areas in the vicinity to the North and Baltic Sea. The Harz and the Thuringian-Franconian mid-range mountain areas, however, which were identified to host the historically most pronounced windthrow index values, are projected to be affected by comparably modest (largely not robust) increases only. Most areas over the rest of the North of Germany are characterized by less pronounced increases, indifferent changes or even small decreases. However, the fact that robustness is identified only for a small share of areas indicates the substantial uncertainty with respect to the climate change signal of the windthrow index.

Admittedly, the initial research question – to deduce changes in the likelihood for grid outages – can be answered to a limited extent only by the conducted analysis. This relates

to several reasons hampering to establish a quantitative relation between windthrow and electricity outages: Firstly, the windthrow index is meant to reflect general factors that do not depend on human preferences or managing methods. In consequence, the index cannot be used to assess whether windthrow actually occurs or not, but enables a comparison for the climate conditions for windthrow. Secondly, there is a lack of information on the exact routing of OHLs and their proximity to trees. Thirdly, grid infrastructure damages also depend on prevention measures undertaken by operators. Such information are neither publicly available nor could an adaptation of these measures be robustly projected in the context of climate model simulations. Finally, a damaged infrastructure does not necessarily imply electricity outages, due to redundancies in the electricity network. Hence, a quantification of the impacts of singular interruptions would require the application of electricity flow models, which should be addressed in a spatially higher resolved analysis (compare *outlook* paragraph at the end of this chapter)

Despite these limitations, the information on regional differences in the climatic conditions for windthrow, its projected future changes as well as accompanied uncertainties, can provide decisive knowledge on how to adapt vegetation management along the routings of OHL to changing climate conditions. The grids' exposure to an increase of windthrow-favoring climate conditions could be reduced by efforts preventing interruptions, such as regular clearings of the power-line corridors, or more redundant network architectures. However, decisions on the cost-efficiency of such measures also depend on the economic loss resulting from distribution grid interruptions. This is addressed by the subsequent research question.

What is the economic impact related to a grid interruption?

Having investigated climate related changes in the likelihood for windthrow, the analysis conducted in Ch. 4 focused on determining the economic implications related to interruptions of the distribution grid. To this end, the Value of Lost Load concept was employed as a starting point to investigate the economic value of the electricity distribution grid infrastructure. Due to deficits in the methodology to facilitate cost-efficient decision making with regard to grid extension requirements and altered climatic conditions, an expansion of the VoLL concept – introduced as Value of Lost Grid (VoLG) – was proposed.

This allows for an operator- and voltage level-specific analysis of the relative economic value of the grid infrastructure. The results reveal pronounced interregional variability of the VoLG, which indicates substantial regional differences with respect to the economic consequences of an outage. Especially the medium voltage level – identified as the grid level the most often subjected to windthrow-induced grid interruptions – is characterized by outstanding variability.

Further, it was concluded, that areas of comparably high economic importance are often operated by DGOs characterized by a high ratio of electricity consumption to network area, which is often found in densely populated regions. Apparently, in these regions, less infrastructure is needed to supply comparably high amounts of electricity of often higher added value.

Hence, if outage probabilities were spatially uniform, there was an economic argument to opt for a relatively safer design of the infrastructure in these regions, compared to those with less relative economic importance of the infrastructure. However, the analysis conducted in Ch. 3 illustrated the likelihood for windthrow not to be spatially uniform.

What is the risk associated with climate change impacts on the electricity grid infrastructure?

The integration of the results of the two main chapters into one risk measure enabled to identify grid regions of comparably high economic value which are, at the same time, subjected to a comparably high likelihood of windthrow under future climate conditions. The results highlight regions of comparably high risk to be primarily located in the mid-range mountain areas of North-Rhine Westphalia, Baden-Württemberg and Bavaria. For those distribution networks where climate change is projected to increase the economic risk related to windthrow, operators might be subjected to unprecendented conditions to which they need to adapt their vegetation management along the power-lines and network design.

Note that the interpretation of the results of the risk calculation are subjected to the same limitations listed with respect to the methodological approaches in the context of the previous paragraphs. In relation to these limitations, it needs to be stressed that this work cannot answer the posed research question in a qualitative sense, i.e. it cannot be concluded that the grid of operator X is cost-efficiently designed and adapted, while the grid of operator Y is characterized by a too high or too low level of reliability of supply. However, the results clearly indicate a high level of heterogeneity with respect to risk which is neither reflected in the standards according to which the grid is designed (these account for past climatic conditions only) nor in the regulatory schemes incentivizing low (or more precise: cost-efficient) levels of grid outages. Regulatory schemes could for example reflect that outages in certain regions lead to higher economic costs than outages in other regions, by punishing outages in the former region more than outages in the latter.

Outlook

In addition to the presented results a more locally focused analysis, accounting for local features of the grid and its likelihood of being affected by windthrow induced outages,

could be beneficial. Such an analysis would require information on the exact routing of OHLs, the infrastructures proximity to trees and forests, the vulnerability of these tree species to windthrow and past data on the occurrence of windthrow along the lines. With respect to the evaluation of the economic importance of the grid, the suggested VoLG methodology could be applied to individual network entities. Such a regionally focused analysis could be beneficial to reflect differences of the outage likelihoods and the economic importance of infrastructure at a spatial resolution resolving individual lines. Accounting for these would guide decision making with respect to adaptation and grid expansion in a more precise manner. As a prerequisite, information at these resolutions need to be collected and made available.

Nevertheless, the geographical heterogeneity of risk related to windthrow provides important guidance to identify regions or operators for which such an in-depth investigation could be promising. The South of Baden-Württemberg, for example, which was identified to be a high risk region, is also characterized by a comparably high share of OHLs within the medium voltage level of the distribution grid (compare Fig. 3). The same holds for the mid-range mountain areas in the East of Bavaria and some other Bavarian regions. High shares of OHLs do not necessarily imply a high vulnerability to windthrow. But these results indicate that a more detailed analysis should be conducted to inquire whether the identified coincidence of high windthrow likelihoods and high economic importance of the grid is reflected by more resilient network structures and higher efforts to prevent grid interruptions.

To the author's knowledge, this is the first study in the context of climate change induced risks for the electricity grid infrastructure integrating climate change information with information on the economic relevance of electricity distribution networks. Therefore, the proposed methods are to be interpreted as an example of an interdisciplinary methodological contribution aiming to strengthen and support the scientific basis for climate services to the electricity distribution sector, and as a tool to identify distribution grids which should be more closely analyzed with respect to climate change induced outage risks.

References

Abu-Hamdeh, N. H. (2003): Thermal Properties of Soils as affected by Density and Water Content. *Biosystems Engineering*, **86**(1), 97–102. doi:10.1016/S1537-5110(03)00112-0

Agricola, A.-C., B. Höflich, P. Richard, J. Völker, C. Rehtanz, M. Greve, B. Gwisdorf, J. Kays, T. Noll, J. Schwippe, A. Seack, J. Teuwsen, G. Brunekreeft, R. Meyer and V. Liebert (2012): Ausbau- und Innovationsbedarf der Stromverteilnetze in Deutschland bis 2030. Report, Deutsche Energie Agentur (dena). https://www.dena.de/themen-projekte/projekte/energiesysteme/dena-verteilnetzstudie/

Arent, D., R. Tol, E. Faust, J. Hella, S. Kumar, K. Strzepek, F. Tóth and D. Yan (2014): Key economic sectors and services. In Climate Change 2014: Impacts, Adaptation, and Vulnerability. Part A: Global and Sectoral Aspects. Contribution of Working Group II to the Fifth Assessment Report of the Intergovernmental Panel on Climate Change (edited by C. Field, V. Barros, D. Dokken, K. Mach, M. Mastrandre, T. Bilir, M. Chatterjee, K. Ebi, Y. Estrada, R. Genova, B. Girma, E. Kissel, A. Levy, S. MacCracken, P. Mastrandrea and L. White), Cambridge University Press, Cambridge, United Kingdom and New York, NY, USA, pp. 659–708

Bayod-Rújula, A. A. (2009): Future development of the electricity systems with distributed generation. *Energy*, **34**(3), 377–383. doi:10.1016/j.energy.2008.12.008

BDEW (2014): Energie-Info: Stromverbrauch im Haushalt. Report, Bundesverband der Energie- und Wasserwirtschaft e.V., Berlin. www.bdew.de/internet.nsf/id/6966C7CB65D8D8FAC1257D5E0043D565/$file/705_BDEW_Stromverbrauch im Haushalt_Stand_September 2014.pdf

Becker, G. S. (1965): A Theory of the Allocation of Time. *The Economic Journal*, **75**(299), 493–517. doi:doi:10.2307/2228949

Behrens, P., M. T. H. van Vliet, T. Nanninga, B. Walsh and J. F. D. Rodrigues (2017): Climate change and the vulnerability of electricity generation to water stress in the European Union. *Nature Energy*, **2**(114). doi:10.1038/nenergy.2017.114

BGR (2015): PhyGru1000_250 V1.0, Soil depths dataset

Bliem, M. (2005): Eine makroökonomische Bewertung zu den Kosten eines Stromausfalls im österreichischen Versorgungsnetz. *IHSK Discussion Paper*, (02), 1–22. http://www.kihs.at/studien/Discussion paper_Kosten Stromausfall.pdf

Braden, J., O. Panferov and C. Döring (2013): Indikatoren für kombinierte Wald-Risiken im Klimawandel, Analyse von REMO und CLM-Daten. Report, Fakultät für Forstwissenschaften und Waldökologie der Universität Göttingen, Abteilung Bioklimatologie. http://www.kliff-niedersachsen.de.vweb5-test.gwdg.de/wp-content/uploads/2012/11/T2-Jelka-Braden-Oleg-Panferov.pdf (accessed 4 May, 2018)

Bräuninger, M., S. Kruse, A. Wolf, P. Bodehser, M. Kleiner, J. Thiele, V. Böckers, J. Haucap and B. Pagel (2014): Stromtransport in Deutschland: Rahmenbedingungen und Perspektiven. Report, Hamburgisches WeltWirtschaftsInstitut (HWWI), Hamburg. http://www.hwwi.org/fileadmin/hwwi/Publikationen/Partnerpublikationen/HSH/2014_04_08_HSH_HWWI_Stromnetze.pdf (accessed 5 October, 2016)

Büchner, J., J. Katzfey, O. Flörcken, A. Moser, H. Schuster, S. Dierkes, T. van Leeuwen, L. Verheggen, M. Uslar and M. van Amelsvoort (2014): Moderne Verteilernetze für Deutschland (Verteilernetzstudie). Report. https://www.bmwi.de/Redaktion/DE/Publikationen/Studien/verteilernetzstudie.html (accessed 4 October, 2016)

Bundesanstalt für Geowissenschaften und Rohstoffe (2015): Bodenuebersichtskarte von Deutschland 1:200.000 (BUEK200)

Bundesministerium für Ernährung und Landwirtschaft BMEL (2019): Inventurverfahren: Vermessung des Waldes. https://www.bundeswaldinventur.de/dritte-bundeswaldinventur-2012/inventurverfahren/ (accessed 27 February, 2019)

Bundesnetzagentur (2015): Evaluierungsbericht nach § 33 Anreizregulierungsverordnung. Report

Bundesnetzagentur (2018): Tabellarische Auflistung der Versorgungsunterbrechungen Strom 2006 bis 2017. https://www.bundesnetzagentur.de/DE/Sachgebiete/ElektrizitaetundGas/Unternehmen_Institutionen/Versorgungssicherheit/Versorgungsunterbrechungen/Auswertung_Strom/Versorgungsunterbrech_Strom_node.html (accessed 5 November, 2018)

Burger, B. (2019): Net public electricity generation in Germany in 2018. Report, Fraunhofer Institute for Solar Energy Systems ISE, Freiburg. https://www.ise.fraunhofer.de/content/dam/ise/en/documents/News/Stromerzeugung_2018_2_en.pdf (accessed 20 February, 2019)

Cardona, O., M. van Aalst, J. Birkmann, M. Fordham, G. McGregor, R. Perez, R. Pulwarty, E. Schipper and B. Sinh (2012): Determinants of Risk: Exposure and Vulnerability. In Managing the Risks of Extreme Events and Disasters to Advance Climate Change Adaptation (edited by C. Field, V. Barros, T. Stocker, D. D. D. Qin, K. Ebi, M. Mastrandre, K. Mach, G.-K. Plattner, S. Allen, M. Tignor and P. Midgley), Cambridge University Press, Cambridge, UK, and New York, NY, USA, pp. 65–108. ISBN: 9781139177245. doi:10.1017/CBO9781139177245.005

de Nooij, M., C. Koopmans and C. Bijvoet (2007): The value of supply security. *Energy Economics*, **29**(2), 277–295. doi:10.1016/j.eneco.2006.05.022

de Nooij, M., R. Lieshout and C. Koopmans (2009): Optimal blackouts: Empirical results on reducing the social cost of electricity outages through efficient regional rationing. *Energy Economics*, **31**(3), 342–347. doi:10.1016/j.eneco.2008.11.004

de Nooij, M., B. Baarsma, G. Bloemhof, H. Slootweg and H. Dijk (2010): Development and application of a cost-benefit framework for energy reliability. Using probabilistic methods in network planning and regulation to enhance social welfare: The N-1 rule. *Energy Economics*, **32**(6), 1277–1282. doi:10.1016/j.eneco.2010.06.005

Dee, D. P., S. M. Uppala, A. J. Simmons, P. Berrisford, P. Poli, S. Kobayashi, U. Andrae, M. A. Balmaseda, G. Balsamo, P. Bauer, B. Bechthold, A. C. M. Beljaars, L. van de Berg, J. Bidlot, N. Bormann, C. Delsol, R. Dragani, M. Fuentes, A. J. Geer, L. Haimberger, S. B. Healy, H. Hersbach, E. V. Holm, L. Isaken, P. Kållberg, M. Köhler, M. Matricardi, A. P. McNally, B. M. Monte-Sanz, J.-J. Morcrette, B.-K. Park, C. Peubey, P. de Rosnay, C. Tavolato, J.-N. Thépaut and F. Vitart (2011): The ERA-Interim reanalysis: configuration and performance of the data assimilation system. *Quarterly Journal of the Royal Meteorological Society*, **137**, 553–597. doi:10.1002/qj.828

Deutsches Institut für Normung (2005): DIN EN 50423-3-4 (VDE 0210-12)

Deutschländer, T. and H. Mächel (2016): Temperatur inklusive Hitzewellen. In Klimawandel in Deutschland: Entwicklung, Folgen, Risiken und Perspektiven (edited by G. P. Brasseur, D. Jacob and S. Schuck-Zöller), Springer, pp. 47–56. doi: 10.1007/978-3-662-50397-3

Dobbertin, M. (2002): Influence of stand structure and site factors on wind damage comparing the storms Vivian and Lothar. *Forest Snow and Landscape Research*, **77**, 187–205

European Commission (2013): Adapting infrastructure to climate change: An EU Strategy on adaptation to climate change. Report.

https://ec.europa.eu/europeaid/sites/devco/files/swd-2013-138_en_12.pdf (accessed 20 March, 2016)

Federal Statistical Offices (2015): Gemeindeverzeichnis, Gebietsstand: 31.12.2014. https://www.destatis.de/DE/ZahlenFakten/LaenderRegionen/Regionales/Gemeindeverzeichnis/Gemeindeverzeichnis.html (accessed 11 January, 2016)

Feldmann, H., G. Schädler, H. J. Panitz and C. Kottmeier (2013): Near future changes of extreme precipitation over complex terrain in Central Europe derived from high resolution RCM ensemble simulations. *International Journal of Climatology*, **33**(8), 1964–1977. doi:10.1002/joc.3564

Feser, F., M. Barcikowska, O. Krueger, F. Schenk, R. Weisse and L. Xia (2015): Storminess over the North Atlantic and northwestern Europe-A review. *Quarterly Journal of the Royal Meteorological Society*, **141**(687), 350–382. doi:10.1002/qj.2364

Forestry Commission and Forest Research (2015): ForestGALES, A wind risk decision support tool for forest management in Britain. www.forestry.gov.uk/forestresearch

Forum Netztechnik/Netzbetrieb (2017): Störungs- und Verfügbarkeitsstatistiken (Berichtsjahre 2004-2015). https://www.vde.com/de/fnn/themen/versorgungsqualitaet/versorgungszuverlaessigkeit/archiv-fnn-stoerungsstatistiken (accessed 13 May, 2017)

Franken, F., S. Franz and A. Müterthies (2013): Erfassung der durch den Sturm Kyrill geschädigten Waldgebiete in Nordrhein-Westfalen anhand von digitalen Luftbildern und Orthophotos. waldwissen.net

Gadm.org (2015): GADM database of Global Administrative Areas (Vers. 2.8). gadm.org

Gardiner, B., K. Byrne, S. Hale, K. Kamimura, S. J. Mitchell, H. Peltola and J. C. Ruel (2008): A review of mechanistic modelling of wind damage risk to forests. *Forestry*, **81**(3), 447–463. doi:10.1093/forestry/cpn022

Giorgi, F., C. Jones and G. R. Asrar (2009): Addressing climate information needs at the regional level: the CORDEX framework. *World Meteorological Organization Bulletin*, **58**(3), 175–183. doi:10.1109/ICASSP.2009.4960141

Gößling-Reisemann, S., H. Bardt, H. Biebeler, O. Dördelmann, A. Herrmann, S. Stührmann and J. Wachsmuth (2012): Klimawandel: Regionale Verwundbarkeit der Energieversorgung in Deutschland. *Energiewirtschaftliche Tagesfragen*, **62. Jg.**(4), 60–63

Groenemeijer, P., N. Becker, M. Djidara, K. Gavin, T. Hellenberg, A. M. Holzer, I. Juga, P. Jokinen, K. Jylhä, I. Lehtonen, H. Mäkelä, O. M. Napoles, K. Nissen, D. Paprotny, P. Prak, T. Púčik, L. Tijssen and A. Vajda (2015): Past Cases of Extreme Weather Impact on Critical Infrastructure in Europe. Report 608166. http://rain-project.eu/wp-content/uploads/2015/11/D2.2-Past-Cases-final.compressed.pdf (accessed 16 March, 2019)

Groth, M., S. Bender, J. Cortekar, T. Remke and M. Stankoweit (2018): Auswirkungen des Klimawandels auf den Energiesektor in Deutschland. *Zeitschrift für Umweltpolitik & Umweltrecht*, **3**, 324–355

Growitsch, C., R. Malischek, S. Nick and H. Wetzel (2014): The Costs of Power Interruptions in Germany: A Regional and Sectoral Analysis. *German Economic Review*, **16**(3), 307–323. doi:10.1111/geer.12054

Hale, S. A., B. Gardiner, A. Peace, B. Nicoll, P. Taylor and S. Pizzirani (2015): Comparison and validation of three versions of a forest wind risk model. *Environmental Modelling and Software*, **68**, 27–41. doi:10.1016/j.envsoft.2015.01.016

Hasfurther, V., R. D. Burman and J. Nunn (1972): Technical Report No. 178: A Model for Predicting Soil Temperature from Air Temperature

Hines, P., J. Apt and S. Talukdar (2009): Large blackouts in North America: Historical trends and policy implications. *Energy Policy*, **37**(12), 5249–5259. doi:10.1016/j.enpol.2009.07.049

Hofherr, T. and M. Kunz (2010): Extreme wind climatology of winter storms in Germany. *Climate Research*, **41**(2), 105–123. doi:10.3354/cr00844

Hundecha, Y. and A. Bárdossy (2005): Trends in daily precipitation and temperature extremes across western Germany in the second half of the 20th century. *International Journal of Climatology*, **25**(9), 1189–1202. doi:10.1002/joc.1182

IPCC (2014): Annex II: Glossary. In Climate Change 2014: Synthesis Report. Contribution of Working Groups I, II and III to the Fifth Assessment Report of the Intergovernmental Panel on Climate Change (edited by K. Mach, S. Planton, C. G. eds.) von Stechow, Core Writing Team, R. Pachauri and L. R. eds.) Meyer), IPCC, Geneva, Switzerland, pp. 117–130

Jacob, D. (2001): A note to the simulation of the annual and inter-annual variability of the water budget over the Baltic Sea drainage basin. *Meteorology and Atmospheric Physics*, **77**(1-4), 61–73. doi:10.1007/s007030170017

Jacob, D. and R. Podzun (1997): Sensitivity studies with the regional climate model REMO. *Meteorology and Atmospheric Physics*, **63**(1-2), 119–129. doi:10.1007/BF01025368

Jacob, D., J. Petersen, B. Eggert, A. Alias, O. B. Christensen, L. M. Bouwer, A. Braun, A. Colette, M. Déqué, G. Georgievski, E. Georgopoulou, A. Gobiet, L. Menut, G. Nikulin, A. Haensler, N. Hempelmann, C. Jones, K. Keuler, S. Kovats, N. Kröner, S. Kotlarski, A. Kriegsmann, E. Martin, E. van Meijgaard, C. Moseley, S. Pfeifer, S. Preuschmann, C. Radermacher, K. Radtke, D. Rechid, M. Rounsevell, P. Samuelsson, S. Somot, J. F. Soussana, C. Teichmann, R. Valentini, R. Vautard, B. Weber and P. Yiou (2014): EURO-CORDEX: New high-resolution climate change projections for European impact research. *Regional Environmental Change*, **14**(2), 563–578. doi:10.1007/s10113-013-0499-2

Jönsson, A. M., F. Lagergren and B. Smith (2013): Forest management facing climate change - an ecosystem model analysis of adaptation strategies. *Mitigation and Adaptation Strategies for Global Change*, **20**(2), 201–220. doi:10.1007/s11027-013-9487-6

Kamimura, K., K. Kitagawa, S. Saito and H. Mizunaga (2012): Root anchorage of hinoki (Chamaecyparis obtuse (Sieb. Et Zucc.) Endl.) under the combined loading of wind and rapidly supplied water on soil: Analyses based on tree-pulling experiments. *European Journal of Forest Research*, **131**(1), 219–227. doi:10.1007/s10342-011-0508-2

Klaus, M., A. Holsten, P. Hostert and J. P. Kropp (2011): Integrated methodology to assess windthrow impacts on forest stands under climate change. *Forest Ecology and Management*, **261**(11), 1799–1810. doi:10.1016/j.foreco.2011.02.002

Klawa, M. and U. Ulbrich (2003): A model for the estimation of storm losses and the identification of severe winter storms in Germany. *Natural Hazards and Earth System Sciences*, **3**(6), 725–732. doi:10.5194/nhess-3-725-2003

Knist, S., K. Goergen, E. Buonomo, O. B. Christensen, A. Colette, R. M. Cardoso, R. Fealy, J. Fernández, M. García-Díez, D. Jacob, S. Kartsios, E. Katragkou, K. Keuler, S. Mayer, E. Van Meijgaard, G. Nikulin, P. M. Soares, S. Sobolowski, G. Szepszo, C. Teichmann, R. Vautard, K. Warrach-Sagi, V. Wulfmeyer and C. Simmer (2017): Land-atmosphere coupling in EURO-CORDEX evaluation experiments. *Journal of Geophysical Research*, **122**(1), 79–103. doi:10.1002/2016JD025476

Knorr, K., D. Horst, S. Bofinger and P. Hochloff (2017): Energiewirtschaftliche Bedeutung der Offshore-Windenergie für die Energiewende, Update 2017. Report, Fraunhofer-Institut für Windenergie und Energiesystemtechnik IWES. https://www.offshore-

stiftung.de/sites/offshorelink.de/files/documents/Studie_Energiewirtschaftliche Bedeutung Offshore Wind.pdf (accessed 20 February, 2019)

Knutti, R., R. Furrer, C. Tebaldi, J. Cermak and G. A. Meehl (2009): Challenges in Combining Projections from Multiple Climate Models. *Journal of Climate*, **23**(10), 2739–2758. doi:10.1175/2009jcli3361.1

Koch, H., H. Karl, M. Kersting, R. Lucas and N. Werbeck (2016): Infrastrukturen und Dienstleistungen in der Energie- und Wasserversorgung. In Klimawandel in Deutschland: Entwicklung, Folgen, Risiken und Perspektiven (edited by G. P. Brasseur, D. Jacob and S. Schuck-Zöller), Springer, pp. 243–252. doi:10.1007/978-3-662-50397-3

Kohnle, U. and S. Gauckler (2003): Vulnerability of Forests to Storm Damage in a Forest District of South-Western Germany situated in the Periphery of the 1999 Storm (Lothar)

König, A. (1995): Sturmgefährdung von Beständen im Altersklassenwald - Ein Erklärungs- und Prognosemodell. PhD thesis, Technical University of Munich

Kotlarski, S. (2007): A Subgrid Glacier Parameterisation for Use in Regional Climate Modelling. *Reports on Earth System Science*, **42**. doi:10.17617/2.994357

Kropp, J., A. Holsten, T. Lissner, O. Roithmeier, F. Hattermann, S. Huang, J. Rock, F. Wechsung, A. Lüttger, S. Pompe, I. Kühn, L. Costa, M. Steinhäuser, C. Walther, M. Klaus, S. Ritchie and M. Metzger (2009): Klimawandel in Nordrhein-Westfalen, Regionale Abschätzung der Anfälligkeit ausgewählter Sektoren. Potsdam Insitute for Climate Impact Research (PIK), 250 pp. ISBN: 4933128820709

Kumar, R., L. Samaniego and S. Attinger (2013): Implications of distributed hydrologic model parameterization on water fluxes at multiple scales and locations. *Water Resources Research*, **49**(1), 360–379. doi:10.1029/2012WR012195

Lagergren, F., A. M. Jönsson, K. Blennow and B. Smith (2012): Implementing storm damage in a dynamic vegetation model for regional applications in Sweden. *Ecological Modelling*, **247**, 71–82. doi:10.1016/j.ecolmodel.2012.08.011

Lanquaye, C. O. (2003): Empirical Modelling of Windthrow Risk and Hazard Mapping Using Geogrpahic Information Systems. PhD thesis, University of British Columbia

Leahy, E. and R. S. J. Tol (2011): An estimate of the value of lost load for Ireland. *Energy Policy*, **39**(3), 1514–1520. doi:10.1016/j.enpol.2010.12.025

Lengsfeld, P., R. Röspel, R. Lenkert and H. Ebner (2015): Technikfolgenabschätzung (TA), Moderne Stromnetze als Schlüsselelement einer nachhaltigen Stromversorgung. Report, Ausschuss für Bildung und Technikfolgenabschätzung. https://www.tab-beim-bundestag.de/de/pdf/publikationen/berichte/TAB-Arbeitsbericht-ab162.pdf (accessed 23 June, 2017)

Leuschner, U. (2007): Zahlreiche Stromausfälle durch Orkan "Kyrill". http://www.udo-leuschner.de/energie-chronik/070105.htm (accessed 22 September 2018)

Liang, L. L., D. A. Riveros-Iregui, R. E. Emanuel and B. L. McGlynn (2014): A simple framework to estimate distributed soil temperature from discrete air temperature measurements in data-scarce regions. *Journal of Geophysical Research: Atmospheres*, **119**(2), 407–417. doi:10.1002/2013JD020597

Linares, P. and L. Rey (2013): The costs of electricity interruptions in Spain: Are we sending the right signals? *Energy Policy*, **61**, 751–760. doi:10.1016/j.enpol.2013.05.083

Lutum + Tappert DV-Beratung GmbH (2016): Shapefile data of distribution grid operators in Germany

Mann, H. B. and D. Whitney (1947): On a Test of Whether one of Two Random Variables is Stochastically Larger than the Other. *The Annals of Mathematical Statistics*, **18**(1), 50–60

McDermott, G. R. and Ø. A. Nilsen (2011): Electricity Prices, River Temperatures and Cooling Water Scarcity. *NHH Dept. of Economics Discussion Paper*, (May 2011). doi: 10.2139/ssrn.1941820

McSweeney, C. F., R. G. Jones and B. B. Booth (2012): Selecting ensemble members to provide regional climate change information. *Journal of Climate*, **25**(20), 7100–7121. doi:10.1175/JCLI-D-11-00526.1

Mitscherlich, G. (1981): Wald, Wachstum und Umwelt: Eine Einführung in die ökologischen Grundlagen des Waldwachstums; 2. Band (Waldklima und Wasserhaushalt). Sauerländer's Verlag, Frankfurt am Main, 2nd ed.

Moberg, A. and P. D. Jones (2005): Trends in indices for extremes in daily temperature and precipitation in central and western Europe, 1901-99. *International Journal of Climatology*, **25**(9), 1149–1171. doi:10.1002/joc.1163

Moss, R. H., J. A. Edmonds, K. A. Hibbard, M. R. Manning, S. K. Ros, D. P. van Vuuren, T. R. Carter, S. Emori, M. Kainuma, T. Kram, G. A. Meehl, J. F. B. Mitchell,

N. Nakicenovi, K. Riahi, S. J. Smith, R. J. Stouffer, A. M. Thomson, J. P. Weyant and T. J. Wilbanks (2010): The next generation of scenarios for climate change research and assessment. *Nature*, **463**(7282), 747–756. doi:10.1038/nature08823

N-tv (2007): Drei Tage nach "Kyrill": Strom fließt wieder. https://www.n-tv.de/panorama/Strom-fliesst-wieder-article209565.html (accessed 22 September, 2018)

National Academy of Sciences and Engineering (acatech), German National Academy of Sciences Leopoldina and Union of the German Academies of Sciences and Humanities (2016): Flexibility concepts for the German power supply in 2050, Ensuring stability in the age of renewable energies. In Series on Science-Based Policy Advice (edited by S. Byfield and D. Vetter), National Academy of Sciences and Engineering (acatech), German National Academy of Sciences Leopoldina, Union of the German Academies of Sciences and Humanities, Berlin. ISBN: 978-3-8047-3549-1

Nicoll, B. C., B. A. Gardiner, B. Rayner and A. J. Peace (2006): Anchorage of coniferous trees in relation to species, soil type, and rooting depth. *Canadian Journal of Forest Research*, **36**(7), 1871–1883. doi:10.1139/x06-072

Outten, S. D. and I. Esau (2013): Extreme winds over Europe in the ENSEMBLES regional climate models. *Atmospheric Chemistry and Physics*, **13**(10), 5163–5172. doi:10.5194/acp-13-5163-2013

Panferov, O., C. Doering, E. Rauch, A. Sogachev and B. Ahrends (2009): Feedbacks of windthrow for Norway spruce and Scots pine stands under changing climate. *Environmental Research Letters*, **4**(4). doi:10.1088/1748-9326/4/4/045019

Panferov, O., A. Sogachev and B. Ahrends (2010): Changes of Forest Stands Vulnerability to Future Wind Damage Resulting from Different Management Methods. *The Open Geography Journal*, **3**, 80–90. doi:1874-9232/10

Pechan, A. and K. Eisenack (2014): The impact of heat waves on electricity spot markets. *Energy Economics*, **43**, 63–71. doi:10.1016/j.eneco.2014.02.006

Peltola, H., S. Kellomäki and H. Väisänen (1999a): Model computations of the impact of climatic change on the windthrow risk of trees. *Climatic Change*, **41**(1), 17–36. doi:10.1023/A:1005399822319

Peltola, H., S. Kellomäki and H. Väisänen (1999b): Model computations of the impact of climatic change on the windthrow risk of trees. *Climatic Change*, **41**(1), 17–36. doi:10.1023/A:1005399822319

Perera, A. H., B. R. Sturtevant and L. J. Buse (2015): Simulation modeling of forest landscape disturbances. *Simulation Modeling of Forest Landscape Disturbances*, pp. 1–321. doi:10.1007/978-3-319-19809-5

Pesch, T., H. J. Allelein and J. F. Hake (2014): Impacts of the transformation of the German energy system on the transmission grid. *The European Physical Journal Special Topics*, **2575**, 2561–2575. doi:10.1140/epjst/e2014-02214-y

Petermann, T., H. Bradke, A. Lüllmann, M. Poetzsch and U. Riehm (2010): Gefährdung und Verletzbarkeit moderner Gesellschaften - am Beispiel eines großräumigen Ausfalls der Stromversorgung. Report 141. http://www.tab-beim-bundestag.de/de/untersuchungen/u137.html (accessed 6 March, 2017)

Pfeifer, S., K. Bülow, A. Gobiet, A. Hänsler, M. Mudelsee, J. Otto, D. Rechid, C. Teichmann and D. Jacob (2015): Robustness of Ensemble Climate Projections Analyzed with Climate Signal Maps: Seasonal and Extreme Precipitation for Germany. *Atmosphere*, **6**(5), 677–698. doi:10.3390/atmos6050677

Piaszeck, S., A. Wolf and L. Wenzel (2014): Regional diversity in the costs of electricity outages: Results for German counties. *HWWI Research Paper*, **142**. doi:10.1016/j.jup.2014.08.004

Pinto, J. G. and M. Reyers (2016): Winde und Zyklonen. In Klimawandel in Deutschland: Entwicklung, Folgen, Risiken und Perspektiven (edited by G. P. Brasseur, D. Jacob and S. Schuck-Zöller), Springer, pp. 67–75. doi:10.1007/978-3-662-50397-3

Praktiknjo, A. J. (2014): Stated preferences based estimation of power interruption costs in private households: An example from Germany. *Energy*, **76**, 82–90. doi:10.1016/j.energy.2014.03.089

Rademaekers, K., J. van de Laan, S. Boeve, W. Lise, J. van Hienen, B. Metz, P. Haigh, K. de Groot, S. Dijkstra, J. Jansen, T. Bole, P. Lako and C. Kirchsteiger (2011): Investment needs for future adaptation measures in EU nuclear power plants and other electricity generation technologies due to effects of climate change. Report, DG Energy. https://ec.europa.eu/energy/sites/ener/files/documents/2011_03_eur24769-en.pdf (accessed 12 February, 2018)

Rauthe, M., M. Kunz and C. Kottmeier (2010): Changes in wind gust extremes over Central Europe derived from a small ensemble of high resolution regional climate models. *Meteorologische Zeitschrift*, **19**(3), 299–312. doi:10.1127/0941-2948/2010/0350

Röpke, L. (2013): The development of renewable energies and supply security: A trade-off analysis. *Energy Policy*, **61**, 1011–1021. doi:10.1016/j.enpol.2013.06.015

Salb, C., S. Gül, C. Cuntz, Y. Monschauer and J. Weishäupl (2018): Climate Action in Figures: Facts, Trends and Incentives for German Climate Policy. Report, Federal Ministry for the Environment, Nature Conservation and Nuclear Safety (BMU), Frankfurt am Main. https://www.bmu.de/fileadmin/Daten_BMU/Pools/Broschueren/klimaschutz_in_zahlen_2018_en_bf.pdf (accessed 18 February, 2019)

Samaniego, L., R. Kumar and S. Attinger (2010): Multiscale parameter regionalization of a grid-based hydrologic model at the mesoscale. *Water Resources Research*, **46**(5), 1–25. doi:10.1029/2008WR007327

Sanghvi, A. P. (1982): Economic costs of electricity supply interruptions. US and foreign experience. *Energy Economics*, **4**(3), 180–198. doi:10.1016/0140-9883(82)90017-2

Schindler, D., J. Bauhus and H. Mayer (2012): Wind effects on trees. *European Journal of Forest Research*, **131**(1), 159–163. doi:10.1007/s10342-011-0582-5

Schmid, E., B. Knopf and A. Pechan (2016): Putting an energy system transformation into practice: The case of the German Energiewende. *Energy Research & Social Science*, **11**, 263–275. doi:10.1016/j.erss.2015.11.002

Schmidt, M., J. Bayer and G. Kändler (2005): Sturm "Lothar" - Ansatz einer inventurbasierten Risikoanalyse, vol. 9. 12–16 pp. ISBN: 1614-7707

Schröder, T. and W. Kuckshinrichs (2015): Value of Lost Load: An Efficient Economic Indicator for Power Supply Security? A Literature Review. *Frontiers in Energy Research*, **3**(55), 1–12. doi:10.3389/fenrg.2015.00055

Schubert, D. K. J., T. Meyer, A. von Selasinsky, A. Schmidt, S. Thuß, N. Erdmann, M. Erndt and D. Möst (2013): Gefährden Stromausfälle die Energiewende? Einfluss auf Akzeptanz und Zahlungsbereitschaft. *Energiewirtschaftliche Tagesfragen*, **10**, 35–37. http://nbn-resolving.de/urn:nbn:de:bsz:14-qucosa-117777 (accessed 17 October, 2017)

Schubert, S., H. Vennegeerts and D. Quadflieg (2008): Findings from the FNN disturbances statistics. http://www.fgh.rwth-aachen.de/verein/publikat/vortraeg/ErkenntnisseFNN-Stoerungsstatistik_ Vennegeerts.pdf (accessed 21 October, 2016)

Schwab, A. J. (2012): Elektroenergiesysteme. 1051 pp. ISBN: 9783642219573. doi: 10.1007/978-3-642-21958-0

Stankoweit, M., M. Groth and D. Jacob (2017): On the Heterogeneity of the Economic Value of Electricity Distribution Networks: an Application to Germany. *Working Paper Series in Economics*, (371). www.leuphana.de/institute/ivwl/publikationen/working-papers.html (accessed 22 March, 2019)

Statistisches Bundesamt (2015): Zeitverwendungserhebung; Aktivitäten in Stunden und Minuten für ausgewählte Personengruppen (2012/2013). https://www.destatis.de/DE/Publikationen/Thematisch/EinkommenKonsumLebensbedingungen/Zeitbudgeterhebung/Zeitverwendung5639102139004.pdf?___blob=publicationFile (accessed 10 April, 2016)

Stegger, U. and C. Vinnemann (2013): Bodenübersichtskarte der Bundesrepublik Deutschland 1:1.000.000 (BUEK 1000)

Süddeutsche Zeitung (2010): Versicherer schätzen Schaden auf eine Milliarde Euro. www.sueddeutsche.de/panorama/orkan-kyrill-versicherer-schaetzen-schaden-auf-eine-milliarde-euro-1.921086 (accessed 22 September, 2018)

The Council of the European Union (2008): Council Directive 2008/114/EC of 8 December 2008 on the indentification and designation of European critical infrastructures and the assessment of the need to improve their protection. *Official Journal of the European Union*, pp. 75–82

The SciPy Community (2018): NumPy v1.16.dev0 Manual. www.numpy.org/devdocs/reference/generated/numpy.fft.fft.html#numpy.fft.fft (accessed 9 September, 2018)

Thünen Institut (2012): Third Federal Tree Inventory. gdi.thuenen.de/wo/waldatlas/?workspace=bwi3-tnr-voll3-shp&typ=Trakt&instanz=wo-bwi (accessed 27 February, 2018)

Tobin, I., R. Vautard, I. Balog, F. M. Br??on, S. Jerez, P. M. Ruti, F. Thais, M. Vrac and P. Yiou (2014): Assessing climate change impacts on European wind energy from ENSEMBLES high-resolution climate projections. *Climatic Change*, **128**(1-2), 99–112. doi:10.1007/s10584-014-1291-0

Tol, R. S. J. (2007): New Analysis - The Value of Lost Load. In Security of Supply in Ireland 2007 (edited by F. O'Leary, M. Bazilian, M. Howley and B. O'Gallachoir), Sustainable Energy Ireland, Energy Policy Statistical Support Unit, Cork, pp. 63–67. http://www.seai.ie/Publications/Statistics_Publications/Energy_Security_in_Ireland/SEI_EPSSU_Security_of_Supply_Third_Report.pdf

Usbeck, T., T. Wohlgemuth, M. Dobbertin, C. Pfister, A. Bürgi and M. Rebetez (2010): Increasing storm damage to forests in Switzerland from 1858 to 2007. *Agricultural and Forest Meteorology*, **150**(1), 47–55. doi:10.1016/j.agrformet.2009.08.010

van Vuuren, D. P., J. Edmonds, M. Kainuma, K. Riahi, A. Thomson, K. Hibbard, G. C. Hurtt, T. Kram, V. Krey, J.-F. Lamarque, T. Masui, M. Meinshausen, N. Nakicenovic, S. J. Smith and S. K. Rose (2011): The representative concentration pathways: an overview. *Climatic Change*, **109**(1-2), 5–31. doi:10.1007/s10584-011-0148-z

Ward, D. M. (2013a): The effect of weather on grid systems and the reliability of electricity supply. *Climatic Change*, **121**(1), 103–113. doi:10.1007/s10584-013-0916-z

Ward, D. M. (2013b): Supplementary Material: The effect of weather on grid systems and the reliability of electricity supply. *Climatic Change*, **121**(1), 103–113. doi:10.1007/s10584-013-0916-z

Warner, T. (2010): Numerical Weather and Climate Prediction. Cambridge University Press, Cambridge, United Kingdom and New York, NY, USA. doi:10.1017/CBO9780511763243.001

Welle, A. V. D. and B. V. D. Zwaan (2007): An Overview of Selected Studies on the Value of Lost Load. *Energy research Centre of the Netherlands (ECN)*, pp. 5–25. http://www.transust.org/workplan/papers/wp2_task_5_lost_load.pdf (accessed 8 February, 2016)

Wolf, A. and L. Wenzel (2015): Welfare implications of power rationing: An application to Germany. *Energy*, **84**, 53–62. doi:10.1016/j.energy.2015.02.095

World Meteorological Organization (WMO) (2011): Manual on Codes, International Codes, Annex II to the WMO Technical Regulations, Part A - Alphanumeric Codes, vol. Volume I.1. ISBN: 978-92-63-10306-2. https://www.wmo.int/pages/prog/www/WMOCodes/WMO306_vI2/Publications/2011editionUP2014/WMO306_vI2_2011UP2014.pdf

World Meteorological Organization (WMO) (2019): Frequently Asked Questions: What is climate? http://www.wmo.int/pages/prog/wcp/ccl/faqs.php (accessed 26 February, 2019)

Zachariadis, T. and A. Poullikkas (2012): The costs of power outages: A case study from Cyprus. *Energy Policy*, **51**, 630–641. doi:10.1016/j.enpol.2012.09.015

Zander, W., S. Lemkens, U. Macharey, T. Langrock, D. Nailis, M. Zdrallek, K. F. Schäfer, P. Steffens, T. Kornrumpf, K. Hummel and H. Schalle (2017): Optimierter Einsatz von Speichern für Netz-und Marktanwendungen in der Stromversorgung. Report, Deutsche Energie-Agentur GmbH (dena), Berlin. https://shop.dena.de/fileadmin/denashop/media/Downloads_Dateien/esd/9191_dena_Netzflexstudie.pdf (accessed 21 February, 2019)

Zolina, O., C. Simmer, A. Kapala, S. Bachner, S. Gulev and H. Maechel (2008): Seasonally dependent changes of precipitation extremes over Germany since 1950 from a very dense observational network. *Journal of Geophysical Research Atmospheres*, **113**(6), 1–17. doi:10.1029/2007JD008393

A Appendix

A.1 Sensitivities of trees to windthrow

Lagergren et al. (2012) suggest species-dependent species-dependent vulnerability coefficient of 1.0 for Norway spruce, 0.5 for Scots pine and 0.1 for the remaining species. *Kohnle* and *Gauckler* (2003) suggest vulnerability coefficient of 0.16, 0.2 and 0.06 for beech, oak and other deciduous tree species respectively. In order to deduce vulnerability coefficients that also depend on soil depth and -type, this thesis resorts to the soil anchorage coefficients for the four different soil types and two different soil depths as employed by the mechanistic-empirical model for windthrow ForestGALES (*Forestry Commission* and *Forest Research*, 2015), as explained in the subsequent paragraph:

The mean anchorage coefficient of spruces are, for example, quantified based on the mean of the eight anchorage coefficients (for each combination of soil type and depth): 163.8 Nm/kg. Assuming that this coefficient relates to a vulnerability coefficient of 1.0, as assumed for the species in general, deviations of the species-, soil-depth and soil-type dependent anchorage coefficients are used to deduce deviations of a certain soil type/depth-combination from this mean vulnerability coefficient. In the context of the chosen example: Since spruces growing on soil type A and a soil depth below 80 cm have an anchorage coefficient of 153.2 Nm/kg, these are 6% more vulnerable to windthrow than the average coefficient of 163.8 Nm/kg. Consequently, based on a simple cross-multiplication, the vulnerability coefficient of the respective soil type/depth-combination is assumed to amount 1.06.

The same procedure is conducted for Scots pines. However, tree pulling experiments have only been conducted on soil type A (*Nicoll et al.*, 2006), therefore, for the remaining soil types the mean vulnerability coefficient of 0.5 was assumed. The results of these calculations can be found in Tab. 1 of the main body of this dissertation.

A.2 Validation of Soil Temperature Proxy

How realistic is the soil temperature proxy to represent „real-world“ soil temperature? Fig. 35 compares the time series of the historical soil temperature at an arbitrary grid point, to the soil temperature proxy calculated. The proxy is computed for both, the weighting function $C(t)$ derived from the historical simulation and from the evaluation simulation. In either case, the first 30 elements of the weighting function were used ($t \in [0 : 29]$). It can be observed that the soil temperature proxies reproduce the simulated soil temperature to a certain extent, but do not perfectly follow the simulated soil temperature. The next paragraph elaborates on the skill of the proxy over the entire domain of interest.

Deviations of the proxy from the simulated soil temperature become relevant, when the proxy incorrectly reproduces the state of the soil (i.e. the proxy is of negative temperature while the simulated soil temperature is positive or vice versa). To quantify the proxy's skill to correctly reproduce the state of the soil, the number of situations during which the proxy and the simulated soil state indicate a frozen soil ($n = \{S|T_{\text{proxy}} < 0°\text{C} \cap T_{\text{td4}} < 0°\text{C}\}$) were related to all situations (S) during which either the proxy or the simulated soil temperature are below $0°C$ ($N = \{S|T_{\text{proxy}} < 0°\text{C} \cup T_{\text{td4}} < 0°\text{C}\}$). Fig. 36 (a) illustrates the resulting ratio of the two quantities (n/N) for the *historical* simulation based on the weighting factor C deduced from the same simulation. Accordingly, in 70 to 90% of all cases (where either the soil proxy or the soil temperature (T_{D4}) indicate a frozen soil state) the proxy is in agreement with the soil temperature about the soil state. Nonetheless, this skill can in some cases amount to only 30 to 40%, and at very few locations close to the Sea the proxy's skill can even reach 0%.

Fig. 36 (b) highlights that the application of the weighting function C calculated based on the *evaluation* run and applied to the atmospheric temperature of the *historical* run, in almost all cases only marginally decreases (mostly in the range of 0 to 5%) the skill of the proxy to predict the state of the soil. This indicates, that the weighting function derived from the *historical* simulation can also be applied to determine the soil temperature of the *evaluation* simulation based on the *evaluation's* atmospheric temperature. This indicates that the mean of the two weighting functions calculated for each of the two simulations can be applied to any other REMO simulation, and – assuming that REMO physically correctly reproduces energy fluxes from the atmosphere to the soil and within the soil – also in any of the other RCM simulations which are included in the ensembles employed for the analysis conducted in this thesis (compare Sec. 3.3).

A.3 Validation of Soil Moisture Proxy

How realistic is the soil moisture proxy representing actual soil moisture? Fig. 37 compares the time series of the relative soil moisture to the soil moisture proxy calculated based on the weighting function D (compare Subsec. 3.2.2). It can be observed that the soil moisture proxy reproduces the simulated relative soil moisture to a certain extent, but does not perfectly follow the simulated soil temperature.

Fig. 38 illustrates the RMSE between the soil moisture proxy and the simulated moisture saturation of the mHM-based dataset for the same period (1970 to 1999) used to determine the weighting function $D(t)$. The figure indicates that the proxy's skill to reproduce soil moisture varies regionally.

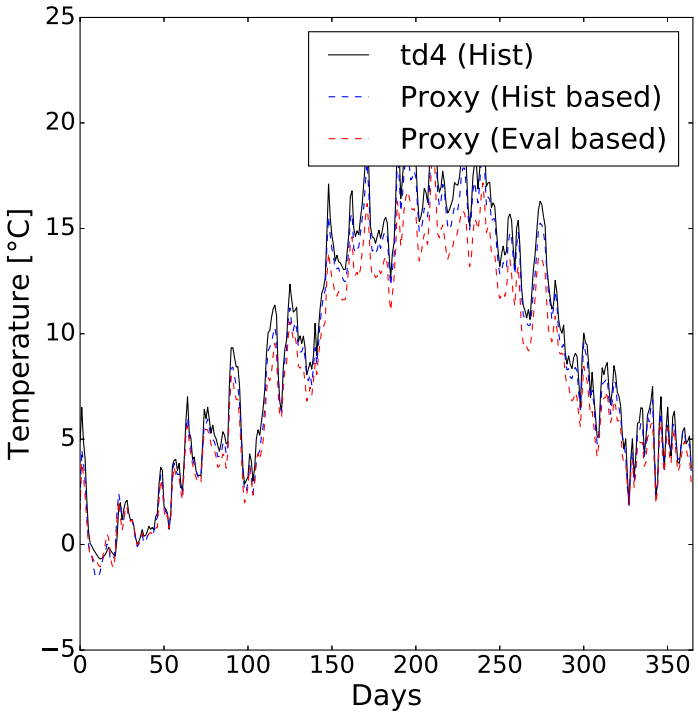

Figure 35: Comparison between (i) the soil temperature in the *historical* simulation of the first realization of GCM MPI-ESM downscaled with REMO2009 (td4) at an arbitrary grid point (11.21°E, 51.44°N) during the year 1990 and (ii) the soil temperature proxy either derived from the *historical* simulation (red) and the *evaluation* simulation (blue).

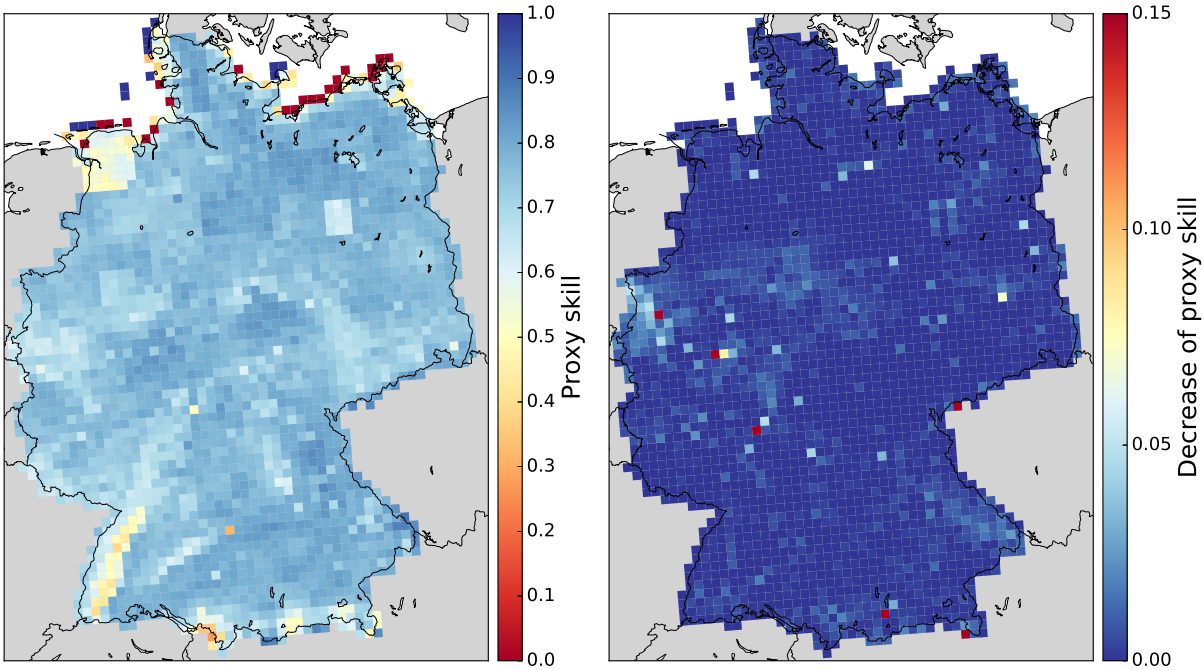

(a) (b)

Figure 36: (a): Skill of the proxy to correctly reproduce the state of the soil for the *historical* simulation, based on the weighting factor $C(t)$ deduced from the same simulation. The colorcode indicates the share of situations during which the proxy and the simulated soil state indicate a frozen soil (n) in relation to all situations during which either the proxy or the simulated soil temperature are below $0°C$ (N). (b): Relative reduction of the proxy's skill when the weighting factor is based on the *evaluation* simulation instead of the *historic* simulation.

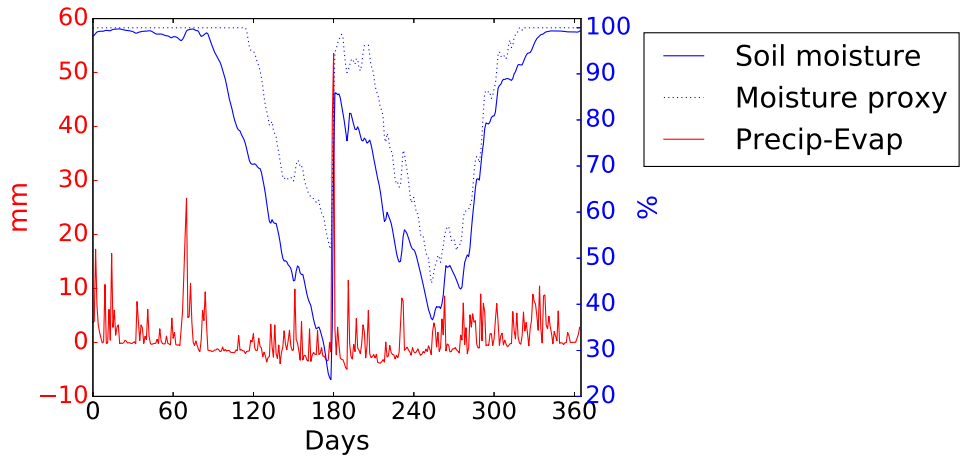

Figure 37: Comparison between the water saturation of the soil (blue), the calculated soil moisture proxy (dotted blue), and the difference between precipitation and evaporation (red) at an arbitrary grid point (11.21°E, 51.44°N) for the year 1990.

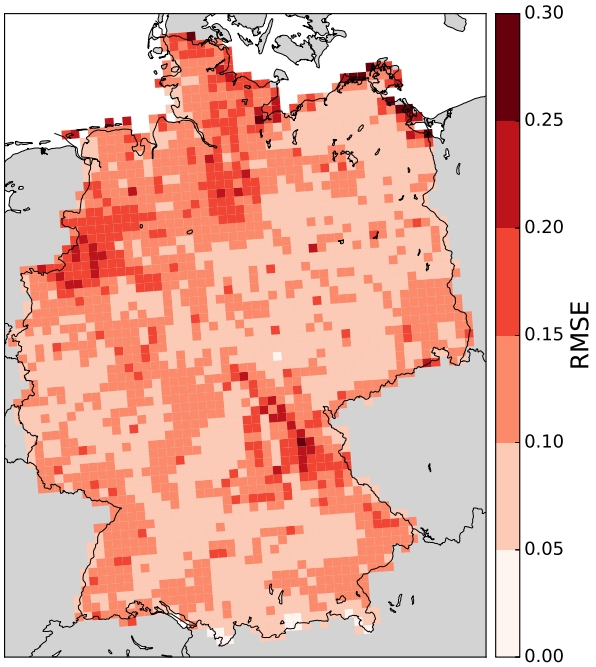

Figure 38: The RMSE of the soil moisture proxy compared to the soil moisture to which the weighting function D was calibrated (compare Subsec. 3.2.2). The RMSE is calculated for the entire calibration period (1970 to 1999).

Soil categories	Soil acronyms used in BUEK200/BUEK1000 dataset
A	FF, FS, OO, OL, RN, RQ, RR, RZ, TT, TC, DD, BB, LL, Ln, LF, PP, PS, CF, CR, VV, VW, XX, YK, Yk, YE, YO, YY, YU, YV, AO, AQ, AZ, AT, AB, MR, MC, MN, MH, MD, MK, MO UeA, IA, IW, JP, JG, JS, JD, F
B	GG, Gq, GN, SS, Sn, 'SH, SG
C	GM, GH
D	HN, HH, KV, KM, KH

Table 3: Reclassification of BUEK200/1000 soil categories into the four different soil categories: freely-draining mineral soils (A), gleyed mineral soils (B), peaty mineral soils (C), deep peats (D).

A.4 Reclassification of soil data

The raw soil classifications as in the used BUEK200/1000 datasets cannot be directly used, since the vulnerability coefficients of trees are available for four soil types only. Therefore, for each domain of the Federal Tree Inventory, the dominant soil types according to the subdivision into the four different soil types were determined, based on the dominant soil category in the overlap area between the shapefile of the respective domain of the Federal Tree Inventory and the shapefile of the BUEK200/1000 soil type file. To this end, the different soil types in the raw data were reclassified into the four categories A to D. Tab. 3 shows, which soil acronyms of the BUEK data were assigned to which soil type.

A.5 Mapping of Household's Electricity Consumption

As indicated in section 4.2.2, it is not a straightforward task to combine structural grid data, as published by each DGO, with VoLLs determined from macroeconomic data on county resolution. To be able to combine these data sets, both need to relate to the same reference unit. Hence, a harmonization of the resolutions is required, which motivated a mapping of electricity consumption (attached with each sector's county-specific VoLL) from county to operator resolution. For this purpose, it was made use of geographic intersections between counties and operators, as specified below.

The suggested methodology to determine the electricity consumption by households with respect to each DGO requires information on the population living in county c supplied by operator o: $P^{(u)a}(c, o)$. The superscript ua/a indicates whether population was unambiguously or ambiguously assigned from county c to operator o. $P^{(u)a}(c, o)$ was determined on the basis of a five step process as elaborated on in the following paragraphs. To facilitate understanding, the following nomenclature is introduced: Let C be a set of

all counties and O be a set of all DGOs. $A(c)$ and $A(o)$ shall constitute the geographic domain of county $c \epsilon C$ and DGO $o \epsilon O$ respectively. Further, let $A(o,c)$ be the geographic intersection of county c and DGO o: $A(o,c) := A(c) \cap A(o)$. Further, $a(c)$, $a(o)$ and $a(o,c)$ denote the geographic domain size of $A(c)$, $A(o)$ and $A(o,c)$.

At the beginning of the five step process, those DGOs o were identified for which $a(o,c) > 0.99 \cdot a(c)$ holds. This condition implies that o is an (almost) complete subdomain of only one county c. Consequently, all inhabitants of c were unambiguously assigned to operator o.

In step two, those DGOs were identified which, in conjunction with any of those DGOs to which population has been assigned already in step one, exactly cover a county. Precisely formulated, this means: Assuming, that o_1 overlaps with county c_1 (overlapping area: $a(o_1, c_1)$), and that people from county c_1 had already been assigned to an arbitrary number of other DGOs o_j ($j \neq 1$) in step one (which means, that these o_j are (almost) completely geographically covered by county c_1). Then, the remaining population of c_1 (which has not yet an unambiguous link to any DGO) was unambiguously mapped to o_1. These conditions can be expressed in the following inequality:

$$a(o_1, c_1) + \sum_{\forall j \text{ of step } 1} (a(o_j, c_1)) \geq 0.99 \cdot a(c_1)$$

Thereafter, in step three, it was made use of population reporting on municipality resolution[31]. Analogously to step one, the population of a municipality was mapped onto a county o, if its geographic intersection is at least 99% of the municipality's domain size.

In step four, those population numbers were mapped, which have not been unambiguously assigned to any DGO yet. Based on the size of the geographic intersections with the overlapping counties, a maximum number of people from each county was determined, which could potentially consume from that specific DGO. This maximum number of people was constrained either by the total number of people living in the county domain which have not been unambiguously mapped onto another DGO yet or by a maximum population density of 5000 inhabitants/km^2. The second constraint prohibits that small geographical intersections exert unrealistic influence on the calculation[32].

After these four steps, onto each DGO a certain population number has been (un)-ambiguously ambiguously mapped from counties to operators ($P^{ua}(c,o)$ and $P^{a}(c,o)$). For some DGOs it was possible to further increase the share of unambiguously mapped population; namely in those instances where the difference between unambiguously as-

[31]Each county is subdivided into at least one municipality. In Germany there are about 11,300 of the latter.

[32]This constraint was chosen heuristically, derived from the population density of the most densely populated municipality in Germany, which is 4,601 persons/km^2 (*Federal Statistical Offices*, 2015).

signed population and the total population supplied by a specific DGO could only be explained if a certain fraction of the so-far ambiguously assigned population, $P^{\mathrm{a}}(c,o)$, is instead unambiguously assigned to the same operator. Mathematically, this implies that as long as the inequality

$$\left(\sum_c P^{ua}(c,o)\right) + \left(\sum_c P^{\mathrm{a}}(c,o)\right) - P^{a}(c,o) < P(o)$$

holds (with $P(o)$ being the number of people supplied by each DGO), population was shifted from $P^{a}(c,o)$ to $P^{ua}(c,o)$.

A.6 Mapping of other Economic Sectors' Electricity Consumption

Based on the determination of total electricity consumption by households, the electricity consumption which is to be assigned to the remaining economic sectors was determined. For these sectors, in analogy to the assignment of the population data, an unambiguous and an ambiguous mapping based on geographic overlaps was performed. However, for most of the other economic sectors it is unclear from which voltage level the electricity is consumed. Therefore, the fraction of ambiguously mapped electricity is significantly larger than for the household sector. The heuristic rationales according to which the mapping was performed are the following: (a) The *manufacturing & mining* sector withdraws the majority of its electricity supply from the higher voltage levels (high and medium voltage grid). (b) The sectors *agriculture* and *services* withdraw the majority of its electricity supply from the low and medium voltage grid. (c) The higher the geographic intersection between a county and a DGO , the higher the probability that sectors located in c consumed its electricity from the intersecting DGO o. (d) Only for the construction sector, it was unambiguously mapped onto the low voltage level (in case the DGO was certain).

We operationalize the previous observations as follows: Based on (d) and (c), it was assumed that when the geographic intersection area $a(c,o)$ is above 80% (90%, 95%, 99%) of $a(c)$, 15% (30%, 60%, 100%) of electricity consumption by the construction sector can be unambiguously assigned to the low voltage grid of the respective DGO o. The remaining 85% (70%, 40%, 0%) were mapped unambiguously onto the low voltage grid. From (a) and (b) was deduced, that an unambiguous mapping is not possible for the remaining sectors, due to the uncertainty from which voltage level these sectors consume electricity. Hence, these sectors' electricity consumption was ambiguously mapped in the following manner: (i) I ambiguously mapped 100% of the electricity consumed in county c by the agricultural and the services sector, and 10% of the manufacturing & mining

sector onto the low voltage level of the respective geographically intersecting operator o; (ii) I ambiguously mapped 100% (100%, 100%) of the electricity consumed in county c by the agricultural (services, manufacturing & mining) sector onto the medium voltage level of the respective operator; (iii) I ambiguously mapped 10% (10%, 100%) of the electricity consumed in county c by the agricultural (services, manufacturing & mining) sector onto the high voltage level of operator o. Issue (c) was reflected by reducing the maximum amount of electricity ambiguously assigned to a DGO o, if the geographic intersection ratio $a(c,o)/a(c)$ is small: Concretely, in case of a geographic intersection ratio $a(c,o)/a(c)$ of less than 20% (10%, 5%, 1%), not more than 60% (40%, 20%, 10%) of the electricity consumption of economic sectors in county c were assigned to the consumption from any voltage level of the geographically intersecting DGO o.

Finally, in analogy to step five of the mapping of population data (compare Appendix A.5), the share of unambiguously mapped electricity consumption was increased by shifting fractions of so-far ambiguously assigned electricity consumption to the unambiguously assigned consumption. This can be performed for those ambiguously assigned electricity consumptions $EC^{\mathrm{a}}(s,c,v,o)$ for which the following inequality holds:

$$\left(\sum_{c} EC^{\mathrm{ua}}(s,c,v,o)\right) + \left(\sum_{c} EC^{\mathrm{a}}(s,c,v,o)\right) - EC^{\mathrm{a}}(s,c,v,o) < EC(v,o)$$

with $EC(v,o)$ being the total electricity consumption from voltage level v of operator o.

A.7 Uncertainty of the VoLL and VoLG on operator resolution

Based on the minimum and maximum values of the VoLL, a measure was introduced that mirrors the uncertainty induced by the partially ambiguous mapping process. To this end, a probability distribution function (pdf) of the VoLL of a random kWh of electricity was determined, based on the ambiguously assigned electricity consumption and its assigned VoLL.

This, however, does not constitute a useful measure to quantify the uncertainty attached to the actual amount of electricity consumed, which can be illustrated by the following example: Assume that the low voltage grid of a certain DGO delivered 10 GWh of electricity annually. The mapping process enables to determine for 7 GWh, which sectors in which county unambiguously consumed from this DGO's grid. Assume a scenario, according to which for the remaining 3 GWh, a number of sectors, whose consumption add up to 4 GWh, potentially (ambiguously) consumed from that specific operator. The uncertainty attached to the VoLL of the 3 GWh is certainly much lower, compared to an-

other scenario (with identical probability distribution of VoLLs), where the ambiguously assigned consumption amounts 40 GWh instead of 4 GWh. Hence, the pdf of the VoLL of a random kWh of electricity of the ambiguously assigned electricity consumption does not constitute a meaningful measure.

Due to the discrete nature of this mathematical problem, one cannot resort to the mathematics of combinatorics to determine a probability distribution of the resulting VoLL or VoLG for a voltage level of a DGO. In consequence, this study opted for minimum and maximum values of VoLL and VoLG as a measure of uncertainty in the manner already described . In order to facilitate a quick comparison between uncertainties attached to the mean VoLG, the relative average deviation of minimum and maximum from the mean value ($d = 1/2 \cdot (\text{VoLG}_{max} - \text{VoLG}_{min})/\text{VoLG}_{mean}$) was determined.

Acknowledgements

First of all, I would like to express a thank to my supervisor Prof. Dr. Daniela Jacob for her scientific support during the period of my PhD, and her trust in me and my work by encouraging me to defend my PhD-work in the context of the institute's evaluation. I am very grateful that Prof. Dr. Markus Quante and Prof. Dr. Klaus Eisenack volunteered as referees of the final thesis and I would like to express my thank for the inspiring and constructive discussion during the disputation of the thesis. Further, I am very grateful for the proofreading efforts, feedback and ideas of my doctoral adviser Dr. Markus Groth, as well as for his encouragement to present my work at international conferences.

The many friendly and helpful colleagues at GERICS helped getting through the downs of the three and a half years and made GERICS a place where I enjoyed to be – not only during lunchtimes and summer ice-cream breaks. Especially my most-of-the-time office-mate Thomas deserves an outstanding mentioning for always taking the time to discuss a question, for his valuable proofreading efforts, and – last but most worth mentioning – the family-like spirit and the culture of mutual support in our office and beyond.

Also people outside the office played a crucial part in the compilation of this thesis: I would like to thank my family, Monika and Philip, for their unconditional support and believe in me. Beyond, my thanks go to Adrian, Benjamin, Bettina, Katharina, Lorenz, Meike, Philipp, Theresa and Thomas, which overwhelmingly contributed to my everyday motivation during the final writing process with tiny once-a-day messages that either brought a warm smile to my face or caused a full-throated laughter.

Last but not least, I would like to dearly thank my wife Theresa for having moderated my PhD-related moods, for her believe in the value of my work and for simply being with me.